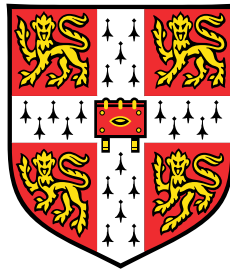


# Sensitivity Analysis in Low Order Thermoacoustic Networks



**José Guillermo Aguilar Pérez**

Department of Engineering  
University of Cambridge

First Year Report  
*Supervisor: Prof. Matthew Juniper*



## Declaration

I hereby declare that except where specific reference is made to the work of others, the contents of this dissertation are original and have not been submitted in whole or in part for consideration for any other degree or qualification in this, or any other university. This dissertation is my own work and contains nothing which is the outcome of work done in collaboration with others, except as specified in the text and Acknowledgements. This dissertation contains fewer than 30,000 words including appendices, bibliography, footnotes, tables and equations and has fewer than 50 figures.

José Guillermo Aguilar Pérez  
December 2015



## Abstract

Strict gas emission regulations are pushing gas turbine manufactures to develop devices that operate under conditions that encourage the appearance of combustion instabilities. Although methods to predict and control unstable modes inside combustion chambers have been actively developed in the last decades, in some cases they might be computationally expensive. Recently there has been a surge in sensitivity analysis aided by adjoint methods that at a very low computational cost provide valuable gradient information of the system. This report introduces the adjoint methods and their application in low order network models to predict and control thermoacoustic oscillations. The approach derives in a nonlinear eigenvalue problem, thus proper adjoint methods are used to obtain the sensitivities of the system. Using a discrete approach, base state sensitivities to parameters like reflection coefficients or flame parameters are computed and discussed in order to stabilize the system. Afterwards, structural sensitivities are computed by perturbing the system with intrinsic feedback. To gain more insight into the problem a continuous approach is used to derive the thermoacoustic adjoint equations. Finally, some of the equations in the low Mach number limit are derived to compare with those with mean flow.



# Table of contents

<b>List of figures</b>	<b>ix</b>
<b>List of tables</b>	<b>xi</b>
<b>1 Introduction</b>	<b>1</b>
1.1 Thermoacoustic Instabilities . . . . .	1
1.2 Low Order Network Models . . . . .	2
1.3 Adjoint Methods in Stability Analysis . . . . .	4
1.3.1 Definition of the Adjoint Function . . . . .	7
1.4 Scope and Structure . . . . .	9
<b>2 Low Order Thermoacoustic Network</b>	<b>11</b>
2.1 Network Definition . . . . .	11
2.2 Governing Equations . . . . .	12
2.3 The Eigenvalue Problem . . . . .	13
2.3.1 Zeroth order (Mean Flow) variables . . . . .	13
2.3.2 First order (fluctuations) variables . . . . .	14
<b>3 Sensitivity analysis via the Discrete approach</b>	<b>21</b>
3.1 Eigenvalue drift . . . . .	21
3.2 Base state sensitivity . . . . .	22
3.2.1 Taylor Tests . . . . .	24
3.3 Structural Sensitivity . . . . .	24
<b>4 Sensitivity Analysis via a Continuous Approach</b>	<b>33</b>
4.1 Continuous Adjoint formulation . . . . .	33
4.2 Continuous Adjoint Equations and Eigenvalue Problem . . . . .	37
4.3 Continuous eigenvalue drift formula . . . . .	44
4.4 Base state sensitivity . . . . .	44

---

4.5	Structural sensitivity . . . . .	44
<b>5</b>	<b>Equations in the Low Mach number limit</b>	<b>47</b>
5.1	The Eigenvalue Problem . . . . .	47
5.2	Sensitivity analysis using a discrete approach . . . . .	48
5.2.1	Base state sensitivity . . . . .	48
5.2.2	Structural sensitivity . . . . .	50
5.3	Notes on the continuous approach . . . . .	52
<b>6</b>	<b>Conclusions and Future Work</b>	<b>53</b>
6.1	Conclusions . . . . .	53
6.2	Future Work . . . . .	54
	<b>References</b>	<b>57</b>
	<b>Appendix A Derivation of the jump conditions</b>	<b>61</b>
	<b>Appendix B Derivation of the nonlinear eigenvalue drift formula</b>	<b>63</b>
	<b>Appendix C Taylor Tests for Base State sensitivities</b>	<b>65</b>
	<b>Appendix D Perturbed Energy Equation in Terms of Pressure</b>	<b>67</b>
	<b>Appendix E Derivation of Jump Conditions to Perturbations Added to the System</b>	<b>69</b>
	<b>Appendix F Perturbed Wave-Form Solutions in time and frequency domain</b>	<b>71</b>
	<b>Appendix G Structural Sensitivity Taylor Tests</b>	<b>81</b>
	<b>Appendix H Derivation of adjoint equations (adding a perturbation)</b>	<b>85</b>

# List of figures

2.1	Network Model set up . . . . .	11
2.2	Direct pressure mode shape . . . . .	20
2.3	Direct velocity mode shape . . . . .	20
2.4	Direct density mode shape . . . . .	20
3.1	Network model split into 4 sections due to the presence of intrinsic feedback at points $x = a$ and $x = c$ . . . . .	26
3.2	Structural sensitivity - Continuity Equation - Pressure device. — represents the sensitivity using the eigenvalue drift formula. X represents sensitivities at certain points using a finite difference method. . . . .	28
3.3	Structural sensitivity - Continuity Equation - Velocity device. — represents the sensitivity using the eigenvalue drift formula. X represents sensitivities at certain points using a finite difference method. . . . .	29
3.4	Structural sensitivity - Continuity Equation - Density device. — represents the sensitivity using the eigenvalue drift formula. X represents sensitivities at certain points using a finite difference method. . . . .	29
3.5	Structural sensitivity - Momentum Equation - Pressure device. — represents the sensitivity using the eigenvalue drift formula. X represents sensitivities at certain points using a finite difference method. . . . .	30
3.6	Structural sensitivity - Momentum Equation - Velocity device. — represents the sensitivity using the eigenvalue drift formula. X represents sensitivities at certain points using a finite difference method. . . . .	30
3.7	Structural sensitivity - Momentum Equation - Density device. — represents the sensitivity using the eigenvalue drift formula. X represents sensitivities at certain points using a finite difference method. . . . .	31
3.8	Structural sensitivity - Energy Equation - Pressure device. — represents the sensitivity using the eigenvalue drift formula. X represents sensitivities at certain points using a finite difference method. . . . .	31

3.9	Structural sensitivity - Energy Equation - Velocity device. — represents the sensitivity using the eigenvalue drift formula. X represents sensitivities at certain points using a finite difference method. . . . .	32
3.10	Structural sensitivity - Energy Equation - Density device. — represents the sensitivity using the eigenvalue drift formula. X represents sensitivities at certain points using a finite difference method. . . . .	32
4.1	Continuity sensitivity mode shape $\rho^+$ . . . . .	43
4.2	Momentum sensitivity mode shape $u^+$ . . . . .	43
4.3	Energy sensitivity mode shape $p^+$ . . . . .	43
4.4	Structural sensitivity - Continuity Equation - Pressure device. — represents the sensitivity using the discrete approach. X represents sensitivities computed by the continuous approach . . . . .	46
5.1	Pressure and velocity mode shapes under low Mach number conditions.	48
5.2	Structural sensitivities acting on the momentum equation using three methods: Discrete, Continuous and Finite difference . . . . .	51
6.1	Gantt Chart of research plan. . . . .	55
C.1	Taylor test for base state variables: reflection coefficients ( $R_u, R_d$ ). . . . .	65
C.2	Taylor test for base state variables: time delays ( $\tau_u, \tau_d$ ). . . . .	66
C.3	Taylor test for base state variables: flame model ( $\beta, \tau$ ). . . . .	66
G.1	Testing structural sensitivity of continuity equation - pressure device. . . . .	81
G.2	Testing structural sensitivity of continuity equation - velocity device. . . . .	82
G.3	Testing structural sensitivity of continuity equation - density device. . . . .	82
G.4	Testing structural sensitivity of momentum equation - pressure device. . . . .	82
G.5	Testing structural sensitivity of momentum equation - velocity device. . . . .	83
G.6	Testing structural sensitivity of momentum equation - density device. . . . .	83
G.7	Testing structural sensitivity of Energy equation - pressure device. . . . .	83
G.8	Testing structural sensitivity of Energy equation - velocity device. . . . .	84
G.9	Testing structural sensitivity of Energy equation - density device. . . . .	84

# List of tables

2.1	Geometry and flow conditions . . . . .	19
3.1	Base state sensitivities for the first unstable eigenvalue of the network characterized by table 2.1 ( $s_1 = (0.0116 + 2.0980i) \cdot 10^3 \text{ s}^{-1}$ ) . . . . .	23
5.1	Base state sensitivities for the first unstable eigenvalue of the network characterized by table 2.1 under zero mean flow ( $s_1 = (147.75 + 2190.75i)\text{s}^{-1}$ ) . . . . .	49



# Chapter 1

## Introduction

### 1.1 Thermoacoustic Instabilities

F-1 engines used in the Saturn V rockets carry in their design probably the most expensive but successful attempt to mitigate combustion instabilities; with more than 3200 full-scale tests (Culick, 2006) the Apollo program is the perfect example on why there is a need to develop robust analytical tools to predict the onset of instabilities. More recently, stringent emissions regulations are motivating the development of combustors operating in a lean regime, which runs at lower temperatures to prevent the dissociation of air molecules and therefore reduce the formation of NO<sub>x</sub> gases. However, these operation conditions encourage the development of combustion instabilities (Lieuwen et al., 2001), hence promoting the development of strategies to prevent them.

Thermoacoustic instabilities are a form of unstable combustion that arise in all types of rockets, ramjets, afterburners, and gas turbines among others. All of these devices continuously burn fuel in order to generate either thrust or other form of mechanical energy. In general, the steady state of combustion will be accompanied by small unsteady heat release fluctuations, that when coupled with pressure fluctuations can cause thermoacoustic instabilities. This is because the flame (a source of volume) acts as a distribution of monopoles producing acoustic waves that propagate and then reflect at the boundaries to interact again with the flame. If the unsteadiness of the flame gets in phase with the acoustic field, small amplitude pressure oscillations will begin to grow in time and after many cycles, gain a considerable amplification which could be enough to cause flame blow off or structural damage (Lieuwen, 2003).

The first account of thermoacoustic oscillations was in the 18<sup>th</sup> century due to Higgins who described the generation of *sweet sounds* coming out from a tube burning hydrogen (Higgins, 1802). The phenomenon was not yet completely understood, it took

another century until Lord Rayleigh developed the theory behind the thermoacoustic effect: the Rayleigh criterion (Rayleigh, 1878); which states that whenever unsteady heat release is added during the condensation phase (increasing pressure) on the system, the instabilities will appear, but if unsteady heat is added during rarefaction phase (decreasing pressure), the instabilities are discouraged. The former statement has been generalized (Nicoud and Poinso, 2005) to account for energy dissipation  $\Psi$  across the boundaries and is expressed mathematically as:

$$\int_T \int_\Omega \frac{\gamma - 1}{\gamma \bar{p}} p'(x, t) q'(x, t) \, d\Omega \, dt \geq \int_T \int_S \Psi(x, t) \, dS \, dt \quad (1.1)$$

Where  $p'$  denotes the pressure fluctuations and  $q'$  denotes the unsteady heat release fluctuations. Accounting for no losses across the boundaries ( $\Psi = 0$ ), the original Rayleigh criterion is recovered. In this regime, to predict the onset of instabilities the only requirement is that the left hand side integral be greater than zero, which will happen whenever the pressure and unsteady heat release amplitudes add up to get a larger amplitude wave..

Nicoud et al. (2007) summarize several methods to predict thermoacoustic instabilities, among others: Large Eddy Simulations (LES) currently used to study turbulent combustion but with the drawback of being computationally expensive; Helmholtz solvers which use equations for fluctuations in the frequency domain ( $\omega$ ) to solve the nonlinear eigenvalue problem given by the inhomogeneous Helmholtz equation:

$$\nabla \cdot \left( \frac{1}{\bar{\rho}} \nabla \hat{p} \right) + \frac{\omega^2}{\gamma \bar{p}} \hat{p} = i\omega \frac{\gamma - 1}{\gamma \bar{p}} \hat{q} \quad (1.2)$$

and Network models, being of special interest since they provide a low order framework that can be extensively used in pre-design stages.

## 1.2 Low Order Network Models

Network modeling is a technique often used in the field of thermodynamics to analyze each of the components of a bigger network separately and then couple them together using conservation laws. Their usage in thermoacoustics is based upon the fact that the wave behavior of acoustics inside a duct is linear, therefore being accurately captured by a low order network model; additionally, it provides physical insight using a very simple approach and it is very fast compared to standard CFD computations (Morgans, 2015).

As described by [Dowling and Stow \(2003\)](#) a thermoacoustic network is a collection of acoustic elements such as ducts, plenums, combustors, boundaries and a combustion zone, normally assumed as a compact flame. The element's mean flow quantities are often considered homogeneous and a mode shape for the fluctuations is considered. Both mean flow quantities and fluctuations are joined by jump relationships which in general seek to conserve one or more of these quantities: mass, momentum and energy. There are two major outcomes, one is a dispersion relationship used to compute all of the resonant modes of the system, and the other are the relative amplitudes of the waves considered in the model, which are normally the forward and backward acoustic waves and if there is a flame and an entropy wave (for example, [Goh and Morgans \(2012\)](#)), in 2 or 3 dimensions vorticity waves also play a role ([Lieuwen, 2012](#)). The resonant modes of the system, will then depend on the configuration of the system. Through this report only longitudinal waves are considered, but for a different geometry the inclusion of radial or azimuthal modes is necessary, for instance in the case of annular combustors ([Stow and Dowling, 2001](#))

[Chu and Kovásznyai \(1958\)](#) showed that to first order any wave can be considered as a linear superposition of acoustic, entropy or vorticity fluctuations. This is because the acoustic fluctuations which travel at the speed of sound ( $\bar{c}$ ) are treated as isentropic and irrotational, entropy fluctuations which travel at the mean flow speed ( $\bar{u}$ ) are treated as incompressible and irrotational, and vorticity waves which travel at the mean flow speed ( $\bar{u}$ ) are treated as incompressible and isentropic. To second order there are some interactions between these fluctuations and can no longer be considered independent. Since the models used through this report are only one dimensional, and knowing that vorticity modes are produced by the baroclinic mechanism ([Lieuwen, 2001](#)) only acoustic and entropy disturbances are considered.

To guarantee that the flame can be treated as an infinitely compact source of heat release [Dowling \(1995\)](#) suggests that the wave length of the acoustic variables ( $L_a$ ) be much larger than the length of the flame ( $L_f$ ), that is  $L_f/L_a \ll 1$ . However, on the presence of convected disturbances like equivalence ratio fluctuations or hot spots (entropy waves) a stricter consideration must be made, which implies that the wave length of the convected variable ( $L_c$ ) must be much smaller than the length of the flame ( $L_f/L_c \ll 1$ ). As the name suggests these type of disturbances convect away with the mean flow, therefore, depending on the boundary at the exit, the latter condition can be relaxed, which is not the case of a boundary condition that generates acoustic waves from entropy disturbances such as the exit nozzle studied by [Marble and Candel \(1977\)](#).

The last piece to complete a network model is to state the form of the unsteady heat release. Following from Crocco's combustion time lag theory, the famous  $n - \tau$  model can be derived from the form of heat release:

$$Q = \rho u c_p \Delta T \quad (1.3)$$

when linearized provides an unsteady mechanism that can depend on both the density and the velocity fluctuations, from both [Lieuwen \(2003\)](#) proves that the velocity coupling mechanism is potentially a stronger source of acoustic amplification. These fluctuations are normally delayed, given that they need to convect from their source of origin, for instance the location of the fuel injectors, until they reach the flame. Then the unsteady heat release model can be thought as:

$$q' = \beta_1 u'(x_i, t - \tau) + \beta_2 \rho'(x_i, t - \tau) \quad (1.4)$$

if this model is substituted in equation (1.1), it is clear that the time delay ( $\tau$ ) is then the major source of instabilities (and non-linearities) that occur in the system. Unsteady heat release can be chosen to saturate at certain limits (imposed for example by the type of fuel) so that limit cycles of finite amplitude can be studied as done by [Dowling \(1997\)](#).

### 1.3 Adjoint Methods in Stability Analysis

[Magri \(2015\)](#) discusses how thermoacoustic systems being defined by a wide range of parameters, that encompass geometry definitions, operation regimes, forms of heat release etc. characterize the properties of its eigenvalues. Whenever one of the eigenvalues is unstable it is common to start changing any of the parameters until a stable solution is found. The power of adjoint methods relies in the ability to show for the desired eigenvalue how every single parameter is affected, therefore giving gradient information. The main advantage of this method being that it only requires one calculation apart from the one required to compute the eigenvalue. given these features of the adjoint methods they are perfectly suited for optimization and sensitivity problems.

To give some specific examples, in aerodynamic design [Jameson \(1995\)](#) used control theory aided by adjoint methods to compute the optimal design of a wing. In his paper it is shown how an iterative algorithm coupled with gradient information is used to reduce the drag of the wing by almost 50 percent. In this case, however, the

main objective was not the eigenvalue but the drag coefficient. Another example in the same area is done by [Nielsen et al. \(2010\)](#) where adjoint methods are used again for large scale shape optimization of both a jet fighter and a tilted rotor on dynamic unstructured grids. This time a handful of geometries including wings, tails, camber angles, and thickness of blades are optimized for a specified flight regime.

Stability analysis using adjoint methods has as primary objective the study of the properties of the eigenvalues. In flow instability, eigenvalue sensitivity is used to calculate the forced response of the flow to external forcing or the sensitivity of the eigenvalues to perturbations of the system, for example by changing a boundary condition. Pioneering this field was [Hill \(1992\)](#) working with the flow around a cylinder which presented for the first time adjoint based global mode stabilization. It is well known that in an open flow, the wake behind a cylinder becomes unstable by increasing the Reynolds number to around 47. At this point the flow bifurcates into the von Kármán Vortex Street, which is a two dimensional periodic oscillation. The onset of instability was studied experimentally by [Strykowski and Sreenivasan \(1990\)](#) by inserting a second smaller cylinder to get the response (stability/instability) of the system and mapping the overall behavior. The novelty of Hill's work was mapping the sensitivity of the unstable mode to external disturbances, and finding the point where the system is most sensitive to them by using the adjoint equations. The same problem was studied later by [Giannetti and Luchini \(2007\)](#) while performing global analysis on the flow around the cylinder, however, this time the concept of *structural sensitivity*<sup>1</sup> was brought to deal with the problem. These two approaches were still diverging from the experimental results mainly to the fact that sensitivity analysis do not perturb the mean flow, but the experiments did. The final resolution that combined the effect of the perturbation on the mean flow and the time varying disturbance was done by [Marquet et al. \(2008\)](#) and [Luchini et al. \(2009\)](#) which produced sensitivity maps that match very well with the experimental results of [Strykowski and Sreenivasan \(1990\)](#). A thorough review of this problem along with other instabilities in fluids such as the Tollmien-Schlichting waves and the Görtler instability is given by [Luchini and Bottaro \(2014a\)](#).

From this work in stability analysis, the applications soared. To show some in the field of hydrodynamics, using incompressible flow [Marino and Luchini \(2009\)](#) explored the stability of forward facing step. Another application in this area is given by [Pralits et al. \(2010\)](#) studying the flow around a rotating cylinder. In low Mach number flows

---

<sup>1</sup>The structural sensitivity turns out to be the proportional to the product of the direct and adjoint eigenfunctions.

Qadri et al. (2013) studied the spiral vortex breakdown of swirling flows. In the field of compressible flows Spagnoli and Airiau (2008) proposed noise mitigation strategies by using adjoint fields to identify the sources of noise in compressible mixing layers, and Freund (2011) used adjoint based optimization to produce an iterative algorithm that reduces jet noise.

In thermoacoustics one of the first applications of adjoint methods was done by Juniper (2011) where an optimization routine is aided with adjoint looping of the governing equations using a discretized Galerkin method to identify triggering of self-sustained oscillations inside an electrically heated Rijke tube. Continuing with the same model Magri and Juniper (2013b) used a time delayed thermoacoustic system in low Mach number conditions and adjoint methods to assess the stability of its eigenvalues. In that paper they study the changes to any of the parameters on the system (base state sensitivity) and also those generated by a generic passive control device acting on it (structural sensitivity). One of the major outcomes was that of a fine drag mesh used in the second half of the tube near the exit to help stabilize the system. This theory has been experimentally tested by Rigas et al. (2015) where they measure the linear stability of the system to quantify the growth rate and the frequency shift, as well as testing the drag mesh as a control device. As expected, the experiments had very good agreement with theory at least while measuring the growth rate. The frequency shift measurements were somewhat different because Magri and Juniper (2013b) did not consider a jump in temperature. Afterwards, Magri and Juniper (2013a) extend the theory developed in the electrically heated Rijke tube to consider the infinite rate chemistry diffusion flame, again doing base state and structural sensitivity analysis. Following the same line of research, Magri and Juniper (2014a) introduce the adjoint operators via a toy model, and later develop the adjoint techniques as applied to a ducted flame that considers a jump in temperature. Furthermore, using the same diffusion flame<sup>2</sup> proposed by Balasubramanian (2008) to study its non-normality and nonlinearity, Magri and Juniper (2014b) study both receptivity and sensitivity of the flame, revealing that it is very receptive to open loop forcing of the mixture fraction towards the tip of the flame, something that is not straightforward to obtain from just the sensitivity analyses. Base state sensitivities to stoichiometric mixture fractions, geometries and heat release parameters are studied as well. Adding up, Juniper (2015) introduces the Helmholtz equation (Eq. 1.2) and performs the adjoint of the Helmholtz solver including the study of several passive devices such as a Helmholtz resonator.

---

<sup>2</sup>In this flame, convection and reaction are modeled instead of a time delayed system between velocity and heat release fluctuations.

Given by the fact that in ducts only plane waves propagate, while the others decay exponentially fast, most of the previous reviewed work has been done in 1D, however, [Magri et al. \(2014\)](#) consider a 3D domain of low Mach number combustors and uses adjoints to identify unstable modes and introduce passive feedback mechanisms to help stabilize them. Finally [Juniper et al. \(2014\)](#) introduce a low order model of the Helmholtz equation to later perform uncertainty quantification taking into account the adjoint advantage which according to [Luchini and Bottaro \(2014b\)](#) states that: with fewer outputs than inputs adjoint computation is faster than direct computation. Alongside, nonlinear eigenvalue problems are studied and the eigenvalue drift formulas to first and second order are derived.

### 1.3.1 Definition of the Adjoint Function

Since most of the report will deal with adjoint equations, it is important to set their definition. To begin, consider the following inner product:

$$[\mathbf{a}, \mathbf{b}] = \int_V \int_T \mathbf{a}^* \cdot \mathbf{b} \, dt \, dV \quad (1.5)$$

where the \* represents the complex conjugate. Using the bilinear form described above, the adjoint system is defined as:

$$[\mathbf{q}^+, L\mathbf{q}] - [L^+\mathbf{q}^+, \mathbf{q}] = \text{constant} \quad (1.6)$$

Where  $\mathbf{q}$  is the vector and  $L$  is the operator that define the direct system, and  $\mathbf{q}^+$  is the vector and  $L^+$  is the operator that define the adjoint system. The constant on the right hand side is normally set to zero. The former expression is a simplification of the system presented by [Juniper and Magri \(2014\)](#). To get the adjoint equations, simply put the direct equations in the form presented by Eq. (1.6) and integrate by parts until the direct variables are isolated. The former operation can also be seen from the Lagrangian point of view while doing constrained optimization ([Gunzburger, 1997](#)). To follow that procedure the only requirement is to create a cost function ( $\mathcal{L}$ ) that is to be optimized and take the adjoint variables as Lagrange multipliers:

$$\mathcal{L} \equiv [\mathbf{q}^+, L\mathbf{q}] = [L^+\mathbf{q}^+, \mathbf{q}] + \text{constant} \quad (1.7)$$

Then, the cost function is equal to the adjoint system as defined in Eq.(1.5). To optimize a function one seeks that the derivatives of  $\mathcal{L}$  with respect to the direct ( $\mathbf{q}$ ) or adjoint ( $\mathbf{q}^+$ ) variables are equal to zero for any possible  $\mathbf{q}$  or  $\mathbf{q}^+$  respectively. Hence,

obtaining the adjoint equations, and the bilinear concomitant<sup>3</sup>, which after setting to zero, helps relate the boundary conditions and the initial and final values in time<sup>4</sup>. An ideal example of this process is given by Schmid and Brandt (2014) while deriving the Navier-Stokes adjoint Equations.

In stability analysis it is common to consider an eigenvalue problem of the form:

$$\mathbf{L}\mathbf{q} = \lambda\mathbf{q} \quad (1.8)$$

Where  $\lambda$  is the eigenvalue. Note that under the definition of the inner product (Eq. 1.5) the eigenvalues of the adjoint system are the complex conjugates of the direct system. The system can now be perturbed in two different ways:

- Perturbing the operator  $\mathbf{L}$ . This implies changing a parameter in the operator, which can be the reflection coefficients, the flame interaction index, flame position, etc. The outcome of analyzing the change caused by this perturbation in the eigenvalue is also known as *base state sensitivity*.
- Perturbing the system by adding a small intrinsic feedback source. This implies adding a small source proportional to one of the state variables of vector  $\mathbf{q}$ . In thermoacoustics it is likely to be either mass addition, a force, or some kind of energy. The change in the eigenvalue due to this source is known as *structural sensitivity*.

To first order, the change in the eigenvalue ( $\delta\lambda$ ) is the given by:

$$\delta\lambda = \frac{[\mathbf{q}^+, \delta\mathbf{L}\mathbf{q}]}{[\mathbf{q}^+, \mathbf{q}]} \quad (1.9)$$

where  $\delta\mathbf{L}$  represents the perturbation added to the system. However, it is often that thermoacoustic systems are nonlinear (Juniper et al., 2014):

$$\mathbf{L}(\lambda, p)\mathbf{q} = 0 \quad (1.10)$$

Where  $p$  are the internal parameters of the system. Hence, the eigenvalue drift formula changes to:

$$\delta\lambda = \frac{[\mathbf{q}^+, \delta\mathbf{L}\mathbf{q}]}{[\mathbf{q}^+, \frac{\partial \mathbf{L}}{\partial \lambda} \mathbf{q}]} \quad (1.11)$$

---

<sup>3</sup>Previously referred to as the constants.

<sup>4</sup>By following this procedure it can be shown that the adjoint operator evolves backwards in time.

One key point to ensure that eigenvalue analysis provides useful information, is the non-normality of the system. [Nicoud et al. \(2007\)](#) proved that in a thermoacoustic system the eigenfunctions are not orthogonal to each other due to the presence of the unsteady heat release. This means that transient growth around a fixed point<sup>5</sup> can be driven by linear mechanisms. Nonetheless, [Magri et al. \(2013\)](#) proved that at least in the presence of diffusion flames the non-normality is not as influential, therefore non-modal effects can be ignored.

## 1.4 Scope and Structure

Currently most of the approaches to get the sensitivity of a thermoacoustic system have been developed under a discretized Galerkin method, thus the mode shapes generated to create the sensitivity maps depend on the number of Galerkin modes used. These maps while being correct, display a smooth path through the jumps (low number of modes) or the Gibbs phenomenon (high number of modes) (see for example [Magri and Juniper \(2013b\)](#)). Therefore the first objective of the report is to obtain both the base state and the structural sensitivities using a wave based network model, which eventually displays a

On the other hand, [Dowling and Stow \(2003\)](#) showed that for Mach numbers less than 0.2 ( $M < 0.2$ ) the frequency shift is less than 5 percent thus promoting the use of Low Mach number analysis. The presence of a mean flow will be considered through the first chapters of the report to see the influence in sensitivity of the system. For the structural sensitivity the influence of mass addition, a force or heat addition will be studied therefore analyzing the implications of each device on the acoustic and entropy waves of the system.

The structure of the document is divided into 5 more chapters:

- Chapter 2 will be focused on the eigenvalue problem derived from a simple thermoacoustic network including the effects of mean flow. The problem is derived and the resonant modes are obtained.
- Chapter 3 is focused in obtaining the base state the structural sensitivities of the system using a discrete approach.
- Chapter 4 does the same as chapter 3 but it considers a continuous approach. It is important to note that even when they derive in the same results, both provide a different insight into the sensitivities of the system.

---

<sup>5</sup>The preferred choice for a fixed point are normally the mean values of the system.

- Chapter 5 will discuss the the equations in the low Mach number limit, therefore providing a framework that is comparable to that already developed.
- Chapter 6 will conclude with some remarks on the outcomes and difficulties on the approaches taken in the report, as well as providing a framework for the future work.

# Chapter 2

## Low Order Thermoacoustic Network

### 2.1 Network Definition



The thermoacoustic network is composed of a duct of length ( $L$ ) with a flame located at ( $x = b$ ). Considering that the flame is sufficiently compact, it can be treated as a jump. Therefore, the whole domain is split into two sections governed by a similar set of linearized equations (eq. 2.3). The jump conditions (eq. 2.4) connect the two domains. To solve the system a proper set of boundary conditions at the inlet ( $x = 0$ ) and at the outlet ( $x = L$ ) is required. Details of the network can be found in figure 2.1.

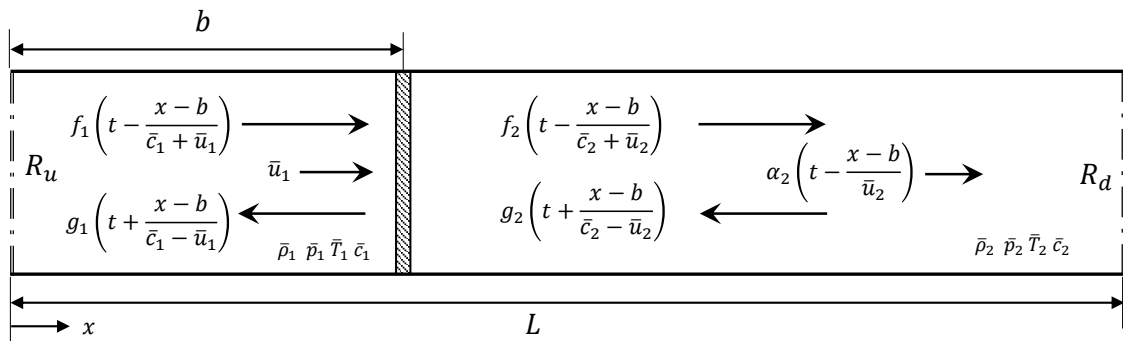


Fig. 2.1 Network Model set up

## 2.2 Governing Equations

In 1D the governing equations for the thermoacoustic system are given by the continuity equation, the momentum equation assuming no viscosity and the energy equation assuming no heat conduction:

$$\frac{\partial \rho}{\partial t} + u \frac{\partial \rho}{\partial x} + \rho \frac{\partial u}{\partial x} = 0 \quad (2.1a)$$

$$\rho \frac{\partial u}{\partial t} + \rho u \frac{\partial u}{\partial x} + \frac{\partial p}{\partial x} = 0 \quad (2.1b)$$

$$\frac{\partial p}{\partial t} + u \frac{\partial p}{\partial x} + \gamma p \frac{\partial u}{\partial x} = 0 \quad (2.1c)$$

The flame is treated as a discontinuity on the flow parameters, requiring a set of jump relationships. These relations are derived<sup>1</sup> from Eq. (2.1):

$$[\rho u]_{b^-}^{b^+} = 0 \quad (2.2a)$$

$$[p + \rho u^2]_{b^-}^{b^+} = 0 \quad (2.2b)$$

$$\frac{\gamma}{(\gamma - 1)} [\rho u]_{b^-}^{b^+} + \left[ \rho \frac{1}{2} u^3 \right]_{b^-}^{b^+} = q \quad (2.2c)$$

Where  $q$  is the heat release added per unit area. Linearizing the governing equations around the mean flow parameters (i.e  $p(x, t) \rightarrow \bar{p} + p'(x, t)$ ) yields:

$$\frac{\partial \rho'}{\partial t} + \bar{u} \frac{\partial \rho'}{\partial x} + \bar{\rho} \frac{\partial u'}{\partial x} = 0 \quad (2.3a)$$

$$\bar{\rho} \frac{\partial u'}{\partial t} + \bar{\rho} \bar{u} \frac{\partial u'}{\partial x} + \frac{\partial p'}{\partial x} = 0 \quad (2.3b)$$

$$\frac{\partial p'}{\partial t} + \bar{u} \frac{\partial p'}{\partial x} + \gamma \bar{p} \frac{\partial u'}{\partial x} = 0 \quad (2.3c)$$

The linearized jump conditions are:

$$[\rho' \bar{u} + \bar{\rho} u']_{b^-}^{b^+} = 0 \quad (2.4a)$$

$$[p' + 2\bar{\rho} \bar{u} u' + \rho' \bar{u}^2]_{b^-}^{b^+} = 0 \quad (2.4b)$$

$$\frac{\gamma}{(\gamma - 1)} [p' \bar{u} + \bar{p} u']_{b^-}^{b^+} + \frac{1}{2} [3\bar{\rho} \bar{u}^2 u' + \bar{u}^3 \rho']_{b^-}^{b^+} = \int_{b^-}^{b^+} q' dx \quad (2.4c)$$

---

<sup>1</sup>See appendix A for their derivation.

For simplicity the form of unsteady heat release is chosen to be an  $n - \tau$  model proportional to the velocity just upstream of the flame:

$$q'(x, t) = \beta u'(b^-, t - \tau) \delta(x - b) \quad (2.5)$$

Where  $\beta$  is the flame interaction index and the time delay ( $\tau$ ) is taken to be the fuel convection time from the injection until it is burned (Dowling and Stow, 2003).

## 2.3 The Eigenvalue Problem

Linearization is done around the mean flow parameters (zeroth order variables), therefore the first step is to solve for them. The second step is to seek for a solution of the fluctuating variables (first order).

### 2.3.1 Zeroth order (Mean Flow) variables

For the upstream mean variables:

- Set two of the three thermodynamic variables (pressure ( $\bar{p}_1$ ), temperature ( $\bar{T}_1$ ) and density ( $\bar{\rho}_1$ )).
- Solve for the third one using the ideal gas relationship ( $\bar{p} = \bar{\rho} R \bar{T}$ ).
- Set the mean velocity ( $\bar{u}_1$ ).
- Compute the speed of sound via the isentropic relationship ( $\bar{c}_1 = \sqrt{\gamma R \bar{T}_1}$ ).
- Compute the Mach number as  $M_1 = \bar{u}_1 / \bar{c}_1$ .

For the downstream variables, use the jump conditions for mean flow Eq. (2.2):

- Get the temperature from the other side of the duct ( $\bar{T}_2$ ) by setting a jump in temperature ( $\bar{T}_2 = \bar{T}_1 + \Delta T$ ).
- Compute the quadratic for the velocity<sup>2</sup>:

$$\bar{u}_2 = \frac{(\bar{u}_1^2 + R\bar{T}_1) - \sqrt{(\bar{u}_1^2 + R\bar{T}_1)^2 - 4\bar{u}_1^2 R\bar{T}_2}}{2\bar{u}_1} \quad (2.6)$$

---

<sup>2</sup>This equation is only valid for *low* Mach numbers. To keep the argument of the square root positive, it is required that:  $M_1 < \left( \sqrt{\bar{T}_2/\bar{T}_1} - \sqrt{\bar{T}_2/\bar{T}_1 - 1} \right) / \sqrt{\gamma}$  which implies that the temperature ratio puts a restriction on the mean flow.

If the mean heat release per unit area ( $\bar{q}$ ) is known instead of the jump in temperature, compute the quadratic from the following expression:

$$\bar{u}_2^2 \left( \bar{\rho}_1 \bar{u}_1 \left( \frac{1}{2} - \frac{\gamma}{\gamma-1} \right) \right) + \bar{u}_2 \left( \frac{\gamma}{\gamma-1} (\bar{p}_1 + \bar{\rho}_1 \bar{u}_1^2) \right) - \left( \frac{\gamma}{\gamma-1} \bar{p}_1 \bar{u}_1 + \frac{1}{2} \bar{\rho}_1 \bar{u}_1^3 + \bar{q} \right) = 0 \quad (2.7)$$

- Compute pressure as:

$$\bar{p}_2 = \bar{p}_1 - \bar{\rho}_1 \bar{u}_1 (\bar{u}_2 - \bar{u}_1) \quad (2.8)$$

- Compute density ( $\bar{\rho}_2$ ) using the ideal gas law, the speed of sound ( $\bar{c}_2$ ) using the isentropic relationship and the Mach number ( $M_2$ ) as for the upstream side.

The former analysis is similar to the one identified as subsonic Rayleigh flow in compressible flow theory ([Anderson, 2003](#)).

### 2.3.2 First order (fluctuations) variables

The linearized governing equations (2.3) are a system of coupled equations. To get the solutions, begin by rewriting them in matrix form using partial differential equations notation:

$$\begin{bmatrix} \rho' \\ u' \\ p' \end{bmatrix}_t + \begin{bmatrix} \bar{u} & \bar{\rho} & 0 \\ 0 & \bar{u} & 1/\bar{\rho} \\ 0 & \gamma\bar{p} & \bar{u} \end{bmatrix} \begin{bmatrix} \rho' \\ u' \\ p' \end{bmatrix}_x = \mathbf{0} \quad (2.9)$$

In simplified form:

$$\mathbf{U}_t + \mathbf{A}\mathbf{U}_x = \mathbf{0} \quad (2.10)$$

These compose a strictly hyperbolic system of equations ([Evans, 2010](#)), whose solutions (coming from the wave equation) are plane waves. Proceed by diagonalizing the real matrix A:

$$\mathbf{A} = \mathbf{S}\mathbf{\Lambda}\mathbf{S}^{-1} = \begin{bmatrix} 1 & 1/\bar{c}^2 & 1/\bar{c}^2 \\ 0 & 1/\bar{\rho}\bar{c} & -1/\bar{\rho}\bar{c} \\ 0 & 1 & 1 \end{bmatrix} \begin{bmatrix} \bar{u} & 0 & 0 \\ 0 & \bar{c} + \bar{u} & 0 \\ 0 & 0 & -(\bar{c} - \bar{u}) \end{bmatrix} \begin{bmatrix} 1 & 0 & -1/\bar{c}^2 \\ 0 & \bar{\rho}\bar{c}/2 & 1/2 \\ 0 & -\bar{\rho}\bar{c}/2 & 1/2 \end{bmatrix} \quad (2.11)$$

Substituting into the simplified form (eq. 2.10) yields:

$$\mathbf{U}_t + \mathbf{S}\mathbf{\Lambda}\mathbf{S}^{-1}\mathbf{U}_x = \mathbf{0} \quad (2.12)$$

Pre-multiply by  $S^{-1}$  to get:

$$S^{-1}\mathbf{U}_t + \Lambda S^{-1}\mathbf{U}_x = \mathbf{0} \quad (2.13)$$

Substitute using  $\mathbf{V} = S^{-1}\mathbf{U}$  to get a fully decoupled system:

$$\mathbf{V}_t + \Lambda\mathbf{V}_x = \mathbf{0} \quad (2.14a)$$

$$\begin{bmatrix} \mathcal{R} \\ \mathcal{U} \\ \mathcal{P} \end{bmatrix}_t + \begin{bmatrix} \bar{u} & 0 & 0 \\ 0 & \bar{c} + \bar{u} & 0 \\ 0 & 0 & -(\bar{c} - \bar{u}) \end{bmatrix} \begin{bmatrix} \mathcal{R} \\ \mathcal{U} \\ \mathcal{P} \end{bmatrix}_x = \mathbf{0} \quad (2.14b)$$

Note that the vector  $\mathbf{V}$  represents the Riemann invariants of the system. Now the system has become a set of three transport equations:

$$\mathcal{R}_t + \bar{u}\mathcal{R}_x = 0 \quad (2.15a)$$

$$\mathcal{U}_t + (\bar{c} + \bar{u})\mathcal{U}_x = 0 \quad (2.15b)$$

$$\mathcal{P}_t - (\bar{c} - \bar{u})\mathcal{P}_x = 0 \quad (2.15c)$$

With solutions:

$$\mathcal{R}(x, t) = \alpha \left( t - \frac{x}{\bar{u}} \right) \quad \text{Entropy wave} \quad (2.16a)$$

$$\mathcal{U}(x, t) = f \left( t - \frac{x}{\bar{c} + \bar{u}} \right) \quad \text{Forward traveling wave} \quad (2.16b)$$

$$\mathcal{P}(x, t) = g \left( t + \frac{x}{\bar{c} - \bar{u}} \right) \quad \text{Backward traveling wave} \quad (2.16c)$$

The solutions to the original variables are recovered using  $\mathbf{U} = S\mathbf{V}$ :

$$p'(x, t) = f \left( t - \frac{x}{\bar{c} + \bar{u}} \right) + g \left( t + \frac{x}{\bar{c} - \bar{u}} \right) \quad (2.17a)$$

$$u'(x, t) = \frac{1}{\rho\bar{c}} \left( f \left( t - \frac{x}{\bar{c} + \bar{u}} \right) - g \left( t + \frac{x}{\bar{c} - \bar{u}} \right) \right) \quad (2.17b)$$

$$\rho'(x, t) = \frac{1}{\bar{c}^2} \left( f \left( t - \frac{x}{\bar{c} + \bar{u}} \right) - g \left( t + \frac{x}{\bar{c} - \bar{u}} \right) \right) + \alpha \left( t - \frac{x}{\bar{u}} \right) \quad (2.17c)$$

The domain is split into two sections according to figure 2.1. The wave solutions are centered at  $x = b$ , and labeled with subscripts 1 if they are located upstream of the

flame and 2 if they are downstream. The pressure fluctuations become:

$$p'(x, t) = \begin{cases} f_1 \left( t - \frac{x-b}{\bar{c}_1 + \bar{u}_1} \right) + g_1 \left( t + \frac{x-b}{\bar{c}_1 - \bar{u}_1} \right) & \text{if } x < b \\ f_2 \left( t - \frac{x-b}{\bar{c}_2 + \bar{u}_2} \right) + g_2 \left( t + \frac{x-b}{\bar{c}_2 - \bar{u}_2} \right) & \text{if } x > b \end{cases} \quad (2.18)$$

The velocity fluctuations:

$$u'(x, t) = \begin{cases} \frac{1}{\bar{\rho}_1 \bar{c}_1} \left( f_1 \left( t - \frac{x-b}{\bar{c}_1 + \bar{u}_1} \right) - g_1 \left( t + \frac{x-b}{\bar{c}_1 - \bar{u}_1} \right) \right) & \text{if } x < b \\ \frac{1}{\bar{\rho}_2 \bar{c}_2} \left( f_2 \left( t - \frac{x-b}{\bar{c}_2 + \bar{u}_2} \right) - g_2 \left( t + \frac{x-b}{\bar{c}_2 - \bar{u}_2} \right) \right) & \text{if } x > b \end{cases} \quad (2.19)$$

The density fluctuations:

$$\rho'(x, t) = \begin{cases} \frac{1}{\bar{c}_1^2} \left( f_1 \left( t - \frac{x-b}{\bar{c}_1 + \bar{u}_1} \right) + g_1 \left( t + \frac{x-b}{\bar{c}_1 - \bar{u}_1} \right) + \alpha_1 \left( t - \frac{x-b}{\bar{u}_1} \right) \right) & \text{if } x < b \\ \frac{1}{\bar{c}_2^2} \left( f_2 \left( t - \frac{x-b}{\bar{c}_2 + \bar{u}_2} \right) + g_2 \left( t + \frac{x-b}{\bar{c}_2 - \bar{u}_2} \right) + \alpha_2 \left( t - \frac{x-b}{\bar{u}_2} \right) \right) & \text{if } x > b \end{cases} \quad (2.20)$$

Notice that for simplicity in further calculations the entropy waves are multiplied<sup>3</sup> by  $1/\bar{c}^2$ . Given that there are 3 governing equations, a set of 3 boundary conditions must be provided to solve the system. The first two boundary conditions relate the acoustic waves imposing Dirichlet, Neumann or Robin boundary conditions to the fluctuations at  $x = 0$  and  $x = L$ . This assumption is valid considering that the entropy waves convect away from the flame, and they are not reflected as acoustic fluctuations, which would be the case of choked outlets as a nozzle (See for example [Duran and Moreau \(2013\)](#); [Marble and Candel \(1977\)](#)). The boundary condition at  $x = 0$  gives:

$$f_1(t) = R_u g_1(t - \tau_u) \quad (2.21)$$

$$\tau_u = \frac{2b\bar{c}_1}{\bar{c}_1^2 - \bar{u}_1^2} \quad (2.22)$$

The boundary condition at  $x = L$ :

$$g_2(t) = R_d f_2(t - \tau_d) \quad (2.23)$$

$$\tau_d = \frac{2(L-b)\bar{c}_2}{\bar{c}_2^2 - \bar{u}_2^2} \quad (2.24)$$

---

<sup>3</sup>In the frequency space the amplitude of these waves ( $\mathcal{A}$ ) will compensate for this factor. It is normal to see the entropy waves accompanied by a  $\bar{\rho}/c_p$  factor (for example [Morgans and Annaswamy \(2008\)](#)) but this will have the same effect as our current choice.

The third boundary condition sets the entropy fluctuations at the inlet:

$$\alpha_1(0, t) = \alpha_1 \left( t + \frac{b}{\bar{u}_1} \right) = a_0 \left( t + \frac{b}{\bar{u}_1} \right) \quad (2.25)$$

Substitute the boundary conditions into the linearized jump conditions (eq. 2.4) at  $x = b$ . Multiply the continuity jump condition by  $\bar{c}_1$ , and divide the energy jump condition by  $\bar{c}_1$ . Laplace transform using  $g = Ge^{st}$  and rearrange to get to the following transfer matrix:

$$\mathbf{L}\hat{\mathbf{q}} = \mathbf{X} \quad (2.26)$$

$$\begin{bmatrix} L_{11} & L_{12} & L_{13} \\ L_{21} & L_{22} & L_{23} \\ L_{31} & L_{32} & L_{33} \end{bmatrix} \begin{bmatrix} \mathcal{A}_2 \\ G_1 \\ F_2 \end{bmatrix} = \begin{bmatrix} M_1 \\ M_1^2 \\ \frac{1}{2}M_1^3 \end{bmatrix} A_0(s)$$

Where the matrix L is composed of two matrices:

$$\mathbf{L} = \mathbf{N} + \mathbf{Q} \quad (2.27)$$

$$\mathbf{N} = \begin{bmatrix} N_{11} & N_{12} & N_{13} \\ N_{21} & N_{22} & N_{23} \\ N_{31} & N_{32} & N_{33} \end{bmatrix} \quad \mathbf{Q} = \begin{bmatrix} 0 & 0 & 0 \\ 0 & 0 & 0 \\ 0 & Q_{32} & 0 \end{bmatrix}$$

The components of matrix N are:

$$N_{11} = \frac{\bar{c}_1}{\bar{c}_2} M_2 \quad (2.28a)$$

$$N_{12} = (1 - M_1) - R_u e^{-s\tau_u} (1 + M_1) \quad (2.28b)$$

$$N_{13} = \frac{\bar{c}_1}{\bar{c}_2} \left( (1 + M_2) + R_d e^{-s\tau_d} (M_2 - 1) \right) \quad (2.28c)$$

$$N_{21} = M_2^2 \quad (2.28d)$$

$$N_{22} = -(1 - M_1)^2 - R_u e^{-s\tau_u} (1 + M_1)^2 \quad (2.28e)$$

$$N_{23} = (1 + M_2)^2 + R_d e^{-s\tau_d} (1 - M_2)^2 \quad (2.28f)$$

$$N_{31} = \frac{1}{2} M_2^3 \frac{\bar{c}_2}{\bar{c}_1} \quad (2.28g)$$



$$N_{32} = \frac{1 - \gamma M_1}{\gamma - 1} + \frac{M_1^2}{2} (3 - M_1) - R_u e^{-s\tau_u} \left( \frac{1 + \gamma M_1}{\gamma - 1} + \frac{M_1^2}{2} (3 + M_1) \right) \quad (2.28h)$$

$$N_{33} = \frac{\bar{c}_2}{\bar{c}_1} \left( \frac{1 + \gamma M_2}{\gamma - 1} + \frac{M_2^2}{2} (3 + M_2) + R_d e^{-s\tau_d} \left( \frac{-1 + \gamma M_2}{\gamma - 1} - \frac{M_2^2}{2} (3 - M_2) \right) \right) \quad (2.28i)$$


The matrix Q is a 3 by 3 zeros matrix with the only non zero entry being:


$$Q_{32} = \frac{\beta}{\rho_1 \bar{c}_1^2} e^{-s\tau} (1 - R_u e^{-s\tau_u}) \quad (2.29)$$

There are three possible ways to seek a solution to the problem: 

- Set  $A_0$  to zero. This is the most common approach considering that this are generated by the flame, since there is heat release at the inlet it is natural for this term to be zero. In this case the problem becomes a nonlinear eigenvalue problem for  $s$ . Eigenvalues ( $s_j$ ) are computed by setting the determinant of matrix L to 0. Once the eigenvalues are known, the eigenvectors  $\hat{\mathbf{q}}_j$  can be computed. Using those, the eigenfunctions (mode shapes) can be recovered.
- $A_0$  is a function of  $G_1$ ,  $F_2$  and or  $\mathcal{A}_2$ . Then the system of equations can be rearranged to form another eigenvalue problem as before. 
- $A_0$  is a different function. Then, the equations are forced, the eigenvalues are still computed in the same way as before (they will represent the poles of the system), but there is only one vector of solutions, that will define the amplitudes that satisfy the system, that is: 

$$\hat{\mathbf{q}} = \hat{\mathbf{q}}_j + \hat{\mathbf{q}}_{A_0} \quad (2.30)$$

The first vector ( $\hat{\mathbf{q}}_j$ ) being the one that satisfies the homogeneous problem, while the other ( $\hat{\mathbf{q}}_{A_0}$ ) is satisfies the particular solution (forcing). If all the modes are damped the solution will be dominated by the latter. 

Mode-shapes for the first unstable eigenvalue  $s_1 = (0.0116 + 2.0980i) \cdot 10^3 \text{ s}^{-1}$  of a network characterized by the values in table 2.1 can be seen in figures 2.2, 2.3 and 2.4. The resonant frequency of the system is 333.9Hz. Note that Dirichlet boundary conditions were set for  $p'$  (fig. 2.2), velocity fluctuations (fig. 2.3) do not display a Neumann boundary condition as would be expected from a case with zero mean flow. Also observe that the density fluctuations (fig. 2.4) are proportional to the pressure fluctuations upstream of the flame, and that they display the same boundary condition at that location; downstream due to the presence of entropy waves this is not true anymore. 

Description	Value
Constants	
$\gamma$	1.4
R (dry air)	287.1 Jkg <sup>-1</sup> K <sup>-1</sup>
Geometry	
Length	1m
Boundary conditions	
Inlet boundary: $R_u$ (Open end)	-1
Outlet boundary: $R_d$ (Open end)	-1
Inlet entropy waves: $A_0$	0
Flow conditions	
Inlet pressure ( $\bar{p}_1$ )	101,300Pa
Inlet temperature ( $\bar{T}_1$ )	700K
Inlet velocity ( $\bar{u}_1$ )	60ms <sup>-1</sup>
Jump in temperature ( $\Delta\bar{T}$ )	1300K
Unsteady Heat Release	
Flame location ( $b$ )	0.3m
Flame interaction index ( $\beta$ )	360,000ms <sup>2</sup> kg <sup>-1</sup>
Time delay ( $\tau$ )	0.001s

Table 2.1 Geometry and flow conditions

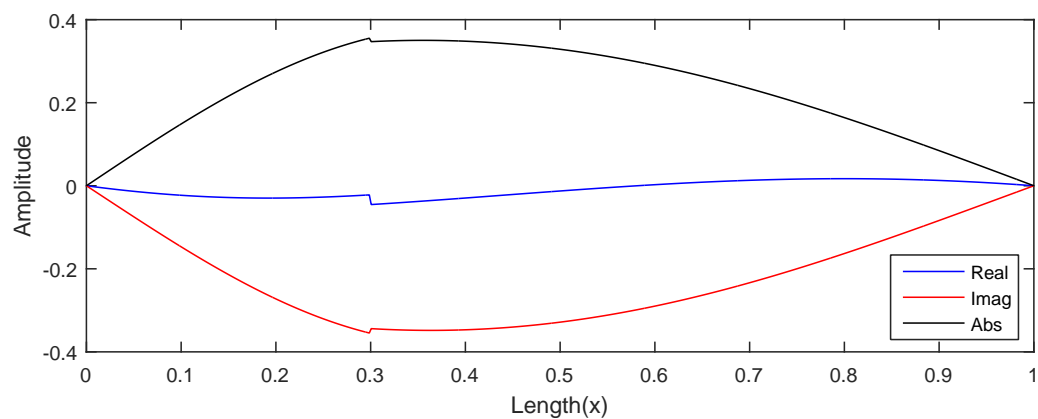


Fig. 2.2 Direct pressure mode shape

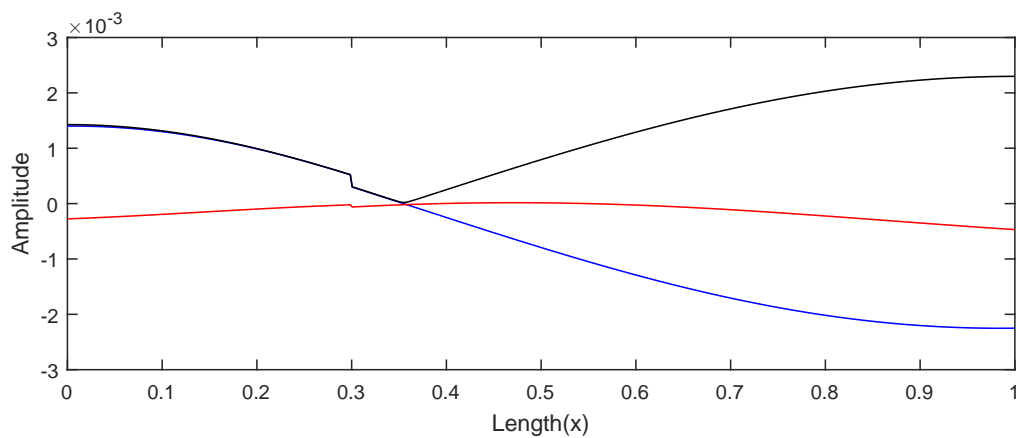


Fig. 2.3 Direct velocity mode shape

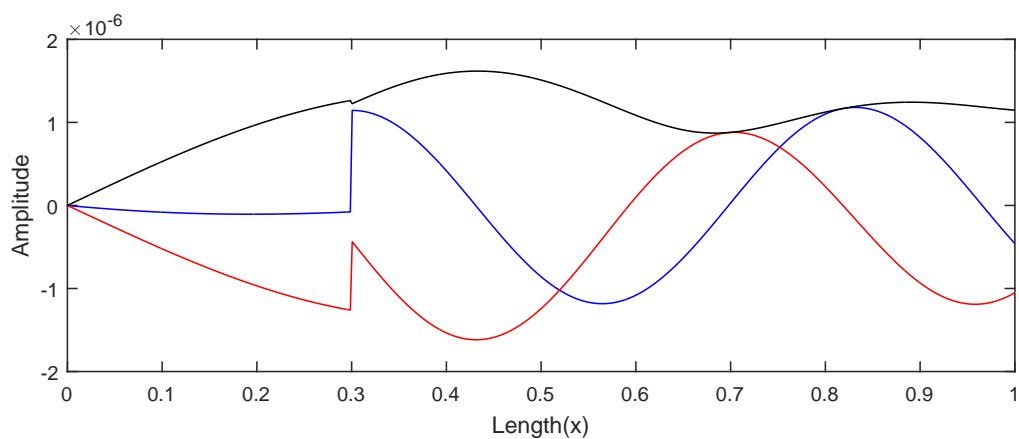


Fig. 2.4 Direct density mode shape

# Chapter 3

## Sensitivity analysis via the Discrete approach

### 3.1 Eigenvalue drift

Matrix  $L$  from Eq. (2.26) produces a nonlinear eigenvalue problem for  $s$ . For this case, Juniper et al. (2014) derived the following eigenvalue drift formula<sup>1</sup>:

$$\delta s = -\frac{(\hat{\mathbf{q}}^\dagger)^H \delta L(s_j, p_0) \hat{\mathbf{q}}}{(\hat{\mathbf{q}}^\dagger)^H \left. \frac{\partial L(s_j, p)}{\partial s_j} \right|_{s_j, p_0} \hat{\mathbf{q}}} \quad (3.1)$$

To apply this formula to the network model, the matrix  $\partial L / \partial s_j$  needs to be computed, which is done analytically as:

$$\frac{\partial L}{\partial s_j} = \frac{\partial N}{\partial s_j} + \frac{\partial Q}{\partial s_j} \quad (3.2)$$

where

$$\frac{\partial N}{\partial s_j} = \begin{bmatrix} N'_{11} & N'_{12} & N'_{13} \\ N'_{21} & N'_{22} & N'_{23} \\ N'_{31} & N'_{32} & N'_{33} \end{bmatrix} \quad (3.3)$$

---

<sup>1</sup>Derived also in appendix B.

$$N'_{11} = 0 \quad (3.4a)$$

$$N'_{12} = \tau_u R_u e^{-s_j \tau_u} (1 + M_1) \quad (3.4b)$$

$$N'_{13} = \frac{\bar{c}_1}{\bar{c}_2} \left( -\tau_d R_d e^{-s_j \tau_d} (M_2 - 1) \right) \quad (3.4c)$$

$$N'_{21} = 0 \quad (3.4d)$$

$$N'_{22} = \tau_u R_u e^{-s_j \tau_u} (1 + M_1)^2 \quad (3.4e)$$

$$N'_{23} = -\tau_d R_d e^{-s_j \tau_d} (1 - M_2)^2 \quad (3.4f)$$

$$N'_{31} = 0 \quad (3.4g)$$


$$N'_{32} = \tau_u R_u e^{-s_j \tau_u} \left( \frac{1 + \gamma M_1}{\gamma - 1} + \frac{M_1^2}{2} (3 + M_1) \right) \quad (3.4h)$$

$$N'_{33} = \frac{\bar{c}_2}{\bar{c}_1} \left( -\tau_d R_d e^{-s_j \tau_d} \left( \frac{-1 + \gamma M_2}{\gamma - 1} - \frac{M_2^2}{2} (3 - M_2) \right) \right) \quad (3.4i)$$

The matrix  $\partial Q / \partial s_j$  has only one non zero element:

$$\frac{\partial Q_{32}}{\partial s_j} = \frac{\beta}{\bar{\rho}_1 \bar{c}_1^2} e^{-s \tau} \left( R_u e^{-s_j \tau_u} (\tau_u + \tau) - \tau \right) \quad (3.5)$$

## 3.2 Base state sensitivity

As stated in section 1.5,  base state sensitivity gives the change of the eigenvalue with respect to any change in a parameter of the system. For this particular case it is worth looking at the following base state values: reflection coefficients:  $R_u$  and  $R_d$ , geometric time delays:  $\tau_u$  and  $\tau_d$  and unsteady heat release parameters:  $\tau$  and  $\beta$ . Then a generic change in the matrix  $L$  is given by:

$$\delta L = \frac{\partial L}{\partial R_u} \delta R_u + \frac{\partial L}{\partial R_d} \delta R_d + \frac{\partial L}{\partial \tau_u} \delta \tau_u + \frac{\partial L}{\partial \tau_d} \delta \tau_d + \frac{\partial L}{\partial \tau} \delta \tau + \frac{\partial L}{\partial \beta} \delta \beta \quad (3.6)$$

Where the base state sensitivity matrices are:

$$\frac{\partial L}{\partial R_u} = \begin{bmatrix} 0 & -e^{-s_j \tau_u} (1 + M_1) & 0 \\ 0 & -e^{-s_j \tau_u} (1 + M_1)^2 & 0 \\ 0 & -e^{-s_j \tau_u} \left( \frac{1 + \gamma M_1}{\gamma - 1} + \frac{M_1^2}{2} (3 + M_1) + \frac{\beta}{\bar{\rho}_1 \bar{c}_1^2} e^{-s_j \tau} \right) & 0 \end{bmatrix} \quad (3.7a)$$

$$\frac{\partial \mathbf{L}}{\partial R_d} = \begin{bmatrix} 0 & 0 & \frac{\bar{c}_1}{\bar{c}_2} e^{-s_j \tau_d} (M_2 - 1) \\ 0 & 0 & e^{-s_j \tau_d} (1 - M_2)^2 \\ 0 & 0 & \frac{\bar{c}_2}{\bar{c}_1} e^{-s_j \tau_d} \left( \frac{-1 + \gamma M_2}{\gamma - 1} - \frac{M_2^2}{2} (3 - M_2) \right) \end{bmatrix} \quad (3.7b)$$

$$\frac{\partial \mathbf{L}}{\partial \tau_u} = \begin{bmatrix} 0 & s_j R_u e^{-s_j \tau_u} (1 + M_1) & 0 \\ 0 & s_j R_u e^{-s_j \tau_u} (1 + M_1)^2 & 0 \\ 0 & s_j R_u e^{-s_j \tau_u} \left( \frac{1 + \gamma M_1}{\gamma - 1} + \frac{M_1^2}{2} (3 + M_1) + \frac{\beta}{\rho_1 \bar{c}_1^2} e^{-s_j \tau} \right) & 0 \end{bmatrix} \quad (3.7c)$$

$$\frac{\partial \mathbf{L}}{\partial \tau_d} = \begin{bmatrix} 0 & 0 & -\frac{\bar{c}_1}{\bar{c}_2} s_j R_d e^{-s_j \tau_d} (M_2 - 1) \\ 0 & 0 & -s_j R_d e^{-s_j \tau_d} (1 - M_2)^2 \\ 0 & 0 & -\frac{\bar{c}_2}{\bar{c}_1} s_j R_d e^{-s_j \tau_d} \left( \frac{-1 + \gamma M_2}{\gamma - 1} - \frac{M_2^2}{2} (3 - M_2) \right) \end{bmatrix} \quad (3.7d)$$

$$\frac{\partial \mathbf{L}}{\partial \tau} = \begin{bmatrix} 0 & 0 & 0 \\ 0 & 0 & 0 \\ 0 & -s_j \frac{\beta}{\rho_1 \bar{c}_1^2} e^{-s_j \tau} (1 - R_u e^{-s_j \tau_u}) & 0 \end{bmatrix} \quad (3.7e)$$

$$\frac{\partial \mathbf{L}}{\partial \beta} = \begin{bmatrix} 0 & 0 & 0 \\ 0 & 0 & 0 \\ 0 & \frac{e^{-s_j \tau}}{\rho_1 \bar{c}_1^2} (1 - R_u e^{-s_j \tau_u}) & 0 \end{bmatrix} \quad (3.7f)$$

For the same case described in the last part of section 2.3.2 the base state sensitivities are shown in table 3.1. The results provide a complex number, where the real part provides the sensitivity of the growth rate and the imaginary part the sensitivity of the frequency. It should be clear that the system is very sensitive to changes in the time delays. If the system is to be stabilized, only the geometric time delays ( $\tau_u$  and  $\tau_d$ ) can be changed by re-positioning the flame. If the reflection coefficients are allowed to get some damping for example  $R_d = -0.95$  the system will become more stable. The flame interaction index is the least sensitive of the base state variables.

Base state Variable	Value
$R_u$	$(-2.1918 + 1.4662i) \cdot 10^2 \text{ s}^{-1}$
$R_d$	$(-3.5152 - 1.1381i) \cdot 10^2 \text{ s}^{-1}$
$\tau_u$	$(-3.1017 - 4.5814i) \cdot 10^5 \text{ s}^{-1}$
$\tau_d$	$(+2.3469 - 7.3882i) \cdot 10^5 \text{ s}^{-1}$
$\tau$	$(-0.3768 - 3.7229i) \cdot 10^5 \text{ s}^{-1}$
$\beta$	$(+4.9317 - 0.4715i) \cdot 10^{-4} \text{ s}^{-1}$

Table 3.1 Base state sensitivities for the first unstable eigenvalue of the network characterized by table 2.1 ( $s_1 = (0.0116 + 2.0980i) \cdot 10^3 \text{ s}^{-1}$ )

### 3.2.1 Taylor Tests

The eigenvalue drift can be computed using a finite difference method ( $\delta_{FD}$ ), or using the eigenvalue drift formula from eq. (3.1) ( $\delta_{AD}$ ). The main difference between both methods, being that the first is computationally more expensive but it also includes terms of order 2, 3 and beyond. Since both ways of computing the eigenvalue drift are the same to first order, the difference between them ( $\delta_{sFD} - \delta_{sAD}$ ), should increase linearly with the square of the size of the perturbation ( $\epsilon^2$ ) for a small value of  $\epsilon$ . This procedure is called the Taylor Test (Magri, 2015). Taylor test plots for every base state variable are available in appendix C.

## 3.3 Structural Sensitivity

To compute the structural sensitivity of the system, one needs to consider the effects of intrinsic feedback, which is done by introducing small perturbations into the governing equations, for example: mass injection into the continuity equation ( $\mathcal{M}$ ), drag force into the momentum equation ( $\mathcal{F}$ ) or heat addition to the energy equation ( $\mathcal{Q}$ ). In general the governing equations become:

$$\frac{\partial \rho'}{\partial t} + \bar{u} \frac{\partial \rho'}{\partial x} + \bar{\rho} \frac{\partial u'}{\partial x} = \mathcal{M} \quad (3.8a)$$

$$\bar{\rho} \frac{\partial u'}{\partial t} + \bar{\rho} \bar{u} \frac{\partial u'}{\partial x} + \frac{\partial p'}{\partial x} = \mathcal{F} \quad (3.8b)$$

$$\frac{\partial p'}{\partial t} + \bar{u} \frac{\partial p'}{\partial x} + \gamma \bar{p} \frac{\partial u'}{\partial x} = \mathcal{Q} + \bar{c}^2 \mathcal{M} \quad (3.8c)$$

The term  $\bar{c}^2 \mathcal{M}$  in the energy equation (Eq. 3.8c) arises due to the use of the continuity equation to get the energy equation in terms of pressure as shown in appendix D. For simplicity, consider the next expression:

$$\mathcal{E} = \mathcal{Q} + \bar{c}^2 \mathcal{M} \quad (3.9)$$

The quantities  $\mathcal{M}$ ,  $\mathcal{F}$ ,  $\mathcal{E}$  are chosen to be functions of  $p'$ ,  $u'$  and  $\rho'$ :

$$\mathcal{M} = \mathcal{M}_p p' + \mathcal{M}_u u' + \mathcal{M}_r \rho' \quad (3.10a)$$

$$\mathcal{F} = \mathcal{F}_p p' + \mathcal{F}_u u' + \mathcal{F}_r \rho' \quad (3.10b)$$

$$\mathcal{E} = \mathcal{E}_p p' + \mathcal{E}_u u' + \mathcal{E}_r \rho' \quad (3.10c)$$

The main assumption is that **these small perturbations will not produce any change to the mean flow parameters**. To compute the eigenvalue drift (Eq. 3.1) the matrix of perturbations ( $\delta L$ ) is required. Hence, after adding these perturbations the task is to rearrange the expressions to obtain the original matrix from the eigenvalue problem (L) plus some extra terms ( $\delta L$ ) which are a function of the perturbations introduced:

$$L \rightarrow L + \delta L(\mathcal{M}, \mathcal{F}, \mathcal{E}) \quad (3.11)$$

The interest is to know how these perturbations affect the eigenvalue at different positions along the duct, therefore the perturbations must be point functions (i.e Dirac deltas):


$$\frac{\partial \rho'}{\partial t} + \bar{u} \frac{\partial \rho'}{\partial x} + \bar{\rho} \frac{\partial u'}{\partial x} = \mathcal{M} \delta(x - x_0) \quad (3.12a)$$

$$\bar{\rho} \frac{\partial u'}{\partial t} + \bar{\rho} \bar{u} \frac{\partial u'}{\partial x} + \frac{\partial p'}{\partial x} = \mathcal{F} \delta(x - x_0) \quad (3.12b)$$

$$\frac{\partial p'}{\partial t} + \bar{u} \frac{\partial p'}{\partial x} + \gamma \bar{p} \frac{\partial u'}{\partial x} = \mathcal{E} \delta(x - x_0) \quad (3.12c)$$

There are two major implications of using a Dirac delta as part of the model (the second one follows from the first):

### 1. Splitting the domain:

To keep the model as  simple traveling waves, the domain needs to be split and to keep the perturbation it needs to be introduced as a jump in the system (similar to the flame). Since the equations are defined upstream and downstream of the flame this means that the domain will be split into four parts. These are delimited by the inlet, the position of the upstream perturbation at  $x = x_0 = a$ , the position of the flame at  $x = b$ , the position of the downstream perturbation at  $x = x_0 = c$  and the outlet, as shown in figure 3.1.

### 2. Derive two new sets of jump conditions:

A detailed explanation of the derivation of the jump conditions can be found in appendix E. The jump conditions upstream of the flame ( $x = a$ ) are:

$$\bar{u}_1(\rho'_{ii} - \rho'_i) + \bar{\rho}_1(u'_{ii} - u'_i) = \mathcal{M}_{p_1} p'_i + \mathcal{M}_{u_1} u'_i + \mathcal{M}_{r_1} \rho'_i \quad (3.13a)$$

$$\bar{\rho}_1 \bar{u}_1(u'_{ii} - u'_i) + (p'_{ii} - p'_i) = \mathcal{F}_{p_1} p'_i + \mathcal{F}_{u_1} u'_i + \mathcal{F}_{r_1} \rho'_i \quad (3.13b)$$

$$\bar{u}_1(p'_{ii} - p'_i) + \gamma \bar{p}_1(u'_{ii} - u'_i) = \mathcal{E}_{p_1} p'_i + \mathcal{E}_{u_1} u'_i + \mathcal{E}_{r_1} \rho'_i \quad (3.13c)$$

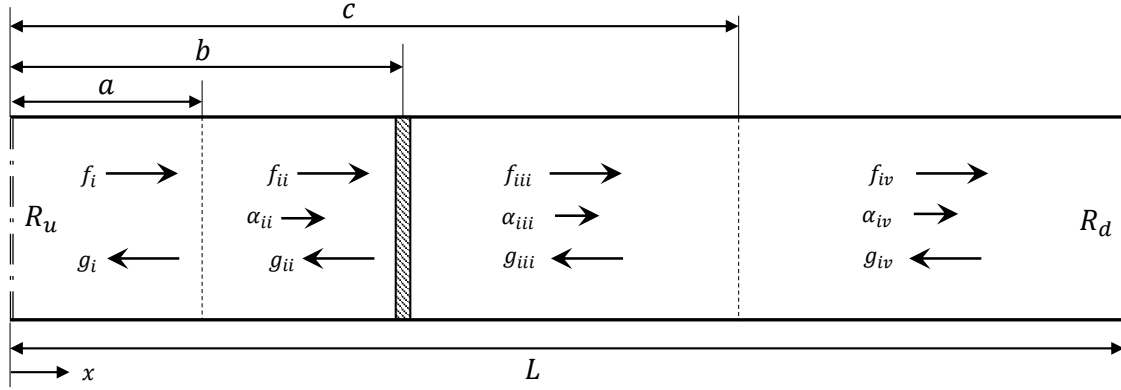


Fig. 3.1 Network model split into 4 sections due to the presence of intrinsic feedback at points  $x = a$  and  $x = c$

The jump conditions downstream of the flame ( $x = c$ ) are:

$$\bar{u}_2(\rho'_{iv} - \rho'_{iii}) + \bar{p}_2(u'_{iv} - u'_{iii}) = \mathcal{M}_{p_2} p'_{iv} + \mathcal{M}_{u_2} u'_{iv} + \mathcal{M}_{r_2} \rho'_{iv} \quad (3.14a)$$

$$\bar{p}_2 \bar{u}_2 (u'_{iv} - u'_{iv}) + (p'_{iv} - p'_{iii}) = \mathcal{F}_{p_2} p'_{iv} + \mathcal{F}_{u_2} u'_{iv} + \mathcal{F}_{r_2} \rho'_{iv} \quad (3.14b)$$

$$\bar{u}_2 (p'_{iv} - p'_{iii}) + \gamma \bar{p}_2 (u'_{iv} - u'_{iii}) = \mathcal{E}_{p_2} p'_{iv} + \mathcal{E}_{u_2} u'_{iv} + \mathcal{E}_{r_2} \rho'_{iv} \quad (3.14c)$$

After adding a perturbation to the governing equations the wave forms will change from their original state to a perturbed state, that is:

$$(f_i = f_1) \rightarrow (f_1 + \delta f_1 = f_{ii}) \quad (f_{iv} = f_2) \rightarrow (f_2 + \delta f_2 = f_{iii}) \quad (3.15a)$$

$$(g_i = g_1) \rightarrow (g_1 + \delta g_1 = g_{ii}) \quad (g_{iv} = g_2) \rightarrow (g_2 + \delta g_2 = g_{iii}) \quad (3.15b)$$

$$(\alpha_i = \alpha_1) \rightarrow (\alpha_1 + \delta \alpha_1 = \alpha_{ii}) \quad (\alpha_{iv} = \alpha_2) \rightarrow (\alpha_2 + \delta \alpha_2 = \alpha_{iii}) \quad (3.15c)$$

From the previous analysis it must be clear that in order to recover the matrix  $L + \delta L$ , the first task is to obtain expressions for the waves that define regions  $ii$  and  $iii$  (perturbed waves) in terms of the waves from regions  $i$  and  $iv$  (unperturbed waves); thereafter, substitute them into the jump conditions at  $x = b$  (Eq. 2.4). To obtain these expressions, put the wave form solutions (Eq. 2.17) of the variables  $p'$ ,  $\rho'$  and  $u'$  into the jump conditions at  $x = a$  and  $x = c$  (Eqs. 3.13 and 3.14), multiply the continuity equation by  $\bar{c}$  and divide the energy equation by  $\bar{c}$ , finally, solve both  $3 \times 3$  linear systems. The full perturbed wave-form solutions derived from these systems are presented in appendix F. For discussion only two of the solutions (one acoustic and one entropic) are presented next, since they have some general characteristics applicable to all waves of their types.

**Perturbed upstream forward traveling wave:**

$$\begin{aligned}
f_{ii}(t) = & f_1(t) + \frac{1}{2(M_1 + 1)} \left( \mathcal{M}_{p1} \bar{c}_1 (f_1(t) + g_1(t - \tau_a)) \cdots \right. \\
& + \frac{\mathcal{M}_{u1}}{\bar{\rho}_1} (f_1(t) - g_1(t - \tau_a)) + \frac{\mathcal{M}_{r1}}{\bar{c}_1} (f_1(t) + g_1(t - \tau_a) + \alpha_1(t + \tau_a)) \cdots \\
& + \mathcal{F}_{p1} (f_1(t) + g_1(t - \tau_a)) + \frac{\mathcal{F}_{u1}}{\bar{\rho}_1 \bar{c}_1} (f_1(t) - g_1(t - \tau_a)) \cdots \\
& + \frac{\mathcal{F}_{r1}}{\bar{c}_1^2} (f_1(t) + g_1(t - \tau_a) + \alpha_1(t + \tau_a)) + \frac{\mathcal{Q}_{p1}}{\bar{c}_1} (f_1(t) + g_1(t - \tau_a)) \cdots \\
& \left. + \frac{\mathcal{Q}_{u1}}{\bar{\rho}_1 \bar{c}_1^2} (f_1(t) - g_1(t - \tau_a)) + \frac{\mathcal{Q}_{r1}}{\bar{c}_1^3} (f_1(t) + g_1(t - \tau_a) + \alpha_1(t + \tau_a)) \right) \quad (3.16)
\end{aligned}$$

Acoustic waves are affected by mass addition, momentum addition, and energy addition; for a perturbation of the same magnitude, mass addition is likely to have the biggest effect, and heat addition the least. In the low Mach number limit the perturbed coefficient will converge to 1/2.

**Perturbed downstream entropy wave:**

$$\begin{aligned}
\alpha_{iii}(t) = & \alpha_2(t) - \frac{1}{M_2} \left( \frac{\mathcal{Q}_{p2}}{\bar{c}_2} (f_2(t + \tau_\gamma) + g_2(t + \tau_c + \tau_\gamma)) \cdots \right. \\
& + \frac{\mathcal{Q}_{u2}}{\bar{\rho}_2 \bar{c}_2^2} (f_2(t + \tau_\gamma) - g_2(t + \tau_c + \tau_\gamma)) \cdots \\
& \left. + \frac{\mathcal{Q}_{r2}}{\bar{c}_2^3} (f_2(t + \tau_\gamma) + g_2(t + \tau_c + \tau_\gamma) + \alpha_2(t)) \right) \quad (3.17)
\end{aligned}$$

Entropy waves are only affected by energy addition, which makes sense considering that entropy waves are convected hot spots. To add up to the former statement [Yu et al. \(1991\)](#) look at how the convected modes follow closely the heat release of the system, supporting that heat addition is likely to modify the amplitude of entropy waves. Note that on the low Mach number limit, the amplitude of the entropy wave tends to infinity. [Dowling and Stow \(2003\)](#) discuss the consequences of obtaining the zero mean flow equations from the those considering mean flow. Also in appendix [F](#) it is explained how the the system is taken into the frequency domain by using the Laplace transform  $g = Ge^{st}$  and then substituting into the jump conditions (Eq. [2.4](#)) of the original problem, resulting in the perturbed problem:

$$(L + \delta L) \hat{\mathbf{q}} = \mathbf{X} + \delta \mathbf{X} \quad (3.18)$$

To get the structural sensitivity plots, the eigenvalue drift from Eq. (3.1) needs to be computed along the duct at various positions that range from 0 to  $L$ . The frequency domain equations of appendix F are useful to compute the matrix  $\delta L$  at those positions. To achieve this, a perturbation proportional to  $\rho'$  or  $p'$  in the continuity, momentum or energy equations is chosen, and the rest of them are set to zero. (If the eigenvalue drift is computed before the flame, perturbations downstream of the flame are set to zero and vice versa). Plots (3.2 to 3.10) show the structural sensitivities of the system for the first unstable eigenvalue, where the real part shows the change in the growth rate, while the imaginary part shows the change in the frequency caused by the introduction of the small feedback mechanism.

Some feedback mechanisms already discussed by Juniper (2015); Magri and Juniper (2013b) are worth mentioning. The velocity device in the momentum equation (fig. 3.6) shows that the growth rate is always positive, with bigger amplitudes towards the inlet or outlet. Therefore, if a force is exerted in the opposite direction, like by positioning a drag mesh at those locations, it is likely to stabilize the system. On the other hand, the pressure device in the continuity equation (fig. 3.2) is useful to show which is the best position to locate Helmholtz resonators in thermoacoustic systems.

There are two ways in which the structural sensitivity can be tested. From one side using a finite difference method, which depends on the same matrix  $\delta L$  and computes the eigenvalues of the perturbed problem to then subtract them from the unperturbed problem, thus giving a more accurate prediction at a higher computational cost. Or else the Taylor tests, which are available in appendix G.

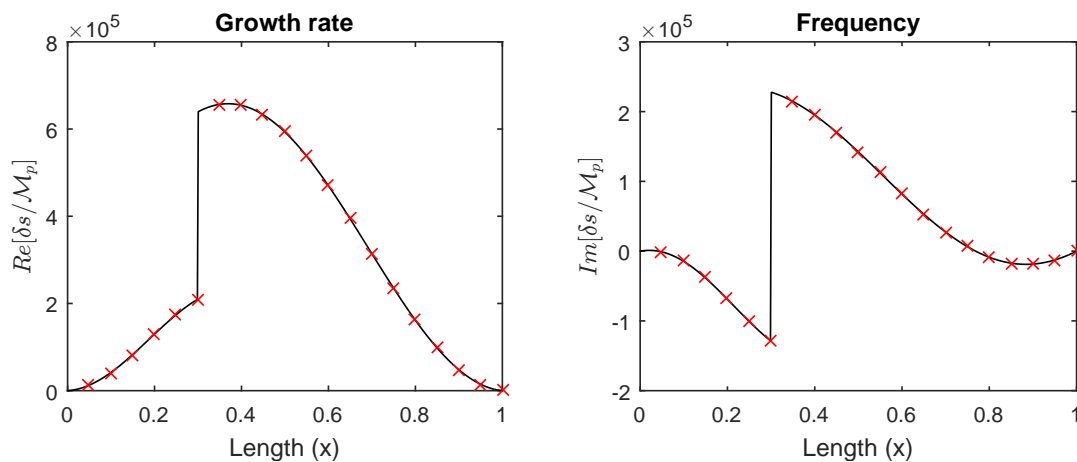


Fig. 3.2 Structural sensitivity - Continuity Equation - Pressure device. — represents the sensitivity using the eigenvalue drift form  $\rho'$  X represents sensitivities at certain points using a finite difference method.

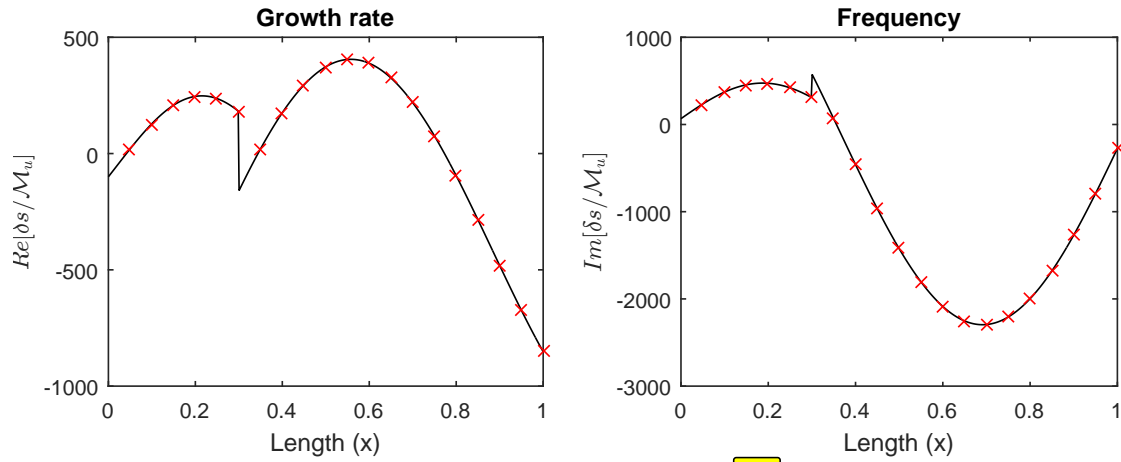



Fig. 3.3 Structural sensitivity - Continuity Equation -  velocity device. — represents the sensitivity using the eigenvalue drift formula. X represents sensitivities at certain points using a finite difference method.

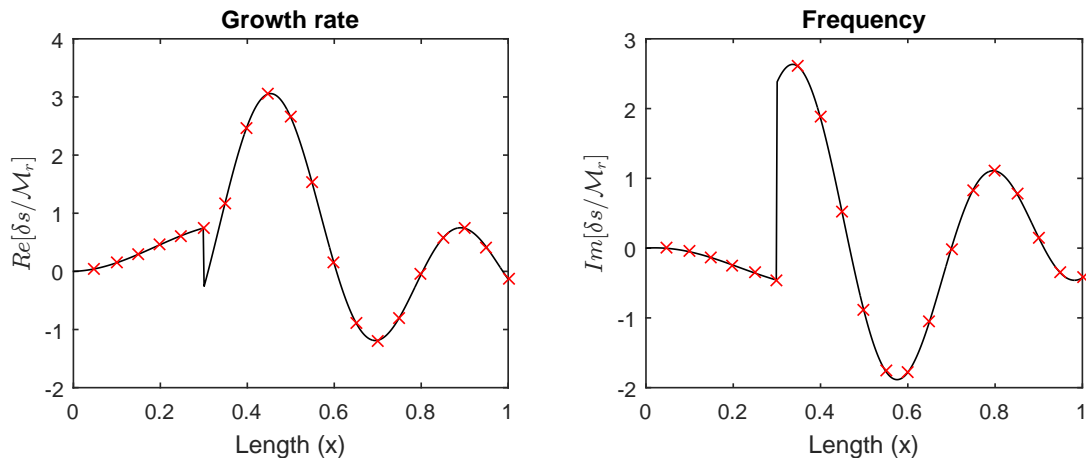


Fig. 3.4 Structural sensitivity - Continuity Equation - Density device. — represents the sensitivity using the eigenvalue drift formula. X represents sensitivities at certain points using a finite difference method.

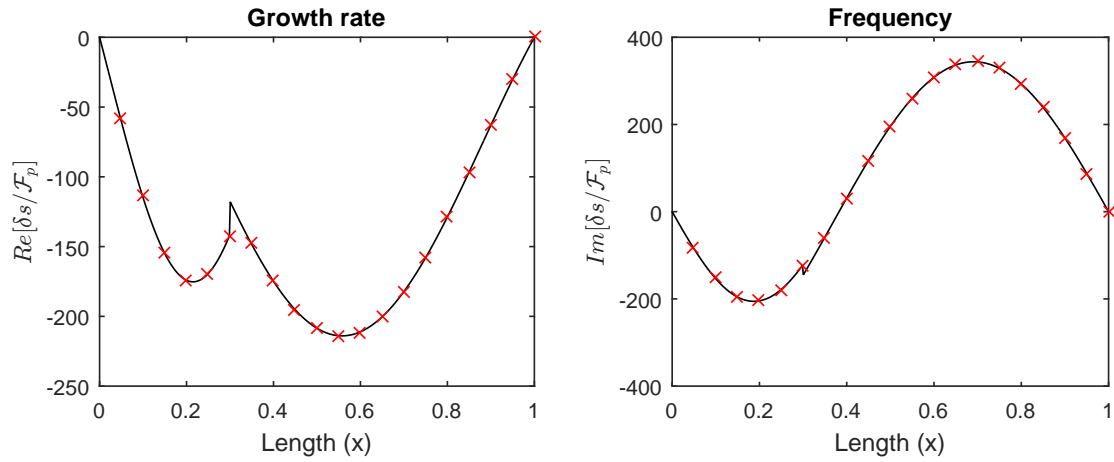


Fig. 3.5 Structural sensitivity - Momentum Equation - Pressure device. — represents the sensitivity using the eigenvalue drift formula. X represents sensitivities at certain points using a finite difference method.

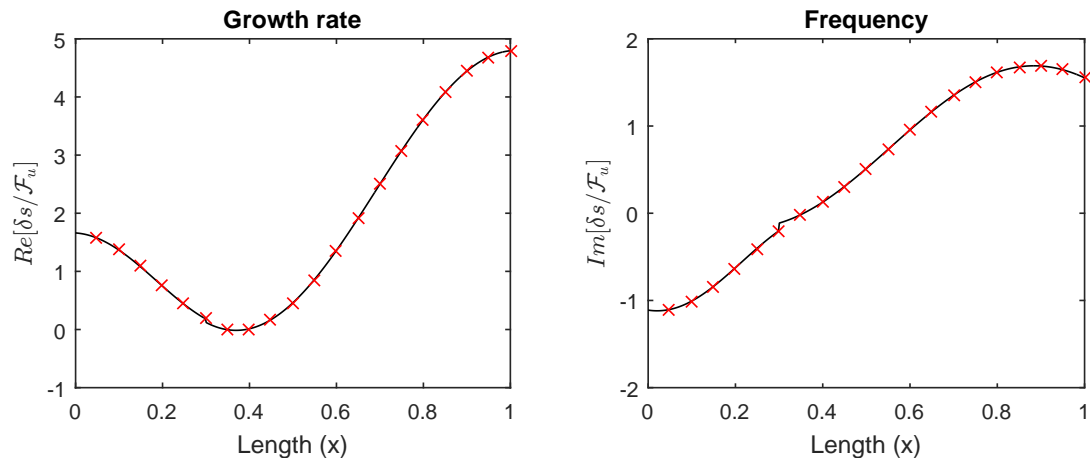


Fig. 3.6 Structural sensitivity - Momentum Equation - Velocity device. — represents the sensitivity using the eigenvalue drift formula. X represents sensitivities at certain points using a finite difference method.

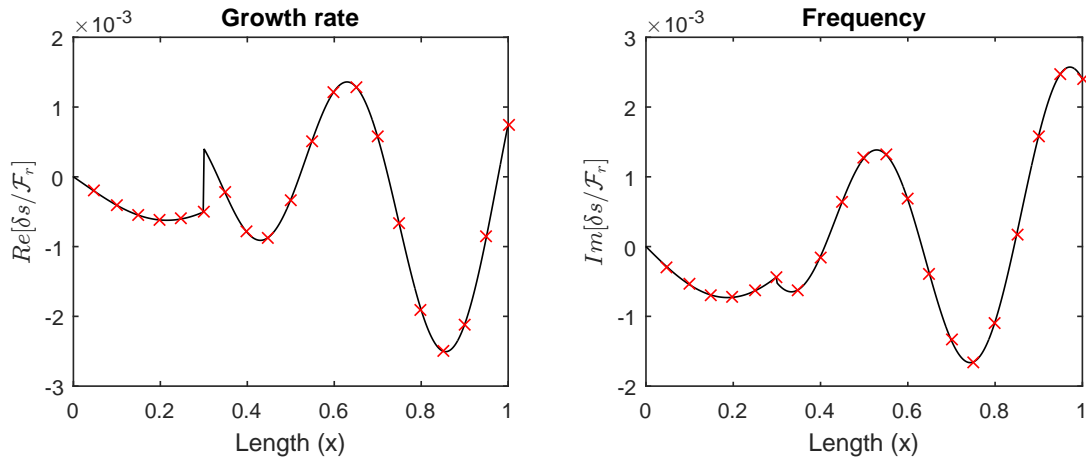


Fig. 3.7 Structural sensitivity - Momentum Equation - Density device. — represents the sensitivity using the eigenvalue drift formula. X represents sensitivities at certain points using a finite difference method.

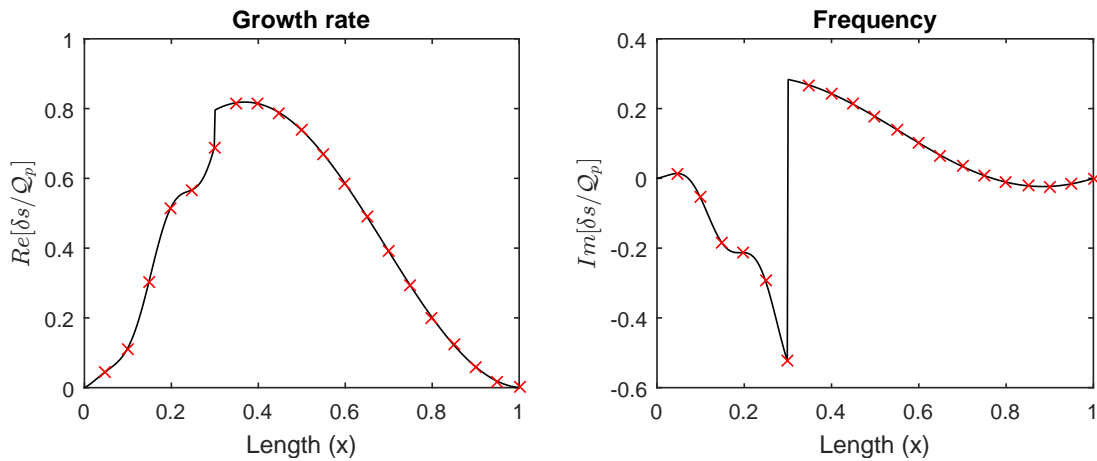


Fig. 3.8 Structural sensitivity - Energy Equation - Pressure device. — represents the sensitivity using the eigenvalue drift formula. X represents sensitivities at certain points using a finite difference method.

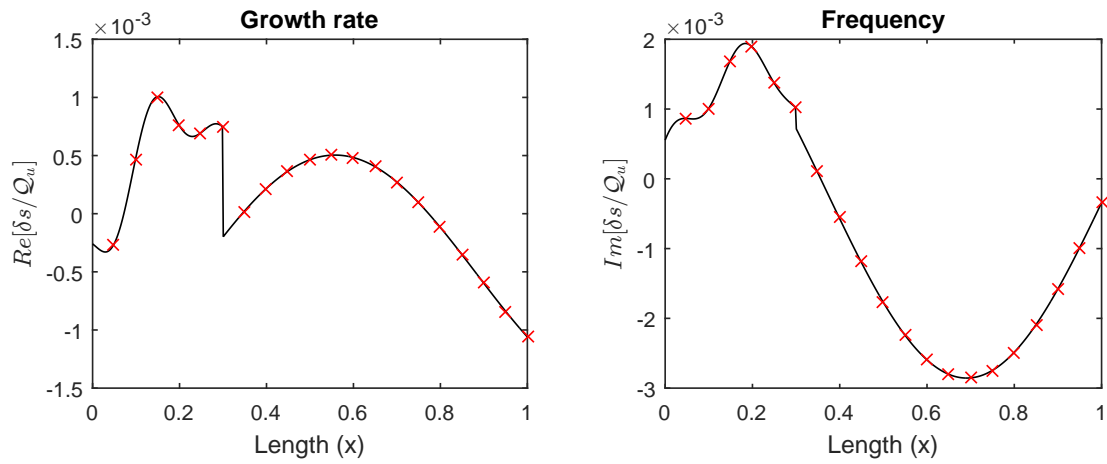


Fig. 3.9 Structural sensitivity - Energy Equation - Velocity device. — represents the sensitivity using the eigenvalue drift formula. X represents sensitivities at certain points using a finite difference method.

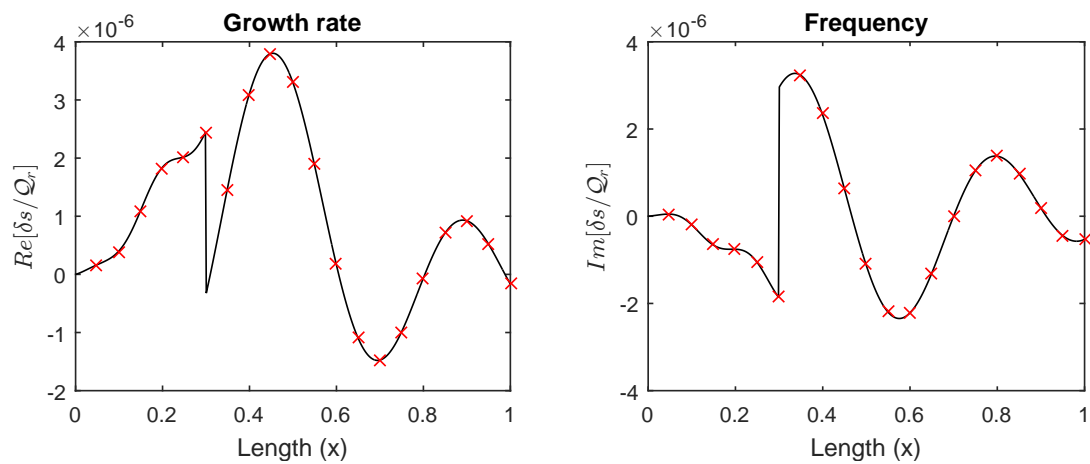


Fig. 3.10 Structural sensitivity - Energy Equation - Density device. — represents the sensitivity using the eigenvalue drift formula. X represents sensitivities at certain points using a finite difference method.

# Chapter 4

## Sensitivity Analysis via a Continuous Approach

### 4.1 Continuous Adjoint formulation

The adjoint system is defined through the system of Eq. (1.6). For the set of governing equations (Eq. 2.3):

$$F_1 \equiv \frac{\partial \rho'}{\partial t} + \bar{u} \frac{\partial \rho'}{\partial x} + \bar{\rho} \frac{\partial u'}{\partial x} = 0 \quad (4.1a)$$

$$F_2 \equiv \bar{\rho} \frac{\partial u'}{\partial t} + \bar{\rho} \bar{u} \frac{\partial u'}{\partial x} + \frac{\partial p'}{\partial x} = 0 \quad (4.1b)$$

$$F_3 \equiv \frac{\partial p'}{\partial t} + \bar{u} \frac{\partial p'}{\partial x} + \gamma \bar{p} \frac{\partial u'}{\partial x} = 0 \quad (4.1c)$$

which are defined on

$$x \in [0, b^-) \cup (b^+, L] \quad (4.2)$$

define a set of adjoint variables  $(\rho^+(x, t), u^+(x, t), p^+(x, t))$ . Similarly, for the set of jump conditions (Eq. 2.4):

$$J_1 \equiv [\rho' \bar{u} + \bar{\rho} u']_{b^-}^{b^+} = 0 \quad (4.3a)$$

$$J_2 \equiv [p' + 2\bar{\rho} \bar{u} u' + \rho' \bar{u}^2]_{b^-}^{b^+} = 0 \quad (4.3b)$$

$$J_3 \equiv \frac{\gamma}{(\gamma - 1)} [p' \bar{u} + \bar{p} u']_{b^-}^{b^+} + \frac{1}{2} [3\bar{\rho} \bar{u}^2 u' + \bar{u}^3 \rho']_{b^-}^{b^+} - \beta u(b^-, t - \tau) = 0$$

which are only defined at  $x = b$  (the flame position), define another set adjoint variables ( $f(t)$ ,  $g(t)$ ,  $h(t)$ ). Define the following inner products:

$$\langle a, b \rangle = \int_0^T \left( \int_0^{b^-} a^* b \, dx + \int_{b^+}^L a^* b \, dx \right) dt \quad (4.4)$$

$$\{a, b\} = \int_0^T a^* b \, dt \quad (4.5)$$

Where the (\*) denotes a complex conjugate. Using the direct equations and the adjoint variables, create a functional:

$$\mathcal{L} \equiv \langle \rho^+, F_1 \rangle + \langle u^+, F_2 \rangle + \langle p^+, F_3 \rangle + \{f, J_1\} + \{g, J_2\} + \{h, J_3\} \quad (4.6)$$

Considering each term in turn:

$$\begin{aligned} \langle \rho^+, F_1 \rangle &= \int_0^{b^-} [\rho^{+*} \rho']_0^T dx + \int_{b^+}^L [\rho^{+*} \rho']_0^T dx \dots \\ &\quad + \int_0^T \left( [\rho^{+*} \bar{u} \rho' + \rho^{+*} \bar{\rho} u']_0^{b^-} + [\rho^{+*} \bar{u} \rho' + \rho^{+*} \bar{\rho} u']_{b^+}^L \right) dt \dots \\ &\quad - \left\langle \frac{\partial \rho^+}{\partial t} + \bar{u} \frac{\partial \rho^+}{\partial x}, \rho' \right\rangle - \left\langle \bar{\rho} \frac{\partial \rho^+}{\partial x}, u' \right\rangle \end{aligned} \quad (4.7a)$$

$$\begin{aligned} \langle u^+, F_2 \rangle &= \int_0^{b^-} [u^{+*} \bar{\rho} u']_0^T dx + \int_{b^+}^L [u^{+*} \bar{\rho} u']_0^T dx \dots \\ &\quad + \int_0^T \left( [u^{+*} \bar{\rho} \bar{u} u' + u^{+*} p']_0^{b^-} + [u^{+*} \bar{\rho} \bar{u} u' + u^{+*} p']_{b^+}^L \right) dt \dots \\ &\quad - \left\langle \bar{\rho} \frac{\partial u^+}{\partial t} + \bar{\rho} \bar{u} \frac{\partial u^+}{\partial x}, u' \right\rangle - \left\langle \frac{\partial u^+}{\partial x}, p' \right\rangle \end{aligned} \quad (4.7b)$$

$$\begin{aligned} \langle p^+, F_3 \rangle &= \int_0^{b^-} [p^{+*} p']_0^T dx + \int_{b^+}^L [p^{+*} p']_0^T dx \dots \\ &\quad + \int_0^T \left( [p^{+*} \bar{u} p' + p^{+*} \gamma \bar{p} u']_0^{b^-} + [p^{+*} \bar{u} p' + p^{+*} \gamma \bar{p} u']_{b^+}^L \right) dt \dots \\ &\quad - \left\langle \frac{\partial p^+}{\partial t} + \bar{u} \frac{\partial p^+}{\partial x}, p' \right\rangle - \left\langle \gamma \bar{p} \frac{\partial p^+}{\partial x}, u' \right\rangle \end{aligned} \quad (4.7c)$$

$$\{f, J_1\} = \int_0^T [f^* \rho' \bar{u} + f^* \bar{\rho} u']_{b^-}^{b^+} dt \quad (4.7d)$$

$$\{g, J_2\} = \int_0^T [g^* p' + g^* 2 \bar{\rho} \bar{u} u' + g^* \rho' \bar{u}^2]_{b^-}^{b^+} dt \quad (4.7e)$$

$$\begin{aligned} \{h, J_3\} &= \int_0^T \left( \frac{\gamma}{(\gamma - 1)} [h^* p' \bar{u} + h^* \bar{p} u']_{b^-}^{b^+} + \frac{1}{2} [h^* 3 \bar{\rho} \bar{u}^2 u' + h^* \bar{u}^3 \rho']_{b^-}^{b^+} \right) dt \dots \\ &\quad - \int_{-\tau}^{T-\tau} h^*(t + \tau) \beta u_1'(t) dt \end{aligned} \quad (4.7f)$$

Note that:

$$[\cdots]_0^{b^-} + [\cdots]_{b^+}^L = [\cdots]_0^L - [\cdots]_{b^-}^{b^+} \quad (4.8)$$

Rearranging the functional by type and in terms of direct variables gives:

$$\begin{aligned} \mathcal{L} \equiv & - \left\langle \frac{\partial \rho^+}{\partial t} + \bar{u} \frac{\partial \rho^+}{\partial x}, \rho' \right\rangle - \left\langle \bar{\rho} \frac{\partial u^+}{\partial t} + \bar{\rho} \bar{u} \frac{\partial u^+}{\partial x} + \bar{\rho} \frac{\partial \rho^+}{\partial x} + \gamma \bar{p} \frac{\partial p^+}{\partial x}, u' \right\rangle \cdots \\ & - \left\langle \frac{\partial p^+}{\partial t} + \bar{u} \frac{\partial p^+}{\partial x} + \frac{\partial u^+}{\partial x}, p' \right\rangle \cdots \end{aligned} \quad (4.9a)$$

$$+ \int_0^{b^-} [\rho^{+*} \rho' + u^{+*} \bar{\rho} u' + p^{+*} p']_0^T dx + \int_{b^+}^L [\rho^{+*} \rho' + u^{+*} \bar{\rho} u' + p^{+*} p']_0^T dx \cdots \quad (4.9b)$$

$$+ \int_0^T [\rho^{+*} \bar{u} \rho' + \rho^{+*} \bar{\rho} u' + u^{+*} \bar{\rho} \bar{u} u' + u^{+*} p' + p^{+*} \bar{u} p' + p^{+*} \gamma \bar{p} u']_0^L dt \cdots \quad (4.9c)$$

$$\begin{aligned} & + \int_0^T \left[ \left( f^* \bar{u} + g^* \bar{u}^2 + \frac{1}{2} h^* \bar{u}^3 - \rho^{+*} \bar{u} \right) \rho' \cdots \right. \\ & + \left. \left( f^* \bar{\rho} + g^* 2 \bar{\rho} \bar{u} + \frac{\gamma}{(\gamma-1)} h^* \bar{p} + \frac{3}{2} h^* \bar{\rho} \bar{u}^2 - \rho^{+*} \bar{\rho} - u^{+*} \bar{\rho} \bar{u} - p^{+*} \gamma \bar{p} \right) u' \cdots \right. \\ & \left. + \left( g^* + \frac{\gamma}{(\gamma-1)} h^* \bar{u} - u^{+*} - p^{+*} \bar{u} \right) p' \right]_{b^-}^{b^+} dt - \int_{-\tau}^{T-\tau} h^*(t+\tau) \beta u_1'(t) dt \end{aligned} \quad (4.9d)$$

All the derivatives of  $\mathcal{L}$  with respect to  $\rho'$ ,  $u'$  and  $p'$  must be zero for any value of  $\rho'$ ,  $u'$  and  $p'$ , hence the equations above have the following interpretation:

- Equation (4.9a) gives the continuous adjoint equations:

$$\frac{\partial \rho^+}{\partial t} + \bar{u} \frac{\partial \rho^+}{\partial x} = 0 \quad (4.10a)$$

$$\bar{\rho} \frac{\partial u^+}{\partial t} + \bar{\rho} \bar{u} \frac{\partial u^+}{\partial x} + \bar{\rho} \frac{\partial \rho^+}{\partial x} + \gamma \bar{p} \frac{\partial p^+}{\partial x} = 0 \quad (4.10b)$$

$$\frac{\partial p^+}{\partial t} + \bar{u} \frac{\partial p^+}{\partial x} + \frac{\partial u^+}{\partial x} = 0 \quad (4.10c)$$

- Equation (4.9b) gives the initial and final conditions for  $\rho^+$ ,  $u^+$  and  $p^+$  at all positions. In the frequency domain this row is redundant.
- Equation (4.9c) gives the boundary conditions for  $\rho^+$ ,  $u^+$  and  $p^+$  at  $x = 0$  and  $x = L$  in terms of those of  $\rho'$ ,  $u'$  and  $p'$ :

$$\rho^{+*} \bar{u} \rho' + \rho^{+*} \bar{\rho} u' + u^{+*} \bar{\rho} \bar{u} u' + u^{+*} p' + p^{+*} \bar{u} p' + p^{+*} \gamma \bar{p} u' = 0 \quad (4.11)$$

- Equation (4.9d) gives the adjoint jump conditions for  $\rho^+$ ,  $u^+$  and  $p^+$ . For simplicity, variables evaluated just before the flame ( $b^-$ ) will use the subscript 1 and variables evaluated just after the flame ( $b^+$ ) will use subscript 2. The derivatives with respect  $\rho'_1$ ,  $u'_1$ ,  $p'_1$ ,  $\rho'_2$ ,  $u'_2$  and  $p'_2$  must be zero, which leads to the following six equations:

$$f\bar{u}_2 + g\bar{u}_2^2 + \frac{1}{2}h\bar{u}_2^3 - \rho_2^+\bar{u}_2 = 0 \quad (4.12a)$$

$$f\bar{\rho}_2 + 2g\bar{\rho}_2\bar{u}_2 + \frac{\gamma}{(\gamma-1)}h\bar{p}_2 + \frac{3}{2}h\bar{\rho}_2\bar{u}_2^2 - \rho_2^+\bar{\rho}_2 - u_2^+\bar{\rho}_2\bar{u}_2 - p_2^+\gamma\bar{p}_2 = 0 \quad (4.12b)$$

$$g + \frac{\gamma}{(\gamma-1)}h\bar{u}_2 - u_2^+ - p_2^+\bar{u}_2 = 0 \quad (4.12c)$$

$$\rho_1^+\bar{u}_1 - f\bar{u}_1 - g\bar{u}_1^2 - \frac{1}{2}h\bar{u}_1^3 = 0 \quad (4.12d)$$

$$\rho_1^+\bar{\rho}_1 + u_1^+\bar{\rho}_1\bar{u}_1 + p_1^+\gamma\bar{p}_1 - f\bar{\rho}_1 - 2g\bar{\rho}_1\bar{u}_1 - \frac{\gamma}{(\gamma-1)}h\bar{p}_1 - \frac{3}{2}h\bar{\rho}_1\bar{u}_1^2 - \beta h(t + \tau) = 0 \quad (4.12e)$$

$$u_1^+ + p_1^+\bar{u}_1 - g - \frac{\gamma}{(\gamma-1)}h\bar{u}_1 = 0 \quad (4.12f)$$

From the first three equations a relation between the adjoint variables defined in the whole domain ( $\rho^+$ ,  $u^+$ ,  $p^+$ ) and the adjoint variables defined at the flame ( $f$ ,  $g$ ,  $h$ ) is derived:

$$f = \rho_2^+ - \bar{u}_2 u_2^+ + \frac{1}{2}(\gamma-1)\bar{u}_2^2 p_2^+ \quad (4.13a)$$

$$g = u_2^+ - (\gamma-1)\bar{u}_2 p_2^+ \quad (4.13b)$$

$$h = (\gamma-1)p_2^+ \quad (4.13c)$$

Finally from the other three, the jump conditions for  $\rho^+$ ,  $u^+$  and  $p^+$ , are obtained:

$$\rho_2^+ + (\bar{u}_1 - \bar{u}_2)u_2^+ + \frac{1}{2}(\gamma - 1)(\bar{u}_1 - \bar{u}_2)^2 p_2^+ - \rho_1^+ = 0 \quad (4.14a)$$

$$\bar{\rho}_1 \rho_2^+ + \bar{\rho}_1(2\bar{u}_1 - \bar{u}_2)u_2^+ + \frac{1}{2}(\gamma - 1)\bar{\rho}_1(3\bar{u}_1^2 - 4\bar{u}_1\bar{u}_2 + \bar{u}_2^2)p_2^+ + \gamma\bar{p}_1 p_2^+ \dots \quad (4.14b)$$

$$-\bar{\rho}_1 \rho_1^+ - \bar{\rho}_1 \bar{u}_1 u_1^+ - \gamma\bar{p}_1 p_1^+ + \beta(\gamma - 1)p_2^+(t + \tau) = 0$$

$$u_2^+ + (\gamma\bar{u}_1 - (\gamma - 1)\bar{u}_2)p_2^+ - u_1^+ - \bar{u}_1 p_1^+ = 0 \quad (4.14c)$$

Which after some arrangement can be cast as:

$$\rho_1^+ - \rho_2^+ - u_1^+ \bar{u}_1 + u_2^+ \bar{u}_2 + \frac{1}{2}(\gamma - 1)(p_1^+ \bar{u}_1^2 - p_2^+ \bar{u}_2^2) = \frac{1}{2}(\gamma + 1)u_1^2 \frac{\beta(\gamma - 1)p_2^+(t + \tau)}{\bar{\rho}_1(\bar{c}_1^2 - \bar{u}_1^2)} \quad (4.15a)$$

$$u_1^+ - u_2^+ - (\gamma - 1)(p_1^+ \bar{u}_1 - p_2^+ \bar{u}_2) = -\gamma \bar{u}_1 \frac{\beta(\gamma - 1)p_2^+(t + \tau)}{\bar{\rho}_1(\bar{c}_1^2 - \bar{u}_1^2)} \quad (4.15b)$$

$$p_1^+ - p_2^+ = \frac{\beta(\gamma - 1)p_2^+(t + \tau)}{\bar{\rho}_1(\bar{c}_1^2 - \bar{u}_1^2)} \quad (4.15c)$$

## 4.2 Continuous Adjoint Equations and Eigenvalue Problem

The adjoint equations are:

$$\frac{\partial \rho^+}{\partial t} + \bar{u} \frac{\partial \rho^+}{\partial x} = 0 \quad (4.16a)$$

$$\bar{\rho} \frac{\partial u^+}{\partial t} + \bar{\rho} \bar{u} \frac{\partial u^+}{\partial x} + \bar{\rho} \frac{\partial \rho^+}{\partial x} + \gamma \bar{p} \frac{\partial p^+}{\partial x} = 0 \quad (4.16b)$$

$$\frac{\partial p^+}{\partial t} + \bar{u} \frac{\partial p^+}{\partial x} + \frac{\partial u^+}{\partial x} = 0 \quad (4.16c)$$

Note that for the adjoint equations to be well defined, they must evolve backwards in time. This is shown in the derivation of the adjoint equations in the frequency domain

in appendix H. The adjoint jump conditions at the flame  $x = b$  are:

$$\begin{aligned} \begin{bmatrix} 1 & -\bar{u}_1 & \frac{1}{2}(\gamma - 1)\bar{u}_1^2 \\ 0 & 1 & -(\gamma - 1)\bar{u}_1 \\ 0 & 0 & 1 \end{bmatrix} \begin{bmatrix} \rho_1^+ \\ u_1^+ \\ p_1^+ \end{bmatrix} &= \begin{bmatrix} 1 & -\bar{u}_2 & \frac{1}{2}(\gamma - 1)\bar{u}_2^2 \\ 0 & 1 & -(\gamma - 1)\bar{u}_2 \\ 0 & 0 & 1 \end{bmatrix} \begin{bmatrix} \rho_2^+ \\ u_2^+ \\ p_2^+ \end{bmatrix} + \dots \\ &+ \begin{bmatrix} \frac{1}{2}(\gamma + 1)\bar{u}_1^2 \\ -\gamma\bar{u}_1 \\ 1 \end{bmatrix} \frac{\beta(\gamma - 1)p_2^+(t + \tau)}{\bar{\rho}_1(\bar{c}_1^2 - \bar{u}_1^2)} \end{aligned} \quad (4.17)$$

Given the adjoint equations a problem of the form  $\mathbf{U}_t^+ + \mathbf{A}^+\mathbf{U}_x^+ = \mathbf{0}$  can be created:

$$\begin{bmatrix} \rho^+ \\ u^+ \\ p^+ \end{bmatrix}_t + \begin{bmatrix} \bar{u} & 0 & 0 \\ 1 & \bar{u} & \bar{c}^2 \\ 0 & 1 & \bar{u} \end{bmatrix} \begin{bmatrix} \rho^+ \\ u^+ \\ p^+ \end{bmatrix}_x = \mathbf{0} \quad (4.18)$$

Diagonalizing  $\mathbf{A}^+$ :

$$\mathbf{A}^+ = \mathbf{S}^+\mathbf{\Lambda}^+\mathbf{S}^{+^{-1}} = \begin{bmatrix} -\bar{c}^2 & 0 & 0 \\ 0 & \bar{c} & -\bar{c} \\ 1 & 1 & 1 \end{bmatrix} \begin{bmatrix} \bar{u} & 0 & 0 \\ 0 & \bar{c} + \bar{u} & 0 \\ 0 & 0 & -(\bar{c} - \bar{u}) \end{bmatrix} \begin{bmatrix} -1/\bar{c}^2 & 0 & 0 \\ 1/2\bar{c}^2 & 1/2\bar{c} & 1/2 \\ 1/2\bar{c}^2 & -1/2\bar{c} & 1/2 \end{bmatrix} \quad (4.19)$$

Substitute  $\mathbf{A}^+$  with the diagonalization matrices and pre-multiplying by  $\mathbf{S}^{+^{-1}}$  to get:

$$\mathbf{S}^{+^{-1}}\mathbf{U}_t^+ + \mathbf{\Lambda}^+\mathbf{S}^{+^{-1}}\mathbf{U}_x^+ = \mathbf{0} \quad (4.20)$$

Substituting  $\mathbf{V}^+ = \mathbf{S}^{+^{-1}}\mathbf{U}^+$ , gives:

$$\mathbf{V}_t^+ + \mathbf{\Lambda}^+\mathbf{V}_x^+ = \mathbf{0} \quad (4.21)$$

$$\begin{bmatrix} \mathcal{R}^+ \\ \mathcal{U}^+ \\ \mathcal{P}^+ \end{bmatrix}_t + \begin{bmatrix} \bar{u} & 0 & 0 \\ 0 & \bar{c} + \bar{u} & 0 \\ 0 & 0 & -(\bar{c} - \bar{u}) \end{bmatrix} \begin{bmatrix} \mathcal{R}^+ \\ \mathcal{U}^+ \\ \mathcal{P}^+ \end{bmatrix}_x = \mathbf{0} \quad (4.22)$$

Note that again the vector  $\mathbf{V}^+$  represents the Riemann invariants of the adjoint system, and that the decoupled system of equations is exactly the same as the decoupled system of direct equations (Eq. 2.14), bringing to light that in a system with homogeneous properties, the mean flow does not make the system not self adjoint. However, a glance at the adjoint jump conditions (Eq. 4.17) reveals that the right hand side terms are

not self adjoint. The solutions of the adjoint system are:

$$\mathcal{R}^+(x, t) = \alpha^+ \left( t - \frac{x}{\bar{u}} \right) \quad \text{Entropy wave} \quad (4.23)$$

$$\mathcal{U}^+(x, t) = f^+ \left( t - \frac{x}{\bar{c} + \bar{u}} \right) \quad \text{Backward traveling wave} \quad (4.24)$$

$$\mathcal{P}^+(x, t) = g^+ \left( t + \frac{x}{\bar{c} - \bar{u}} \right) \quad \text{Forward traveling wave} \quad (4.25)$$

In original variables:

$$\rho^+(x, t) = -\bar{c}^2 \left( \alpha^+ \left( t - \frac{x}{\bar{u}} \right) \right) \quad (4.26)$$

$$u^+(x, t) = \bar{c} \left( f^+ \left( t - \frac{x}{\bar{c} + \bar{u}} \right) - g^+ \left( t + \frac{x}{\bar{c} - \bar{u}} \right) \right) \quad (4.27)$$

$$p^+(x, t) = f^+ \left( t - \frac{x}{\bar{c} + \bar{u}} \right) + g^+ \left( t + \frac{x}{\bar{c} - \bar{u}} \right) + \alpha^+ \left( t - \frac{x}{\bar{u}} \right) \quad (4.28)$$

Similar to the direct problem, the domain is split into two sections. The wave solutions are centered at  $x = b$ , and labeled with subscripts 1 if they are located upstream of the flame and 2 if they are downstream.

$$\rho^+(x, t) = \begin{cases} -\bar{c}_1^2 \left( \alpha_1^+ \left( t - \frac{x-b}{\bar{u}_1} \right) \right) & \text{if } x < b \\ -\bar{c}_2^2 \left( \alpha_2^+ \left( t - \frac{x-b}{\bar{u}_2} \right) \right) & \text{if } x > b \end{cases} \quad (4.29)$$

$$u^+(x, t) = \begin{cases} \bar{c}_1 \left( f_1^+ \left( t - \frac{x-b}{\bar{c}_1 + \bar{u}_1} \right) - g_1^+ \left( t + \frac{x-b}{\bar{c}_1 - \bar{u}_1} \right) \right) & \text{if } x < b \\ \bar{c}_2 \left( f_2^+ \left( t - \frac{x-b}{\bar{c}_2 + \bar{u}_2} \right) - g_2^+ \left( t + \frac{x-b}{\bar{c}_2 - \bar{u}_2} \right) \right) & \text{if } x > b \end{cases} \quad (4.30)$$

$$p^+(x, t) = \begin{cases} f_1^+ \left( t - \frac{x-b}{\bar{c}_1 + \bar{u}_1} \right) + g_1^+ \left( t + \frac{x-b}{\bar{c}_1 - \bar{u}_1} \right) + \alpha_1^+ \left( t - \frac{x-b}{\bar{u}_1} \right) & \text{if } x < b \\ f_2^+ \left( t - \frac{x-b}{\bar{c}_2 + \bar{u}_2} \right) + g_2^+ \left( t + \frac{x-b}{\bar{c}_2 - \bar{u}_2} \right) + \alpha_2^+ \left( t - \frac{x-b}{\bar{u}_2} \right) & \text{if } x > b \end{cases} \quad (4.31)$$

Similar to the direct problem, a set of three boundary conditions needs to be set for the adjoint eigenvalue problem. The boundary condition at  $x = 0$  gives:

$$f_1^+(t) = R_{ua} g_1^+(t - \tau_u) \quad (4.32)$$

$$\tau_u = \frac{2b\bar{c}_1}{\bar{c}_1^2 - \bar{u}_1^2} \quad (4.33)$$

The boundary condition at  $x = L$ :

$$g_2^+(t) = R_{da} f_2^+(t - \tau_d) \quad (4.34)$$

$$\tau_d = \frac{2(L - b)\bar{c}_2}{\bar{c}_2^2 - \bar{u}_2^2} \quad (4.35)$$

Recall that the adjoint operator evolves backwards in time, hence it is more convenient to work with the waves going towards the flame  $f_1^+$  and  $g_2^+$ :

$$g_1^+(t) = R_{ua}^{-1} f_1^+(t + \tau_u) \quad (4.36)$$

$$f_2^+(t) = R_{da}^{-1} g_2^+(t + \tau_d) \quad (4.37)$$

Mirroring the direct equations, the third boundary condition sets the entropy waves in the second part of the duct, this is because the adjoint entropy waves convect in the opposite direction as the direct system.

$$\alpha_2^+(0, t) = \alpha_2^+ \left( t + \frac{b}{\bar{u}_2} \right) = a_0^+ \left( t + \frac{b}{\bar{u}_2} \right) \quad (4.38)$$

The relation between the direct and the adjoint reflection coefficients comes from the boundary terms. At  $x = 0$ :

$$\rho^{+*} \bar{u} \rho' + \rho^{+*} \bar{\rho} u' + u^{+*} \bar{\rho} \bar{u} u' + u^{+*} p' + p^{+*} \bar{u} p' + p^{+*} \gamma \bar{p} u' = 0 \quad (4.39)$$

Which simplifies for the upstream boundary as:

$$2(M_1 + 1) f_1^{+*} f_1 + 2(M_1 - 1) g_1^{+*} g_1 - M_1 (\alpha_2^{+*} \alpha_2) = 0 \quad (4.40)$$

After using the boundary conditions  $f_1 = R_u g_1$  and  $f_1^+ = R_{ua} g_1^+$ , a relation between reflection coefficients is obtained:

$$R_{ua}^* = \frac{1}{R_u} \frac{1 - M_1}{1 + M_1} + \frac{M_1 a_0 (t + \tau_a) a_0^* (t - \tau_a)^*}{2 R_u (1 + M_1) g_1 (t - \tau_u) g_1^* (t - \tau_u)^*} \quad \tau_a = \frac{b \bar{c}_1}{\bar{u}_1 (\bar{c}_1 + \bar{u}_1)} \quad (4.41)$$

For the case where  $a_0$  is set to zero at the inlet, the reflection coefficient becomes:

$$R_{ua} = \frac{1}{R_u^*} \frac{1 - M_1}{1 + M_1} \quad (4.42)$$

For the downstream side the equation becomes:

$$2(M_2 + 1)f_2^{+*} f_2 + 2(M_2 - 1)g_2^{+*} g_2 - M_2(\alpha_2^{+*} \alpha_2) = 0 \quad (4.43)$$

The downstream reflection coefficient is:

$$R_{da}^* = \frac{1}{R_d} \frac{1 + M_2}{1 - M_2} + \frac{M_2 a_0^+(t - \tau_c)^* \alpha_2(t - \tau_c)}{2R_d(M_2 - 1)f_2(t - \tau_d)f_2^+(t - \tau_d)^*} \quad \tau_c = \frac{(L - b)\bar{c}_2}{\bar{u}_2(\bar{c}_2 - \bar{u}_2)} \quad (4.44)$$

If  $a_0$  is set to zero, it would be natural to set  $a_0^+$  to zero as well, giving the simple reflection coefficient:

$$R_{da} = \frac{1}{R_d^*} \frac{1 + M_2}{1 - M_2} \quad (4.45)$$

After substituting the adjoint wave forms ( $\rho^+$ ,  $u^+$ ,  $p^+$ ) into the jump conditions (Eq. 4.17), dividing the first equation by  $\bar{c}_1^2$ , the second by  $\bar{c}_1$  and performing a Laplace transform  $f_1^+ = F_1^+ e^{-s^*t}$  the adjoint transfer matrix is obtained:

$$L^+ \hat{q}^+ = X^+ \quad (4.46)$$

$$\begin{bmatrix} L_{11}^+ & L_{12}^+ & L_{13}^+ \\ L_{21}^+ & L_{22}^+ & L_{23}^+ \\ L_{31}^+ & L_{32}^+ & L_{33}^+ \end{bmatrix} \begin{bmatrix} \mathcal{A}_1^+ \\ F_1^+ \\ G_2^+ \end{bmatrix} = \begin{bmatrix} \frac{\bar{c}_2^2}{\bar{c}_1^2} \left(1 - \frac{1}{2}(\gamma - 1)M_2^2\right) - \frac{1}{2}(\gamma + 1)M_1^2 \frac{\beta(\gamma - 1)e^{-s^*\tau}}{\bar{\rho}_1(\bar{c}_1^2 - \bar{u}_1^2)} \\ \frac{\bar{c}_2}{\bar{c}_1}(\gamma - 1)M_2 + \gamma M_1 \frac{\beta(\gamma - 1)e^{-s^*\tau}}{\bar{\rho}_1(\bar{c}_1^2 - \bar{u}_1^2)} \\ -1 - \frac{\beta(\gamma - 1)e^{-s^*\tau}}{\bar{\rho}_1(\bar{c}_1^2 - \bar{u}_1^2)} \end{bmatrix} A_0^+ \quad (4.47)$$

The matrix  $L^+$  is again composed of two matrices:

$$L^+ = M^+ + Q^+ \quad (4.48)$$

$$M = \begin{bmatrix} M_{11}^+ & M_{12}^+ & M_{13}^+ \\ M_{21}^+ & M_{22}^+ & M_{23}^+ \\ M_{31}^+ & M_{32}^+ & M_{33}^+ \end{bmatrix} \quad Q = \begin{bmatrix} 0 & 0 & Q_{13}^+ \\ 0 & 0 & Q_{23}^+ \\ 0 & 0 & Q_{33}^+ \end{bmatrix}$$

Whose components are:

$$M_{11}^+ = 1 - \frac{1}{2}(\gamma - 1)\bar{M}_1^2 \quad (4.49)$$

$$M_{12}^+ = M_1 - \frac{1}{2}(\gamma - 1)M_1^2 + R_{ua}^{-1}e^{-s^*\tau_u} \left( -M_1 - \frac{1}{2}(\gamma - 1)M_1^2 \right) \quad (4.50)$$

$$M_{13}^+ = \left( M_2 + \frac{1}{2}(\gamma - 1)M_2^2 + R_{da}^{-1}e^{-s^*\tau_d} \left( -M_2 + \frac{1}{2}(\gamma - 1)M_2^2 \right) \right) \frac{\bar{c}_2}{\bar{c}_1} \quad (4.51)$$

$$M_{21}^+ = (\gamma - 1)M_1 \quad (4.52)$$

$$M_{22}^+ = -1 + (\gamma - 1)M_1 + R_{ua}^{-1}e^{-s^*\tau_u} (1 + (\gamma - 1)M_1) \quad (4.53)$$

$$M_{23}^+ = \left( -1 - (\gamma - 1)M_2 + R_{da}^{-1}e^{-s^*\tau_d} (1 - (\gamma - 1)M_2) \right) \frac{\bar{c}_2}{\bar{c}_1} \quad (4.54)$$

$$M_{31}^+ = -1 \quad (4.55)$$

$$M_{32}^+ = -(1 + R_{ua}^{-1}e^{-s^*\tau_u}) \quad (4.56)$$

$$M_{33}^+ = 1 + R_{da}^{-1}e^{-s^*\tau_d} \quad (4.57)$$

The  $Q^+$  matrix has zeros in the first two columns, the third one being:

$$Q_{13}^+ = \frac{(\gamma + 1)M_1^2}{2\bar{\rho}_1(\bar{c}_1^2 - \bar{u}_1^2)} \beta e^{-s^*\tau} (\gamma - 1)(1 + R_{da}^{-1}e^{-s^*\tau_d}) \quad (4.58)$$

$$Q_{23}^+ = -\frac{\gamma M_1}{\bar{\rho}_1(\bar{c}_1^2 - \bar{u}_1^2)} \beta e^{-s^*\tau} (\gamma - 1)(1 + R_{da}^{-1}e^{-s^*\tau_d}) \quad (4.59)$$

$$Q_{33}^+ = \frac{1}{\bar{\rho}_1(\bar{c}_1^2 - \bar{u}_1^2)} \beta e^{-s^*\tau} (\gamma - 1)(1 + R_{da}^{-1}e^{-s^*\tau_d}) \quad (4.60)$$

By setting the determinant of matrix  $L^+$  to zero, one gets the eigenvalues of the adjoint system ( $s_j^+$ ) which are the complex conjugates of the direct ones ( $s_j$ ). For the same parameters given in the direct problem, considering  $A_0^+ = 0$ , the adjoint mode shapes for the same model described in the previous chapters are shown in figures 4.1, 4.2 and 4.3.

There are some remarks to do on the mode shapes. Adjoint density mode shape 4.1 shows only influence of the entropy waves in the upstream side of the duct, which is correct considering that the only place to force them is before they are convected away from the flame. In the adjoint system there is another component affected by entropy waves which is the adjoint pressure. Taking into account that the feedback mechanism is coupled between continuity and energy equations, it is clear that the influence of both will have to be considered as a couple.

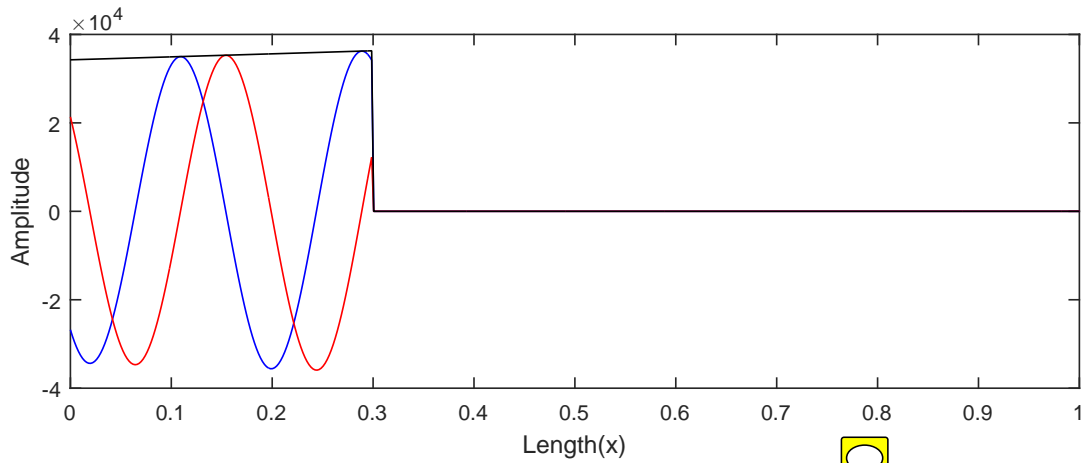


Fig. 4.1 Continuity sensitivity mode shape  $\rho^+$

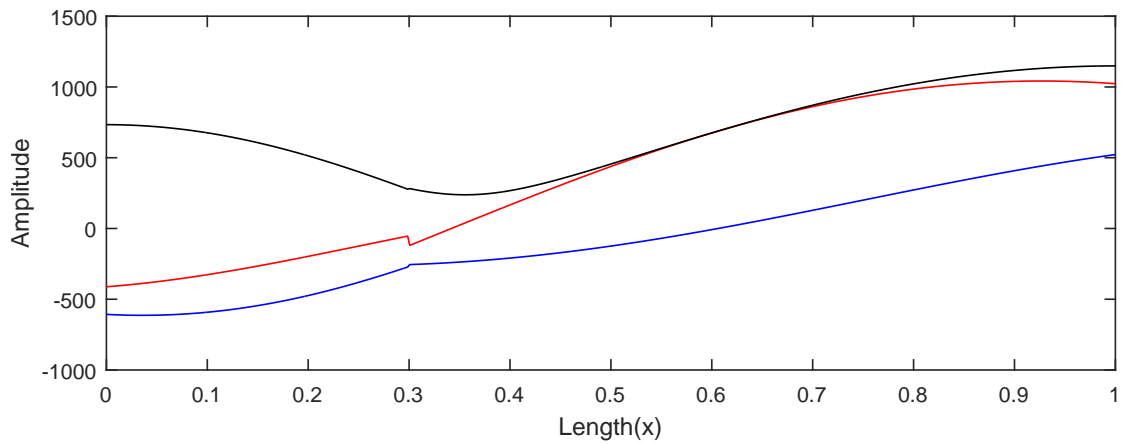


Fig. 4.2 Momentum sensitivity mode shape  $u^+$

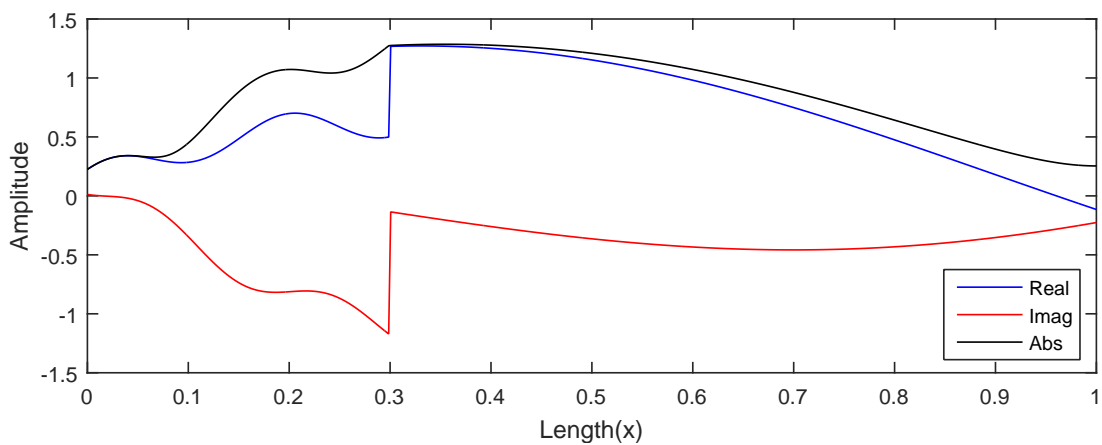


Fig. 4.3 Energy sensitivity mode shape  $p^+$

### 4.3 Continuous eigenvalue drift formula

The eigenvalue drift formula following a continuous approach is derived in appendix H and has as a general expression:

$$\frac{\delta s}{\delta \mathcal{X}} = \frac{Z}{\int_0^{b^-} (\hat{\rho}\rho^{+*} + \bar{\rho}_1 \hat{u}u^{+*} + \hat{p}p^{+*}) dx + \int_{b^+}^L (\hat{\rho}\rho^{+*} + \bar{\rho}_2 \hat{u}u^{+*} + \hat{p}p^{+*}) dx - \beta u_1' e^{-s\tau} (\gamma - 1) p_2^{+*}}$$

Where  $\delta \mathcal{X}$  is a small number related to the slight change in one of the variables of the system (base state) or the size of the perturbation added proportional to one of the native variables (structural) and  $Z$  refers to the inner product of the adjoint and direct eigenfunctions, which appear when the system is slightly modified. The denominator contains the inner products of the adjoint and direct eigenfunctions before and after the flame plus a frequency dependent term at the flame.

### 4.4 Base state sensitivity

Base state sensitivity equations are obtained by slightly changing one of the base state variables, for example, changing  $\beta$  to  $\beta + \delta\beta$  and looking for an expression for  $\delta s$  (see appendix H). The only base state variables analyzed using a continuous approach are  $\beta$  and  $\tau$  (the rest can be worked out using a similar fashion). Keeping in mind that those variables are only defined at the flame  $x = b$ , the base state sensitivities are computed using:

$$\delta \mathcal{X} = \delta\beta \quad Z = u_1' e^{-s\tau} (\gamma - 1) p_2^{+*} \quad (4.61)$$

$$\delta \mathcal{X} = \delta\tau \quad Z = -\beta u_1' s e^{-s\tau} (\gamma - 1) p_2^{+*} \quad (4.62)$$

### 4.5 Structural sensitivity

Structural sensitivity equations are derived by introducing a small perturbation into any of the governing equations, which is proportional to pressure, velocity or density: Upstream of the flame:

$$\frac{\partial \rho'}{\partial t} + \bar{u}_1 \frac{\partial \rho'}{\partial x} + \bar{\rho}_1 \frac{\partial u'}{\partial x} = \mathcal{M}_i \delta(x - a) \quad (4.63a)$$

$$\bar{\rho}_1 \frac{\partial u'}{\partial t} + \bar{\rho}_1 \bar{u}_1 \frac{\partial u'}{\partial x} + \frac{\partial p'}{\partial x} = \mathcal{F}_i \delta(x - a) \quad (4.63b)$$

$$\frac{\partial p'}{\partial t} + \bar{u}_1 \frac{\partial p'}{\partial x} + \gamma \bar{p}_1 \frac{\partial u'}{\partial x} = \mathcal{E}_i \delta(x - a) \quad (4.63c)$$

Downstream of the flame:

$$\frac{\partial \rho'}{\partial t} + \bar{u}_2 \frac{\partial \rho'}{\partial x} + \bar{\rho}_2 \frac{\partial u'}{\partial x} = \mathcal{M}_{iv} \delta(x - c) \quad (4.64a)$$

$$\bar{\rho}_2 \frac{\partial u'}{\partial t} + \bar{\rho}_2 \bar{u}_2 \frac{\partial u'}{\partial x} + \frac{\partial p'}{\partial x} = \mathcal{F}_{iv} \delta(x - c) \quad (4.64b)$$

$$\frac{\partial p'}{\partial t} + \bar{u}_2 \frac{\partial p'}{\partial x} + \gamma \bar{p}_2 \frac{\partial u'}{\partial x} = \mathcal{E}_{iv} \delta(x - c) \quad (4.64c)$$

Where<sup>1</sup>:

$$\begin{aligned} \mathcal{M}_i &= \mathcal{M}_{p_1} p' + \mathcal{M}_{u_1} u' + \mathcal{M}_{r_1} \rho' & \mathcal{M}_{iv} &= \mathcal{M}_{p_2} p' + \mathcal{M}_{u_2} u' + \mathcal{M}_{r_2} \rho' \\ \mathcal{F}_i &= \mathcal{F}_{p_1} p' + \mathcal{F}_{u_1} u' + \mathcal{F}_{r_1} \rho' & \mathcal{F}_{iv} &= \mathcal{F}_{p_2} p' + \mathcal{F}_{u_2} u' + \mathcal{F}_{r_2} \rho' \\ \mathcal{E}_i &= \mathcal{E}_{p_1} p' + \mathcal{E}_{u_1} u' + \mathcal{E}_{r_1} \rho' & \mathcal{E}_{iv} &= \mathcal{E}_{p_2} p' + \mathcal{E}_{u_2} u' + \mathcal{E}_{r_2} \rho' \end{aligned}$$

The presence of a Dirac delta will make the inner product  $Z$  a function evaluated at point  $a$  or  $c$ . The structural sensitivity can be then obtained using:

$$\delta \mathcal{X} = \mathcal{M}_{p_1} \quad Z = p'(a) \left( \rho^+(a)^* + \bar{c}_1^2 p^+(a)^* \right) \quad (4.65a)$$

$$\delta \mathcal{X} = \mathcal{M}_{p_2} \quad Z = p'(c) \left( \rho^+(c)^* + \bar{c}_2^2 p^+(c)^* \right) \quad (4.65b)$$

$$\delta \mathcal{X} = \mathcal{M}_{u_1} \quad Z = u'(a) \left( \rho^+(a)^* + \bar{c}_1^2 p^+(a)^* \right) \quad (4.65c)$$

$$\delta \mathcal{X} = \mathcal{M}_{u_2} \quad Z = u'(c) \left( \rho^+(c)^* + \bar{c}_2^2 p^+(c)^* \right) \quad (4.65d)$$

$$\delta \mathcal{X} = \mathcal{M}_{r_1} \quad Z = \rho'(a) \left( \rho^+(a)^* + \bar{c}_1^2 p^+(a)^* \right) \quad (4.65e)$$

$$\delta \mathcal{X} = \mathcal{M}_{r_2} \quad Z = \rho'(c) \left( \rho^+(c)^* + \bar{c}_2^2 p^+(c)^* \right) \quad (4.65f)$$

$$\delta \mathcal{X} = \mathcal{F}_{p_1} \quad Z = p'(a) u^+(a)^* \quad (4.65g)$$

$$\delta \mathcal{X} = \mathcal{F}_{p_2} \quad Z = p'(c) u^+(c)^* \quad (4.65h)$$

$$\delta \mathcal{X} = \mathcal{F}_{u_1} \quad Z = u'(a) u^+(a)^* \quad (4.65i)$$

$$\delta \mathcal{X} = \mathcal{F}_{u_2} \quad Z = u'(c) u^+(c)^* \quad (4.65j)$$

$$\delta \mathcal{X} = \mathcal{F}_{r_1} \quad Z = \rho'(a) u^+(a)^* \quad (4.65k)$$

$$\delta \mathcal{X} = \mathcal{F}_{r_2} \quad Z = \rho'(c) u^+(c)^* \quad (4.65l)$$

$$\delta \mathcal{X} = \mathcal{Q}_{p_1} \quad Z = p'(a) p^+(a)^* \quad (4.65m)$$

$$\delta \mathcal{X} = \mathcal{Q}_{p_2} \quad Z = p'(c) p^+(c)^* \quad (4.65n)$$

$$\delta \mathcal{X} = \mathcal{Q}_{u_1} \quad Z = u'(a) p^+(a)^* \quad (4.65o)$$

$$\delta \mathcal{X} = \mathcal{Q}_{u_2} \quad Z = u'(c) p^+(c)^* \quad (4.65p)$$

<sup>1</sup>Recall that  $\mathcal{M}$ ,  $\mathcal{F}$  and  $\mathcal{E}$  are small quantities and that  $\mathcal{E} = \mathcal{Q} + \bar{c}^2 \mathcal{M}$ .

$$\delta\mathcal{X} = \mathcal{Q}_{r_1} \quad Z = \rho'(a)p^+(a)^* \quad (4.65q)$$

$$\delta\mathcal{X} = \mathcal{Q}_{r_2} \quad Z = \rho'(c)p^+(c)^* \quad (4.65r)$$



The mode shapes obtained, are the same, to machine precision, to those derived by the discrete adjoint method (figures 3.2 to 3.10). For comparison only one of the modeshapes (fig. 4.4) will be plot following the continuous approach.

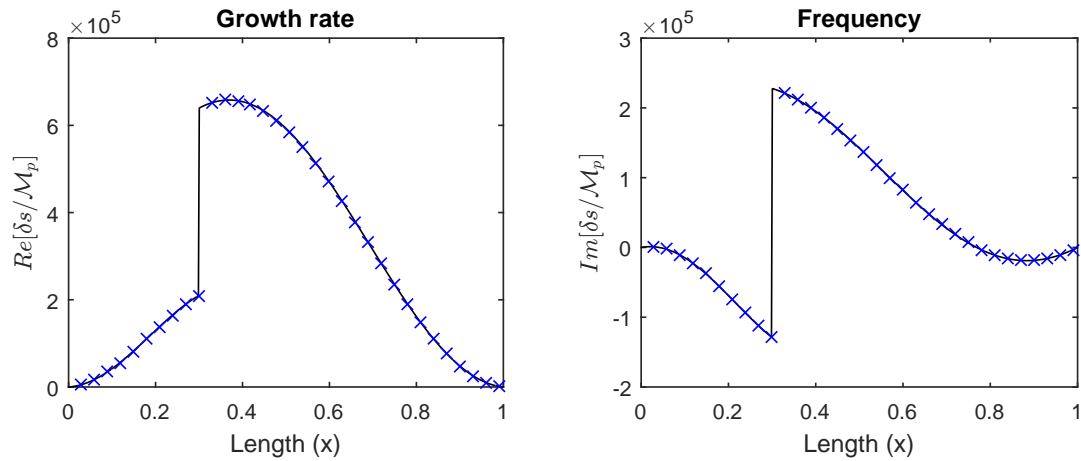


Fig. 4.4 Structural sensitivity - Continuity Equation - Pressure device. — represents the sensitivity using the discrete approach. X represents sensitivities computed by the continuous approach

# Chapter 5

## Equations in the Low Mach number limit

### 5.1 The Eigenvalue Problem

It is common to find combustors operating under low Mach number conditions (Culick, 2006), therefore, the former analyses can be greatly simplified considering this regime. There are a few points to make before writing up the equations: the first one is that under no mean flow, the continuity equation and the energy equation in terms of pressure represent the same dynamics<sup>1</sup> since they are just related by the isentropic relationship  $\bar{c}^2 = p'/\rho' = \bar{c}^2 = \gamma\bar{p}/\bar{\rho}$ . Dowling and Stow (2003) show the effect of the jumps in this limit, concluding that the continuity jump condition is in fact better stated by the energy jump condition. The third point is that there are no convective modes associated, since there is no mean flow considered. The former statement can be proved by looking at the solutions of the system given by the governing equations, which produce the simple wave equation. The following analysis follows the same line as in chapter 2, so it will not be carried out in detail. The governing equations for zero mean flow are:

$$\bar{\rho} \frac{\partial u'}{\partial t} + \frac{\partial p'}{\partial x} = 0 \quad (5.1a)$$

$$\frac{\partial p'}{\partial t} + \gamma\bar{p} \frac{\partial u'}{\partial x} = 0 \quad (5.1b)$$

---

<sup>1</sup>For the computed sensitivities, this means that a feedback to the continuity equation will look very similar to that of the energy equation.

The jump conditions:

$$[p']_{b^-}^{b^+} = 0 \quad (5.2a)$$

$$\frac{\gamma}{(\gamma - 1)} [\bar{p}u']_{b^-}^{b^+} = \beta u(b^-, t - \tau) \quad (5.2b)$$

Following the same definitions from chapter 2, the eigenvalue problem gives:

$$L(s)\hat{q} = \mathbf{0} \quad (5.3)$$

$$\begin{bmatrix} 1 + R_u e^{-s\tau_u} & -(1 + R_d e^{-s\tau_d}) \\ (1 - R_u e^{-s\tau_u}) \left(1 + \frac{\gamma-1}{\gamma\bar{p}_1} \beta e^{-s\tau}\right) & \frac{\bar{c}_2}{\bar{c}_1} (1 - R_d e^{-s\tau_d}) \end{bmatrix} \begin{bmatrix} G_1 \\ F_2 \end{bmatrix} = \begin{bmatrix} 0 \\ 0 \end{bmatrix} \quad (5.4)$$

For the same system that has been considered so far (table 2.1) but assuming zero mean flow, the mode shapes for the first unstable eigenvalue  $s_1 = (147.75 + 2190.75i)s^{-1}$  are shown in figure 5.1. Notice that the eigenvalue has now become more unstable, effectively showing that mean flow stabilizes the system.

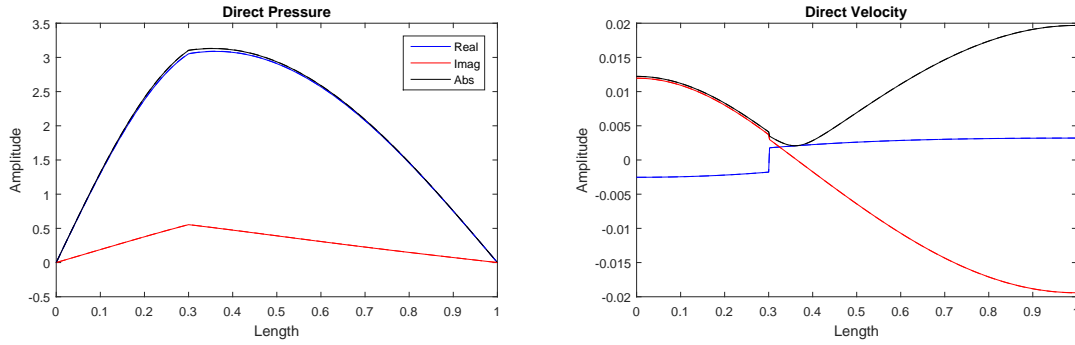


Fig. 5.1 Pressure and velocity mode shapes under low Mach number conditions.

## 5.2 Sensitivity analysis using a discrete approach

### 5.2.1 Base state sensitivity



The eigenvalue drift formula does not change, however its components do. The derivative matrix  $(\partial L(s_j, p)/\partial s_j|_{s_j, p_0})$  is calculated analytically as:

$$\frac{\partial L(s_j)}{\partial s_j} \Big|_{s_j} = \begin{bmatrix} -\tau_u R_u e^{-s_j \tau_u} & \tau_d R_d e^{-s_j \tau_d} \\ \tau_u R_u e^{-s_j \tau_u} + \frac{\gamma-1}{\gamma\bar{p}_1} \beta e^{-s_j \tau} (R_u e^{-s_j \tau_u} (\tau_u + \tau) - \tau) & \frac{\bar{c}_2}{\bar{c}_1} (\tau_d R_d e^{-s_j \tau_d}) \end{bmatrix} \quad (5.5)$$



The base state sensitivity matrices under no mean flow are:

$$\frac{\partial L}{\partial R_u} = \begin{bmatrix} e^{-s_j \tau_u} & 0 \\ -e^{-s_j \tau_u} \left(1 + \frac{\gamma-1}{\gamma \bar{p}_1} \beta e^{-s_j \tau}\right) & 0 \end{bmatrix} \quad (5.6a)$$

$$\frac{\partial L}{\partial R_d} = \begin{bmatrix} 0 & -e^{-s_j \tau_d} \\ 0 & -\frac{\bar{c}_2}{\bar{c}_1} e^{-s_j \tau_d} \end{bmatrix} \quad (5.6b)$$

$$\frac{\partial L}{\partial \tau_u} = \begin{bmatrix} -s_j R_u e^{-s_j \tau_u} & 0 \\ s_j R_u e^{-s_j \tau_u} \left(1 + \frac{\gamma-1}{\gamma \bar{p}_1} \beta e^{-s_j \tau}\right) & 0 \end{bmatrix} \quad (5.6c)$$

$$\frac{\partial L}{\partial \tau_d} = \begin{bmatrix} 0 & s_j R_d e^{-s_j \tau_d} \\ 0 & s_j \frac{\bar{c}_2}{\bar{c}_1} R_d e^{-s_j \tau_d} \end{bmatrix} \quad (5.6d)$$

$$\frac{\partial L}{\partial \tau} = \begin{bmatrix} 0 & 0 \\ -(1 - R_u e^{-s_j \tau_u}) \left(s_j \frac{\gamma-1}{\gamma \bar{p}_1} \beta e^{-s_j \tau}\right) & 0 \end{bmatrix} \quad (5.6e)$$

$$\frac{\partial L}{\partial \beta} = \begin{bmatrix} 0 & 0 \\ (1 - R_u e^{-s_j \tau_u}) \left(\frac{\gamma-1}{\gamma \bar{p}_1} e^{-s_j \tau}\right) & 0 \end{bmatrix} \quad (5.6f)$$

The base state sensitivities are shown in table 5.1. Notice that compared to the mean flow values, the orders of magnitude are exactly the same. The magnitude of the real part (sensitivity to growth rate) varies by around 15 percent which is explained by the change in the eigenvalue. The magnitude of the imaginary part (sensitivity to frequency) varies by around 10 percent or less.



Base state Variable	Value
$R_u$	$(-1.9187 + 1.3741i) \cdot 10^2 \text{ s}^{-1}$
$R_d$	$(-4.0400 - 1.0590i) \cdot 10^2 \text{ s}^{-1}$
$\tau_u$	$(-3.2939 - 4.0004i) \cdot 10^5 \text{ s}^{-1}$
$\tau_d$	$(+1.7231 - 9.0073i) \cdot 10^5 \text{ s}^{-1}$
$\tau$	$(-0.4422 - 3.3177i) \cdot 10^5 \text{ s}^{-1}$
$\beta$	$(+4.2253 - 0.2756i) \cdot 10^{-4} \text{ s}^{-1}$

Table 5.1 Base state sensitivities for the first unstable eigenvalue of the network characterized by table 2.1 under zero mean flow ( $s_1 = (147.75 + 2190.75i)\text{s}^{-1}$ )

## 5.2.2 Structural sensitivity

After following the same procedures as in chapter 3 the perturbed eigenvalue problem becomes:

$$(\mathbf{L}(s) + \delta\mathbf{L})\hat{\mathbf{q}} = \mathbf{0} \quad (5.7)$$

Where the perturbation terms  $\delta\mathbf{L}$  are:

$$\delta\mathbf{L} = \begin{bmatrix} 0 & 0 \\ \mathbf{Q} & 0 \end{bmatrix} + \begin{bmatrix} \mathbf{P}_1 & \mathbf{P}_2 \end{bmatrix} \quad (5.8)$$

$$\mathbf{Q} = \frac{(\gamma - 1)}{\gamma\bar{p}_1} \beta e^{-s\tau} \frac{1}{2} \left( \epsilon_{p_1} \begin{bmatrix} 1 & -1 & -1 & 1 \end{bmatrix} + \frac{\epsilon_{u_1}}{\bar{\rho}_1\bar{c}_1} \begin{bmatrix} -1 & 1 & -1 & 1 \end{bmatrix} \right) \begin{bmatrix} 1 \\ e^{s\tau_a} \\ R_u e^{-s\tau_u} \\ R_d e^{-s(\tau_u + \tau_a)} \end{bmatrix} \quad (5.9)$$

$$\mathbf{P}_1 = \frac{1}{2} \left( \epsilon_{p_1} \begin{bmatrix} 1 & 1 & 1 & 1 \\ 1 & -1 & -1 & 1 \end{bmatrix} + \frac{\epsilon_{u_1}}{\bar{\rho}_1\bar{c}_1} \begin{bmatrix} -1 & -1 & 1 & 1 \\ -1 & 1 & -1 & 1 \end{bmatrix} \right) \begin{bmatrix} 1 \\ e^{s\tau_a} \\ R_u e^{-s\tau_u} \\ R_d e^{-s(\tau_u + \tau_a)} \end{bmatrix} \quad (5.10)$$

$$\mathbf{P}_2 = \frac{1}{2} \begin{bmatrix} 1 & 0 \\ 0 & \frac{\bar{c}_2}{\bar{c}_1} \end{bmatrix} \left( \epsilon_{p_2} \begin{bmatrix} 1 & 1 & 1 & 1 \\ -1 & 1 & 1 & -1 \end{bmatrix} + \frac{\epsilon_{u_2}}{\bar{\rho}_2\bar{c}_2} \begin{bmatrix} 1 & 1 & -1 & -1 \\ -1 & 1 & -1 & 1 \end{bmatrix} \right) \begin{bmatrix} 1 \\ e^{-s\tau_c} \\ R_d e^{-s\tau_d} \\ R_d e^{-s(-\tau_c + \tau_d)} \end{bmatrix} \quad (5.11)$$

In these equations the influence of a device is denoted by  $\epsilon$  which resembles the mechanism used in turn, in this case they correspond to a perturbation to the momentum equation ( $\mathcal{F}$ ). Sensitivity plots (fig. 5.2) match closely those derived under mean flow conditions, so a similar argument on the devices available to control unstable modes can be done.

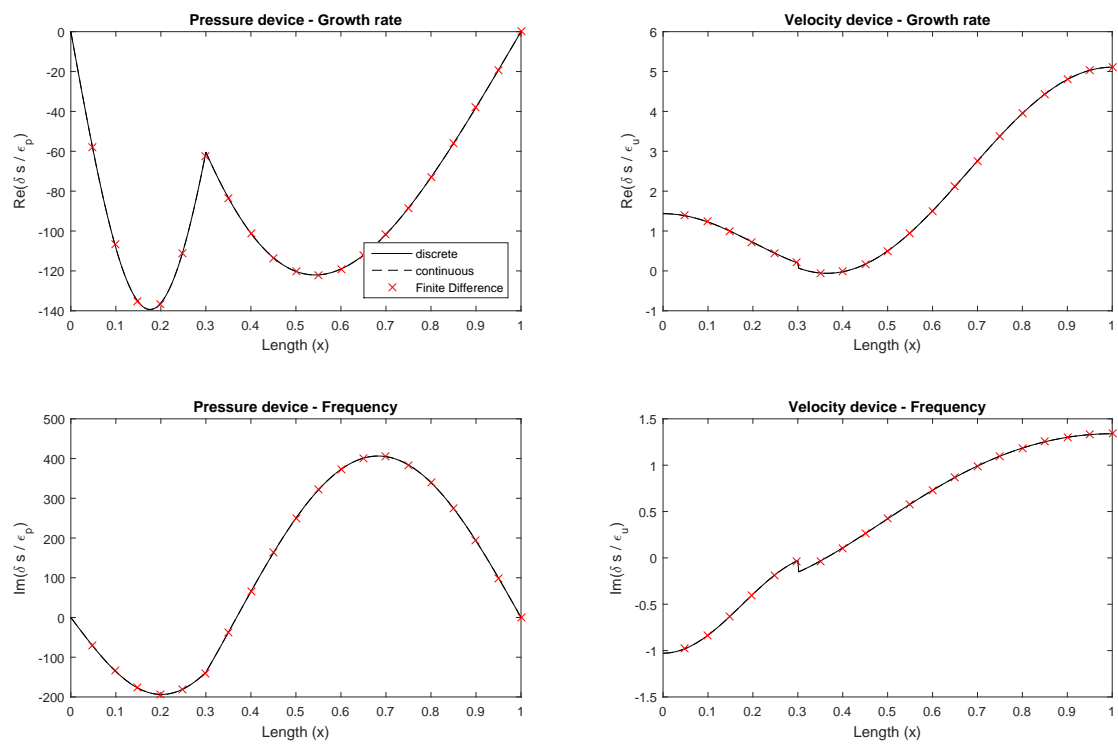


Fig. 5.2 Structural sensitivities acting on the momentum equation using three methods: Discrete, Continuous and Finite difference

### 5.3 Notes on the continuous approach

The continuous adjoint equations can be recovered by taking the limit when  $\bar{u} \rightarrow 0$ , considering that the mass equation is redundant as explained before. Or else the adjoint system can be obtained following the same procedure as in chapter 3. The adjoint equations are:

$$\frac{\partial p^+}{\partial t} + \frac{\partial u^+}{\partial x} = 0 \quad (5.12a)$$

$$\bar{\rho} \frac{\partial u^+}{\partial t} + \gamma \bar{p} \frac{\partial p^+}{\partial x} = 0 \quad (5.12b)$$

Notice that with one variable change the direct equations can be recovered, therefore the parts of the duct governed by this equations, that is the acoustics, are self adjoint. The jump conditions are:

$$p_1^+ - p_2^+ = \frac{(\gamma - 1)}{\gamma \bar{p}_1} \beta p_2^+(t + \tau) \quad (5.13a)$$

$$u_1^+ - u_2^+ = 0 \quad (5.13b)$$

which are essentially different to the direct ones since the heat release term switched to the adjoint pressure jump condition, therefore the system as a whole is not self-adjoint due to the unsteady heat release. The eigenvalue problem becomes:

$$L^+(s) \hat{\mathbf{q}}^+ = \mathbf{0} \quad (5.14)$$

$$\begin{bmatrix} 1 + R_{ua}^{-1} e^{-s\tau_u} & -(1 + R_{da}^{-1} e^{-s\tau_d}) \left(1 + \frac{(\gamma-1)}{\gamma \bar{p}_1} \beta e^{-s\tau}\right) \\ (1 - R_{ua}^{-1} e^{-s\tau_u}) & \frac{\bar{c}_2}{\bar{c}_1} (1 - R_{da}^{-1} e^{-s\tau_d}) \end{bmatrix} \begin{bmatrix} F_1^+ \\ G_2^+ \end{bmatrix} = \begin{bmatrix} 0 \\ 0 \end{bmatrix} \quad (5.15)$$

An important note on this matrix is that it is not Hermitian even without heat release, that is, the conjugate transpose of matrix L is not the same as the one derived through the continuous equations. But it is important to note that without heat release both systems are effectively solving the same set of equations, therefore being self-adjoint.

# Chapter 6


## Conclusions and Future Work

### 6.1 Conclusions

This report presents most of the work done during the first months of the PhD program. In the first chapters convenient literature has been summarized making emphasis on their usefulness or applicability to the project, which is to develop the adjoint of a network model. Direct applications of the results of this project would be to implement this methods in software running low order thermoacoustic networks, to increase the information available for design purposes.


Throughout the report several advantages of the adjoint methods have been brought to light, being the easiness to compute sensitivities the one exploited. As seen in chapters 2 and 3 they provide a direct method to compute the base state sensitivities, or the structural sensitivity maps. A discrete approach and a continuous approach were used to compute most of the sensitivities, it is clear that each method provides different insight into the problem. The discrete method gives a better picture of the what happens to the matrix  $L$  when it is perturbed by intrinsic feedback. However, the continuous adjoint provides a different perspective by showing through the mode shapes the regions that the equations are more sensitive to.

The information that the adjoint method provides is quite useful. In terms of base state sensitivity, they allow the user to know which parameter is the one that affects the eigenvalue the most so that it can be changed to stabilize the system. In some cases the parameters may be difficult to change, however their impact in the eigenvalue can be assessed in the same way. In terms of the structural sensitivity maps, several devices already discussed in literature (Magri and Juniper, 2013b) and proved experimentally (Rigas et al., 2015), where shown to appear even under the presence of mean flow, extending their applicability to this regime. This brings the last important

point discussed through the report  which is the example of how a mean flow helps stabilize the system at least when compared to that on the low Mach number limit.

The content of this report opens the possibility of several applications that will be discussed further in the next section.

## 6.2 Future Work

 From the work done in this report, one of the next step is to implement adjoint methods in the Low Order Thermoacoustic Network (LOTAN) software developed at the University of Cambridge and currently used by Rolls Royce. It is clear that the implementation is not straightforward and that work needs to be done to consider, for example, different types of geometries (annular combustors), changes in cross sectional areas, different types of flames, etc. However, the baseline for this implementation is already set.

On the other hand, a thermoacoustic Helmholtz solver based on a finite element method is going to be developed. This project has already been started by Prof. Juniper and has been proven to be feasible. The project will be done by using the FEniCS project (<http://fenicsproject.org/>) Python based finite element solver. The major aim of this project is to develop a a 2D - 3D thermoacoustic model that can predict the unstable modes of a combustor. The next step will be to derive the adjoint of the system. This stage would be crucial to get all the gradient information available which will lead to obtain all the sensitivities to the parameters apart from the geometry, which include the flame model used. Finally, taking advantage of the adjoint information, the sensitivities due to changes to the shape of the boundary will be obtained and this will be used in the final stage of the project which is to perform shape optimization. For this project proper shape optimization literature is to be reviewed, such as the calculus of moving surfaces as well as Hadamard's formulas for the variations of the eigenvalues at moving boundaries.

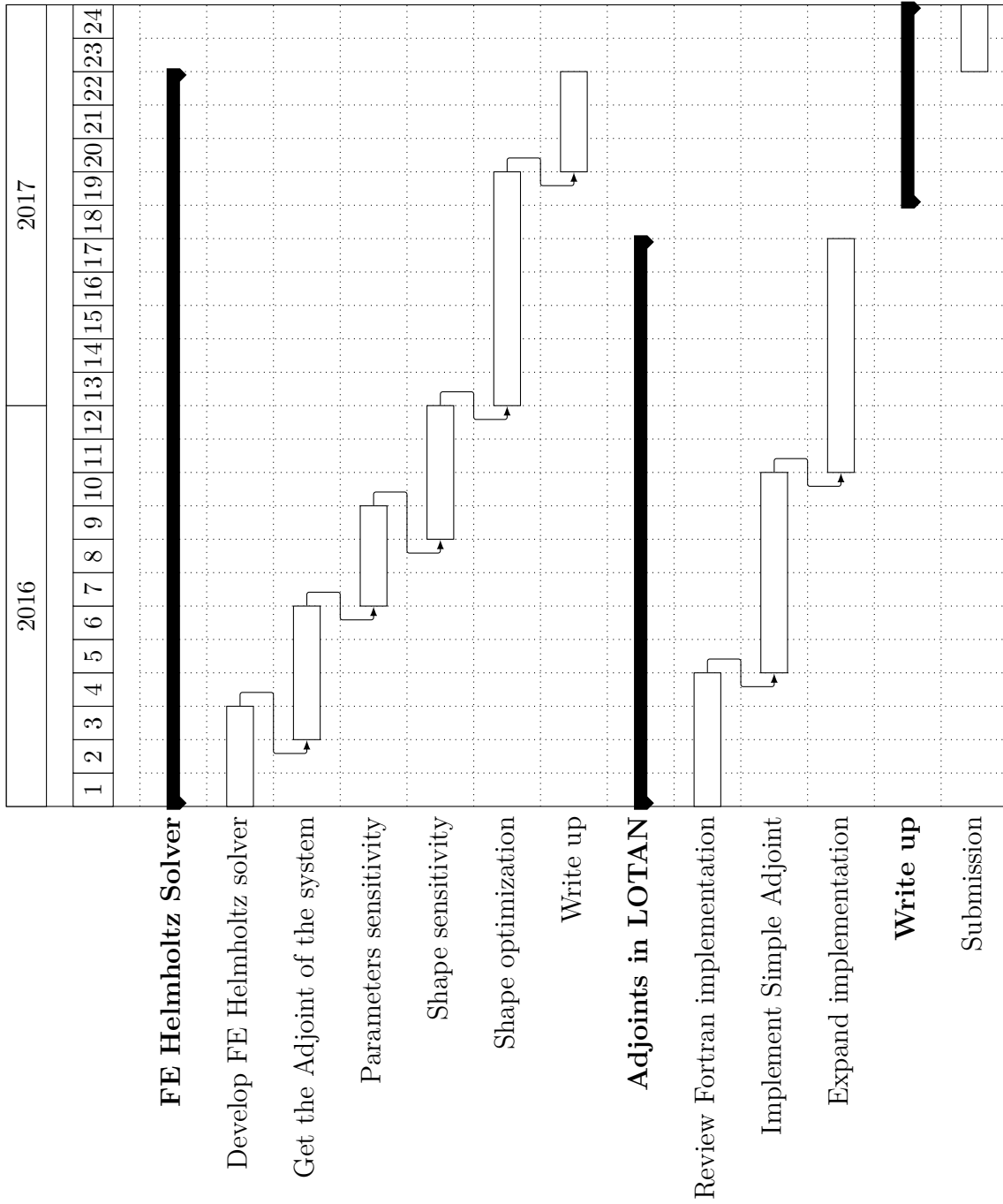


Fig. 6.1 Gantt Chart of research plan.



# References

- Anderson, J. D. J. (2003). *Modern compressible flow*. 3rd edition.
- Balasubramanian, K. (2008). Non-normality and nonlinearity in combustion – acoustic interaction in diffusion flames. *Journal of Fluid Mechanics*, 594:29–57.
- Chu, B.-T. and Kovásznyai, L. S. G. (1958). Non-linear interactions in a viscous heat-conducting compressible gas.
- Culick, F. E. C. (2006). *Unsteady Motions in Combustion Chambers for Propulsion Systems*, volume 323. RTO AGARDograph/AG-AVT-039. North Atlantic Treaty Organization (NATO).
- Dowling, A. (1995). The Calculation of Thermoacoustic Oscillations. *Journal of Sound and Vibration*, 180(4):557–581.
- Dowling, A. P. (1997). Nonlinear self-excited oscillations of a ducted flame. *Journal of Fluid Mechanics*, 346:271–290.
- Dowling, A. P. and Stow, S. R. (2003). Acoustic Analysis of Gas Turbine Combustors Introduction. *Journal of Propulsion and Power*, 19(5):751–764.
- Duran, I. and Moreau, S. (2013). Solution of the quasi-one-dimensional linearized Euler equations using flow invariants and the Magnus expansion. *Journal of Fluid Mechanics*, 723:190–231.
- Evans, L. C. (2010). *Partial Differential Equations*.
- Freund, J. B. (2011). Adjoint-based optimization for understanding and suppressing jet noise. *Journal of Sound and Vibration*, 330(17):4114–4122.
- Giannetti, F. and Luchini, P. (2007). *Structural sensitivity of the first instability of the cylinder wake*, volume 581.
- Goh, C. S. and Morgans, A. S. (2012). The Influence of Entropy Waves on the Thermoacoustic Stability of a Model Combustor. *Combustion Science and Technology*, (March):120816123400009.
- Gunzburger, M. (1997). Introduction into mathematical aspects of flow control and optimization. In *von Karman Institute for Fluid Dynamics*.
- Higgins, B. (1802). On the sound produced by a current of hydrogen gas passing through a tube. *Journal of Natural Philosophy, Chemistry and the Arts*, I:129–131.

- Hill, D. C. (1992). A theoretical approach for analyzing the restabilization of wakes. In *Presented at AIAA Aersopce Science Meeting Exhib. 30th, Reno, NV, AIAA Pap.*, volume 0067.
- Jameson, A. (1995). Optimum aerodynamic design using CFD and control theory.
- Juniper, B. M., Magri, L., and Bauerheim, M. (2014). Sensitivity analysis of thermoacoustic eigenproblems with adjoint methods. *Proceedings of the Summer Program 2014*.
- Juniper, M. P. (2011). Triggering in the horizontal Rijke tube: non-normality, transient growth and bypass transition. *Journal of Fluid Mechanics*, 667:272–308.
- Juniper, M. P. (2015). Adjoint and Passive Control in Thermoacoustics. In *21st CISM-IUTAM International Summer School on Measurement, Analysis, and Passive Control of Thermoacoustic Oscillations, Udine, Italy*, number June, pages 1–30.
- Juniper, M. P. and Magri, L. (2014). Application of receptivity and sensitivity analysis to thermoacoustic instability. In *Progress in Flow Instability Analysis and Laminar-Turbulent Transition Modeling Lecture Series.*, von Karman Institute for Fluid Dynamics.
- Lieuwen, T. (2001). Theoretical investigation of unsteady flow interactions with a premixed planar flame. *Journal of Fluid Mechanics*, 435:289–303.
- Lieuwen, T. (2003). Modeling Premixed Combustion-Acoustic Wave Interactions: A Review. *Journal of Propulsion and Power*, 19(5):765–781.
- Lieuwen, T., Torres, H., Johnson, C., and Zinn, B. T. (2001). A Mechanism of Combustion Instability in Lean Premixed Gas Turbine Combustors. *Journal of Engineering for Gas Turbines and Power*, 123(1):182.
- Lieuwen, T. C. (2012). *Unsteady Combustor Physics*. 1st edition.
- Luchini, P. and Bottaro, A. (2014a). Adjoint Equations in Stability Analysis. *Annual Review of Fluid Mechanics*, 46(1):493–517.
- Luchini, P. and Bottaro, A. (2014b). An introduction to adjoint problems. *Annual Review of Fluid Mechanics*, 46(1):493–517.
- Luchini, P., Giannetti, F., and Pralits, J. (2009). Structural Sensitivity of the Finite-Amplitude Vortex Shedding Behind a Circular Cylinder. In Braza, M. and Hourigan, K., editors, *IUTAM Symposium on Unsteady Separated Flows and their Control*, pages 151–160, New York. Springer.
- Magri, L. (2015). *Adjoint methods in thermo-acoustic and combustion instability*. PhD thesis.
- Magri, L., Balasubramanian, K., Sujith, R. I., and Juniper, M. P. (2013). Non-normality in combustion–acoustic interaction in diffusion flames: a critical revision. *Journal of Fluid Mechanics*, 733:681–683.

- Magri, L. and Juniper, M. P. (2013a). A Theoretical Approach for Passive Control of Thermoacoustic Oscillations: Application to Ducted Flames. *Journal of Engineering for Gas Turbines and Power*, 135(9):091604.
- Magri, L. and Juniper, M. P. (2013b). Sensitivity analysis of a time-delayed thermoacoustic system via an adjoint-based approach. *Journal of Fluid Mechanics*, 719:183–202.
- Magri, L. and Juniper, M. P. (2014a). Adjoint-based linear analysis in reduced-order thermo-acoustic models. *International journal of spray and combustion dynamics*, 6(3).
- Magri, L. and Juniper, M. P. (2014b). Global modes, receptivity, and sensitivity analysis of diffusion flames coupled with duct acoustics. *Journal of Fluid Mechanics*, 752:237–265.
- Magri, L., See, Y. C., Ihme, M., and Juniper, M. P. (2014). Multiple-scale adjoint sensitivity analysis of hydrodynamic / thermo-acoustic instability in turbulent combustion chambers. *Center for Turbulence Research, Summer Program*, (Balaji 2012):199–208.
- Marble, F. and Candel, S. (1977). Acoustic disturbance from gas non-uniformities convected through a nozzle. *Journal of Sound and Vibration*, 55(2):225–243.
- Marino, L. and Luchini, P. (2009). Adjoint analysis of the flow over a forward-facing step. *Theoretical and Computational Fluid Dynamics*, 23(1):37–54.
- Marquet, O., Sipp, D., and Jacquin, L. (2008). Sensitivity analysis and passive control of cylinder flow. *Journal of Fluid Mechanics*, 615:221–252.
- Morgans, A. S. (2015). Low order modelling of combustion instabilities. Technical report, Montestigliano workshop.
- Morgans, a. S. and Annaswamy, a. M. (2008). Adaptive Control of Combustion Instabilities for Combustion Systems with Right-Half Plane Zeros. *Combustion Science and Technology*, 180(9):1549–1571.
- Nicoud, F., Benoit, L., Sensiau, C., and Poinso, T. (2007). Acoustic Modes in Combustors with Complex Impedances and Multidimensional Active Flames. *AIAA Journal*, 45(2):426–441.
- Nicoud, F. and Poinso, T. (2005). Thermoacoustic instabilities: Should the Rayleigh criterion be extended to include entropy changes? *Combustion and Flame*, 142(1-2):153–159.
- Nielsen, E. J., Diskin, B., and Yamaleev, N. K. (2010). Discrete Adjoint-Based Design Optimization of Unsteady Turbulent Flows on Dynamic Unstructured Grids. *AIAA Journal*, 48(6):1195–1206.
- Pralits, J. O., Brandt, L., and Giannetti, F. (2010). Instability and sensitivity of the flow around a rotating circular cylinder. *Journal of Fluid Mechanics*, 650:513.

- Qadri, U. A., Mistry, D., and Juniper, M. P. (2013). Structural sensitivity of spiral vortex breakdown. *Journal of Fluid Mechanics*, 720(1957):558–581.
- Rayleigh, L. (1878). The Explanation of Certain Acoustical Phenomena. *Nature*, 18:319–321.
- Rigas, G., Jamieson, N. P., Li, L. K. B., and Juniper, M. P. (2015). Experimental sensitivity analysis and control of thermoacoustic systems. *Journal of Fluid Mechanics*, Submitted.
- Schmid, P. J. and Brandt, L. (2014). Analysis of fluid systems: stability, receptivity, sensitivity. *Applied Mechanics Reviews*, 66(March 2014).
- Spagnoli, B. and Airiau, C. (2008). Adjoint analysis for noise control in a two-dimensional compressible mixing layer. *Computers & Fluids*, 37(4):475–486.
- Stow, S. R. and Dowling, A. P. (2001). Thermoacoustic oscillations in an annular combustor. *ASME Turbo Expo*, pages 2001–GT–0037.
- Strykowski, P. J. and Sreenivasan, K. R. (1990). On the formation and suppression of vortex ‘shedding’ at low Reynolds numbers. *Journal of Fluid Mechanics*, 218(-1):71.
- Yu, K. H., Trouvé, A., and Daily, J. W. (1991). Low-frequency pressure oscillations in a model ramjet combustor. *Journal of Fluid Mechanics*, 232(-1):47.

# Appendix A

## Derivation of the jump conditions

Consider the network from section 2.1. Begin with the continuity, momentum and energy equations (assume no viscosity and no heat conduction):

$$\frac{D\rho}{Dt} + \rho \nabla \cdot \mathbf{u} = 0 \quad (\text{A.1a})$$

$$\rho \frac{D\mathbf{u}}{Dt} = -\nabla p \quad (\text{A.1b})$$

$$\frac{Dp}{Dt} = -\gamma p \nabla \cdot \mathbf{u} + (\gamma - 1)q \quad (\text{A.1c})$$

Considering flow in 1D:

$$\frac{\partial \rho}{\partial t} + u \frac{\partial \rho}{\partial x} + \rho \frac{\partial u}{\partial x} = 0 \quad (\text{A.2a})$$

$$\rho \frac{\partial u}{\partial t} + \rho u \frac{\partial u}{\partial x} = -\frac{\partial p}{\partial x} \quad (\text{A.2b})$$

$$\frac{\partial p}{\partial t} + u \frac{\partial p}{\partial x} = -\gamma p \frac{\partial u}{\partial x} + (\gamma - 1)q \quad (\text{A.2c})$$

The heat release ( $q$ ) will only be appearing at the flame ( $x = b$ ), for the rest of the ducts it will be equal to zero, hence, it will be treated as a jump. Following the assumption that it is thin enough compared to the wavelength of the acoustic fluctuations, to get the jump conditions, assume a steady state and neglect accumulation terms (i.e time derivatives):

**Continuity:**

$$u \frac{d\rho}{dx} + \rho \frac{du}{dx} = 0$$
$$\frac{d(\rho u)}{dx} = 0 \quad (\text{A.3})$$

**Momentum:**

Use equation (A.3) multiplied by  $u$ :

$$\begin{aligned} \frac{dp}{dx} + \rho u \frac{du}{dx} &= 0 \\ \frac{dp}{dx} + \rho u \frac{du}{dx} + u \frac{d(\rho u)}{dx} &= 0 \\ \frac{dp}{dx} + \frac{d(\rho u^2)}{dx} &= 0 \end{aligned} \quad (\text{A.4})$$

**Energy:**

Rearrange and use equations (A.3) and (A.4):

$$\begin{aligned} u \frac{dp}{dx} + \gamma p \frac{du}{dx} &= (\gamma - 1)q \\ u \frac{dp}{dx} + \gamma \frac{d(pu)}{dx} - \gamma u \frac{dp}{dx} &= (\gamma - 1)q \\ \gamma \frac{d(pu)}{dx} - (\gamma - 1)u \frac{dp}{dx} &= (\gamma - 1)q \\ \frac{\gamma}{(\gamma - 1)} \frac{d(pu)}{dx} + \rho u \cdot u \frac{du}{dx} &= q \\ \frac{\gamma}{(\gamma - 1)} \frac{d(pu)}{dx} + \rho u \frac{d\left(\frac{1}{2}u^2\right)}{dx} &= q \\ \frac{\gamma}{(\gamma - 1)} \frac{d(pu)}{dx} + \frac{d\left(\frac{1}{2}\rho u^3\right)}{dx} &= q \end{aligned} \quad (\text{A.5})$$

Integrating over the flame (located at  $x = b$ , and assuming that the slight variation of  $\gamma$  with temperature is negligible, the jump conditions are obtained:

$$\int_{b^-}^{b^+} \left( \frac{d(\rho u)}{dx} \right) dx = 0 \quad [\rho u]_{b^-}^{b^+} = 0 \quad (\text{A.6})$$

$$\int_{b^-}^{b^+} \left( \frac{dp}{dx} + \frac{d(\rho u^2)}{dx} \right) dx = 0 \quad [p + \rho u^2]_{b^-}^{b^+} = 0 \quad (\text{A.7})$$

$$\int_{b^-}^{b^+} \left( \frac{\gamma}{(\gamma - 1)} \frac{d(pu)}{dx} + \frac{d\left(\frac{1}{2}\rho u^3\right)}{dx} \right) dx = \int_{b^-}^{b^+} q dx \quad \frac{\gamma}{(\gamma - 1)} [pu]_{b^-}^{b^+} + \left[ \frac{1}{2}\rho u^3 \right]_{b^-}^{b^+} = q(b, t) \quad (\text{A.8})$$

# Appendix B

## Derivation of the nonlinear eigenvalue drift formula

The matrix  $L$  from equation 2.26 produces a nonlinear eigenvalue problem for  $s$  of the following form:

$$L(s_j, p)\hat{\mathbf{q}} = \mathbf{0} \quad (\text{B.1})$$

where  $s_j$  is the eigenvalue,  $p$  are the internal parameters of the operator ( $L$ ), and  $\hat{\mathbf{q}}$  is the eigenvector. For the same problem, there exists an adjoint eigenvector  $\hat{\mathbf{q}}^\dagger$  that satisfies:

$$(\hat{\mathbf{q}}^\dagger)^H L(s_j, p) = \mathbf{0} \quad (\text{B.2})$$

By making a small change to the matrix parameters  $p = p_0 + \epsilon\delta p$ , the eigenvalue will change from  $s_j$  to  $s_j + \epsilon\delta s$ , and the eigenvector from  $\hat{\mathbf{q}}$  to  $\hat{\mathbf{q}} + \epsilon\delta\hat{\mathbf{q}}$ . That is:

$$L(s_j + \epsilon\delta s, p_0 + \epsilon\delta p)(\hat{\mathbf{q}} + \epsilon\delta\hat{\mathbf{q}}) = \mathbf{0} \quad (\text{B.3})$$

Performing a Taylor expansion to first order in two variables<sup>1</sup> gives:

$$\left( L(s_j, p) + \frac{\partial L(s_j, p)}{\partial s_j} \Big|_{s_j, p_0} \epsilon\delta s + \frac{\partial L(s_j, p)}{\partial p} \Big|_{s_j, p_0} \epsilon\delta p \right) (\hat{\mathbf{q}} + \epsilon\delta\hat{\mathbf{q}}) = \mathbf{0} \quad (\text{B.4})$$

Gathering all of the terms of order  $\epsilon$ :

$$L(s_j, p)\delta\hat{\mathbf{q}} + \delta s \frac{\partial L(s_j, p)}{\partial s_j} \Big|_{s_j, p_0} \hat{\mathbf{q}} + \delta p \frac{\partial L(s_j, p)}{\partial p} \Big|_{s_j, p_0} \hat{\mathbf{q}} = \mathbf{0} \quad (\text{B.5})$$

---

<sup>1</sup>Using:  $f(x + \Delta x, y + \Delta y) \approx f(x, y) + f_x(x, y)\Delta x + f_y(x, y)\Delta y$

Note that from the definition of the partial derivative, for small  $\delta p$ :

$$\left. \frac{\partial L(s_j, p)}{\partial p} \right|_{s_j, p_0} \approx \frac{L(s_j, p_0 + \delta p) - L(s_j, p_0)}{\delta p} \quad (\text{B.6})$$

Rearranging:

$$\delta p \left. \frac{\partial L(s_j, p)}{\partial p} \right|_{s_j, p_0} \approx L(s_j, p_0 + \delta p) - L(s_j, p_0) = \delta L(s_j, p_0) \quad (\text{B.7})$$



Hence, that the last element of Eq. (B.5) represents the matrix that contains all the perturbed elements. Pre-multiplying that equation by  $(\hat{q}^\dagger)^H$  gives:

$$(\hat{q}^\dagger)^H L(s_j, p) \delta \hat{q} + \delta s (\hat{q}^\dagger)^H \left. \frac{\partial L(s_j, p)}{\partial s_j} \right|_{s_j, p_0} \hat{q} + (\hat{q}^\dagger)^H \delta L(s_j, p_0) \hat{q} = \mathbf{0} \quad (\text{B.8})$$



By definition (Eq. B.2) the first term in the last equation is zero, so it gives:

$$\delta s (\hat{q}^\dagger)^H \left. \frac{\partial L(s_j, p)}{\partial s_j} \right|_{s_j, p_0} \hat{q} = -(\hat{q}^\dagger)^H \delta L(s_j, p_0) \hat{q} \quad (\text{B.9})$$

Rearranging gives the eigenvalue drift:

$$\delta s = - \frac{(\hat{q}^\dagger)^H \delta L(s_j, p_0) \hat{q}}{(\hat{q}^\dagger)^H \left. \frac{\partial L(s_j, p)}{\partial s_j} \right|_{s_j, p_0} \hat{q}} \quad (\text{B.10})$$

# Appendix C

## Taylor Tests for Base State sensitivities

Taylor tests as described in section 3.2.1 are shown here for all computed bases state variables.

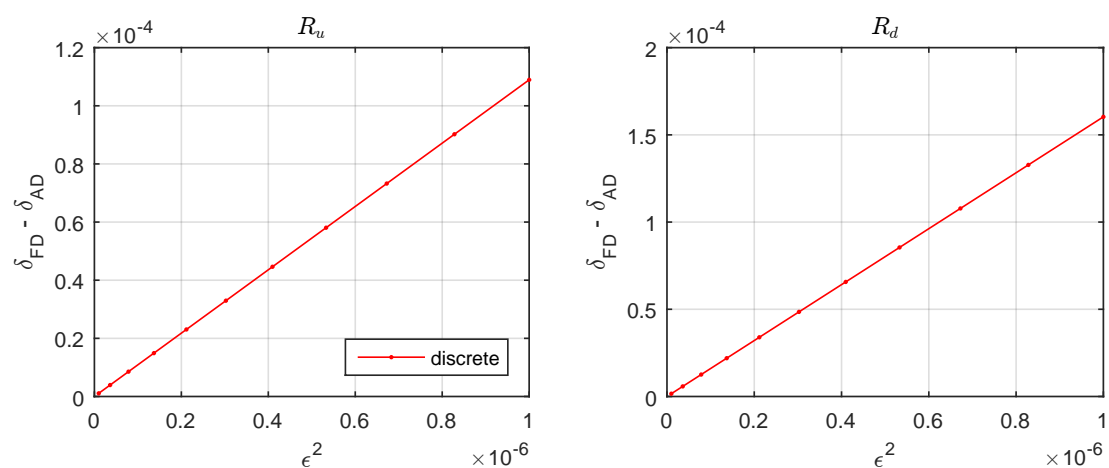


Fig. C.1 Taylor test for base state variables: reflection coefficients ( $R_u$ ,  $R_d$ ).

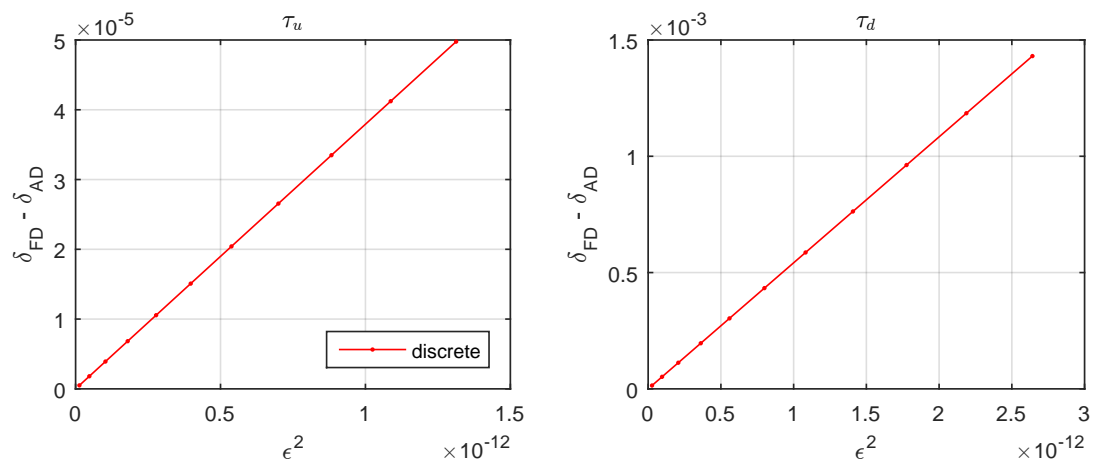


Fig. C.2 Taylor test for base state variables: time delays ( $\tau_u, \tau_d$ ).

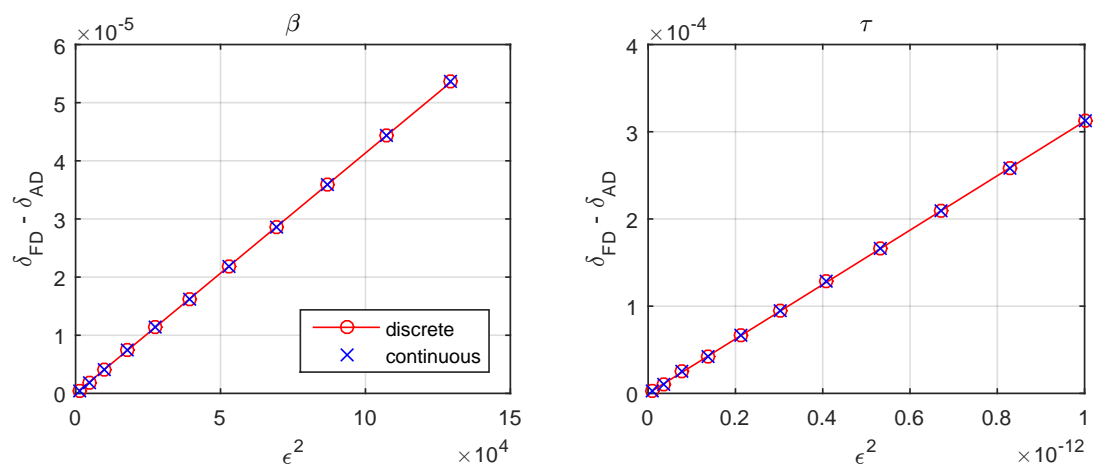


Fig. C.3 Taylor test for base state variables: flame model ( $\beta, \tau$ ).

# Appendix D

## Perturbed Energy Equation in Terms of Pressure

The linearized continuity equation and the energy equation in terms of entropy are:

$$\frac{\bar{D}\rho'}{Dt} + \bar{\rho} \frac{\partial u'}{\partial x} = 0 \quad (\text{D.1})$$

$$\frac{\bar{D}s'}{Dt} = 0 \quad (\text{D.2})$$

Where the operator  $\bar{D}/Dt = \partial/\partial t + \bar{u}\partial/\partial x$ . Now add a perturbation to the continuity equation ( $\mathcal{M}$ ) and to the energy equation ( $\mathcal{S}$ ):

$$\frac{\bar{D}\rho'}{Dt} + \bar{\rho} \frac{\partial u'}{\partial x} = \mathcal{M} \quad (\text{D.3})$$

$$\frac{\bar{D}s'}{Dt} = \mathcal{S} \quad (\text{D.4})$$



Recall that from the definition of entropy  $s = c_v \ln(p/\rho^\gamma)$ , which after linearization becomes:

$$s' = c_v \frac{p'}{\bar{p}} - c_p \frac{\rho'}{\bar{\rho}} \quad (\text{D.5})$$

Assuming that the mean pressure and density are constant along the duct, this gives:

$$\frac{\bar{D}}{Dt} \left( c_v \frac{p'}{\bar{p}} - c_p \frac{\rho'}{\bar{\rho}} \right) = \mathcal{S} \quad (\text{D.6})$$

Which can be rearranged to get this expression:

$$\frac{\bar{D}p'}{Dt} - \frac{\gamma\bar{p}}{\bar{\rho}} \frac{\bar{D}\rho'}{Dt} = \frac{\mathcal{S}\bar{p}}{c_v} \quad (\text{D.7})$$

Substituting the continuity equation:

$$\frac{\bar{D}p'}{Dt} - \frac{\gamma\bar{p}}{\bar{\rho}} \left( \mathcal{M} - \bar{\rho} \frac{\partial u'}{\partial x} \right) = \frac{\mathcal{S}\bar{p}}{c_v} \quad (\text{D.8})$$

Finally (using  $\mathcal{Q} = \mathcal{S}\bar{p}/c_v$ ):

$$\frac{\bar{D}p'}{Dt} + \gamma\bar{p} \frac{\partial u'}{\partial x} = \mathcal{Q} + \bar{c}^2 \mathcal{M} \quad (\text{D.9})$$

Which explains why adding a perturbation to the continuity equation implies perturbing the energy equation if it is used in terms of pressure.

# Appendix E

## Derivation of Jump Conditions to Perturbations Added to the System



The jump conditions are derived from the perturbed equations (Eq. 3.8), neglect accumulation terms and integrate from one side to the other of the perturbation, for example, the continuity jump condition at  $x = a$  would be:

$$\bar{u}_1(\rho'_{ii} - \rho'_i) + \bar{\rho}_1(u'_{ii} - u'_i) = \mathcal{M}(a) \quad (\text{E.1})$$

Notice that the quantity  $\mathcal{M}(a)$  is no longer defined. This happens because density, pressure and velocity fluctuations are not defined at point  $a$  anymore. For the jump condition to make sense, they must acquire a value either just before ( $a^-$ ) or just after ( $a^+$ ) the perturbation. The choice of the side depends on the definition of the system, in this case system studied so far is composed of a duct, a flame and another duct resembled by sections  $ii$  and  $iii$  in figure 3.1. When the perturbations are added, the interest is to know how they produce a change on the system's eigenvalue, therefore they must come from the surroundings (sections  $i$  and  $iv$ ), so the choice for the previous example would be ( $a^-$ ):

$$\bar{u}_1(\rho'_{ii} - \rho'_i) + \bar{\rho}_1(u'_{ii} - u'_i) = \mathcal{M}(a^-) \quad (\text{E.2})$$

where

$$\mathcal{M}(a^-) = \mathcal{M}_i = \mathcal{M}_{p_1}p'_i + \mathcal{M}_{u_1}u'_i + \mathcal{M}_{r_1}\rho'_i \quad (\text{E.3})$$

Therefore, the proper definition for the perturbations added to the system should be:  
Upstream of the flame:

$$\frac{\partial \rho'}{\partial t} + \bar{u}_1 \frac{\partial \rho'}{\partial x} + \bar{\rho}_1 \frac{\partial u'}{\partial x} = \mathcal{M}_i \delta(x - a) \quad (\text{E.4a})$$

$$\bar{\rho}_1 \frac{\partial u'}{\partial t} + \bar{\rho}_1 \bar{u}_1 \frac{\partial u'}{\partial x} + \frac{\partial p'}{\partial x} = \mathcal{F}_i \delta(x - a) \quad (\text{E.4b})$$

$$\frac{\partial p'}{\partial t} + \bar{u}_1 \frac{\partial p'}{\partial x} + \gamma \bar{p}_1 \frac{\partial u'}{\partial x} = \mathcal{E}_i \delta(x - a) \quad (\text{E.4c})$$

Downstream of the flame:

$$\frac{\partial \rho'}{\partial t} + \bar{u}_2 \frac{\partial \rho'}{\partial x} + \bar{\rho}_2 \frac{\partial u'}{\partial x} = \mathcal{M}_{iv} \delta(x - c) \quad (\text{E.5a})$$

$$\bar{\rho}_2 \frac{\partial u'}{\partial t} + \bar{\rho}_2 \bar{u}_2 \frac{\partial u'}{\partial x} + \frac{\partial p'}{\partial x} = \mathcal{F}_{iv} \delta(x - c) \quad (\text{E.5b})$$

$$\frac{\partial p'}{\partial t} + \bar{u}_2 \frac{\partial p'}{\partial x} + \gamma \bar{p}_2 \frac{\partial u'}{\partial x} = \mathcal{E}_{iv} \delta(x - c) \quad (\text{E.5c})$$

The jump conditions will be:

Upstream of the flame:

$$\bar{u}_1 (\rho'_{ii} - \rho'_i) + \bar{\rho}_1 (u'_{ii} - u'_i) = \mathcal{M}_i \quad (\text{E.6a})$$

$$\bar{\rho}_1 \bar{u}_1 (u'_{ii} - u'_i) + (p'_{ii} - p'_i) = \mathcal{F}_i \quad (\text{E.6b})$$

$$\bar{u}_1 (p'_{ii} - p'_i) + \gamma \bar{p}_1 (u'_{ii} - u'_i) = \mathcal{E}_i \quad (\text{E.6c})$$

Downstream of the flame:

$$\bar{u}_2 (\rho'_{iv} - \rho'_{iii}) + \bar{\rho}_2 (u'_{iv} - u'_{iii}) = \mathcal{M}_{iv} \quad (\text{E.7a})$$

$$\bar{\rho}_2 \bar{u}_2 (u'_{iv} - u'_{iii}) + (p'_{iv} - p'_{iii}) = \mathcal{F}_{iv} \quad (\text{E.7b})$$

$$\bar{u}_2 (p'_{iv} - p'_{iii}) + \gamma \bar{p}_2 (u'_{iv} - u'_{iii}) = \mathcal{E}_{iv} \quad (\text{E.7c})$$

# Appendix F

## Perturbed Wave-Form Solutions in time and frequency domain

Upstream of the flame the perturbed wave form solutions (as seen by the flame  $x = b$ ) are:

$$f_{ii}(t) = f_1(t) + \dots \quad (\text{F.1a})$$

$$+ \frac{1}{2(M_1 + 1)} \left( \mathcal{M}_{p_1} \bar{c}_1 (f_1(t) + g_1(t - \tau_a)) + \frac{\mathcal{M}_{u_1}}{\bar{\rho}_1} (f_1(t) - g_1(t - \tau_a)) \dots \right. \\ \left. + \frac{\mathcal{M}_{r_1}}{\bar{c}_1} (f_1(t) + g_1(t - \tau_a) + \alpha_1(t + \tau_\alpha)) \right) \dots \quad (\text{F.1b})$$

$$+ \frac{1}{2(M_1 + 1)} \left( \mathcal{F}_{p_1} (f_1(t) + g_1(t - \tau_a)) + \frac{\mathcal{F}_{u_1}}{\bar{\rho}_1 \bar{c}_1} (f_1(t) - g_1(t - \tau_a)) \dots \right. \\ \left. + \frac{\mathcal{F}_{r_1}}{\bar{c}_1^2} (f_1(t) + g_1(t - \tau_a) + \alpha_1(t + \tau_\alpha)) \right) \dots \quad (\text{F.1c})$$

$$+ \frac{1}{2(M_1 + 1)} \left( \frac{\mathcal{Q}_{p_1}}{\bar{c}_1} (f_1(t) + g_1(t - \tau_a)) + \frac{\mathcal{Q}_{u_1}}{\bar{\rho}_1 \bar{c}_1^2} (f_1(t) - g_1(t - \tau_a)) \dots \right. \\ \left. + \frac{\mathcal{Q}_{r_1}}{\bar{c}_1^3} (f_1(t) + g_1(t - \tau_a) + \alpha_1(t + \tau_\alpha)) \right) \quad (\text{F.1d})$$

$$g_{ii}(t) = g_1(t) + \dots \quad (\text{F.2a})$$

$$+ \frac{1}{2(M_1 - 1)} \left( \mathcal{M}_{p_1} \bar{c}_1 (f_1(t + \tau_a) + g_1(t)) + \frac{\mathcal{M}_{u_1}}{\bar{\rho}_1} (f_1(t + \tau_a) - g_1(t)) \dots \right. \\ \left. + \frac{\mathcal{M}_{r_1}}{\bar{c}_1} (f_1(t + \tau_a) + g_1(t) + \alpha_1(t + \tau_a + \tau_\alpha)) \right) \dots \quad (\text{F.2b})$$

$$- \frac{1}{2(M_1 - 1)} \left( \mathcal{F}_{p_1} (f_1(t + \tau_a) + g_1(t)) + \frac{\mathcal{F}_{u_1}}{\bar{\rho}_1 \bar{c}_1} (f_1(t + \tau_a) - g_1(t)) \dots \right. \\ \left. + \frac{\mathcal{F}_{r_1}}{\bar{c}_1^2} (f_1(t + \tau_a) + g_1(t) + \alpha_1(t + \tau_a + \tau_\alpha)) \right) \dots \quad (\text{F.2c})$$

$$+ \frac{1}{2(M_1 - 1)} \left( \frac{\mathcal{Q}_{p_1}}{\bar{c}_1} (f_1(t + \tau_a) + g_1(t)) + \frac{\mathcal{Q}_{u_1}}{\bar{\rho}_1 \bar{c}_1^2} (f_1(t + \tau_a) - g_1(t)) \dots \right. \\ \left. + \frac{\mathcal{Q}_{r_1}}{\bar{c}_1^3} (f_1(t + \tau_a) + g_1(t) + \alpha_1(t + \tau_a + \tau_\alpha)) \right) \quad (\text{F.2d})$$

$$\alpha_{ii} = \alpha_1(t) + \dots \quad (\text{F.3a})$$

$$+ 0 \dots \quad (\text{F.3b})$$

$$+ 0 \dots \quad (\text{F.3c})$$

$$- \frac{1}{M_1} \left( \frac{\mathcal{Q}_{p_1}}{\bar{c}_1} (f_1(t - \tau_\alpha) + g_1(t - \tau_a - \tau_\alpha)) \dots \right. \\ \left. + \frac{\mathcal{Q}_{u_1}}{\bar{\rho}_1 \bar{c}_1^2} (f_1(t - \tau_\alpha) - g_1(t - \tau_a - \tau_\alpha)) \dots \right. \\ \left. + \frac{\mathcal{Q}_{r_1}}{\bar{c}_1^3} (f_1(t - \tau_\alpha) + g_1(t - \tau_a - \tau_\alpha) + \alpha_1(t)) \right) \quad (\text{F.3d})$$

Where the time delays are:

$$\tau_a = \frac{2(b-a)\bar{c}_1}{\bar{c}_1^2 - \bar{u}_1^2} \quad (\text{F.4a})$$

$$\tau_\alpha = \frac{(b-a)\bar{c}_1}{\bar{u}_1(\bar{c}_1 + \bar{u}_1)} \quad (\text{F.4b})$$

Downstream of the flame the perturbed wave form solutions (as seen by the flame  $x = b$ ) are:

$$f_{iii}(t) = f_2(t) + \dots \quad (\text{F.5a})$$

$$\begin{aligned} & - \frac{1}{2(M_2 + 1)} \left( \mathcal{M}_{p_2} \bar{c}_2 (f_2(t) + g_2(t + \tau_c)) + \frac{\mathcal{M}_{u_2}}{\bar{\rho}_2} (f_2(t) - g_2(t + \tau_c)) \dots \right. \\ & \left. + \frac{\mathcal{M}_{r_2}}{\bar{c}_2} (f_2(t) + g_2(t + \tau_c) + \alpha_2(t - \tau_\gamma)) \right) \dots \quad (\text{F.5b}) \end{aligned}$$

$$\begin{aligned} & - \frac{1}{2(M_2 + 1)} \left( \mathcal{F}_{p_2} (f_2(t) + g_2(t + \tau_c)) + \frac{\mathcal{F}_{u_2}}{\bar{\rho}_2 \bar{c}_2} (f_2(t) - g_2(t + \tau_c)) \dots \right. \\ & \left. + \frac{\mathcal{F}_{r_2}}{\bar{c}_2^2} (f_2(t) + g_2(t + \tau_c) + \alpha_2(t - \tau_\gamma)) \right) \dots \quad (\text{F.5c}) \end{aligned}$$

$$\begin{aligned} & - \frac{1}{2(M_2 + 1)} \left( \frac{\mathcal{Q}_{p_2}}{\bar{c}_2} (f_2(t) + g_2(t + \tau_c)) + \frac{\mathcal{Q}_{u_2}}{\bar{\rho}_2 \bar{c}_2^2} (f_2(t) - g_2(t + \tau_c)) \dots \right. \\ & \left. + \frac{\mathcal{Q}_{r_2}}{\bar{c}_2^3} (f_2(t) + g_2(t + \tau_c) + \alpha_2(t - \tau_\gamma)) \right) \quad (\text{F.5d}) \end{aligned}$$

$$g_{iii}(t) = g_2(t) + \dots \quad (\text{F.6a})$$

$$\begin{aligned} & - \frac{1}{2(M_2 - 1)} \left( \mathcal{M}_{p_2} \bar{c}_2 (f_2(t - \tau_c) + g_2(t)) + \frac{\mathcal{M}_{u_2}}{\bar{\rho}_2} (f_2(t - \tau_c) - g_2(t)) \dots \right. \\ & \left. + \frac{\mathcal{M}_{r_2}}{\bar{c}_2} (f_2(t - \tau_c) + g_2(t) + \alpha_2(t - \tau_c - \tau_\gamma)) \right) \dots \quad (\text{F.6b}) \end{aligned}$$

$$\begin{aligned} & + \frac{1}{2(M_2 - 1)} \left( \mathcal{F}_{p_2} (f_2(t - \tau_c) + g_2(t)) + \frac{\mathcal{F}_{u_2}}{\bar{\rho}_2 \bar{c}_2} (f_2(t - \tau_c) - g_2(t)) \dots \right. \\ & \left. + \frac{\mathcal{F}_{r_2}}{\bar{c}_2^2} (f_2(t - \tau_c) + g_2(t) + \alpha_2(t - \tau_c - \tau_\gamma)) \right) \dots \quad (\text{F.6c}) \end{aligned}$$

$$\begin{aligned} & - \frac{1}{2(M_2 - 1)} \left( \frac{\mathcal{Q}_{p_2}}{\bar{c}_2} (f_2(t - \tau_c) + g_2(t)) + \frac{\mathcal{Q}_{u_2}}{\bar{\rho}_2 \bar{c}_2^2} (f_2(t - \tau_c) - g_2(t)) \dots \right. \\ & \left. + \frac{\mathcal{Q}_{r_2}}{\bar{c}_2^3} (f_2(t - \tau_c) + g_2(t) + \alpha_2(t - \tau_c - \tau_\gamma)) \right) \quad (\text{F.6d}) \end{aligned}$$

$$\alpha_{iii}(t) = \alpha_2(t) + \dots \quad (\text{F.7a})$$

$$+ 0 \dots \quad (\text{F.7b})$$

$$+ 0 \dots \quad (\text{F.7c})$$

$$\begin{aligned} & - \frac{1}{M_2} \left( \frac{\mathcal{Q}_{p2}}{\bar{c}_2} (f_2(t + \tau_\gamma) + g_2(t + \tau_c + \tau_\gamma)) \dots \right. \\ & + \frac{\mathcal{Q}_{u2}}{\rho_2 \bar{c}_2^2} (f_2(t + \tau_\gamma) - g_2(t + \tau_c + \tau_\gamma)) \dots \\ & \left. + \frac{\mathcal{Q}_{r2}}{\bar{c}_2^3} (f_2(t + \tau_\gamma) + g_2(t + \tau_c + \tau_\gamma) + \alpha_2(t)) \right) \end{aligned} \quad (\text{F.7d})$$

Where the time delays are:

$$\tau_c = \frac{2(c - b)\bar{c}_2}{\bar{c}_2^2 - \bar{u}_2^2} \quad (\text{F.8a})$$

$$\tau_\gamma = \frac{(c - b)\bar{c}_2}{\bar{u}_2(\bar{c}_2 + \bar{u}_2)} \quad (\text{F.8b})$$

All of the wave form equations have been split into 4 subequations (a, b, c, d):

- **Subequations (a):** Unperturbed wave form. If there are no perturbations, the original system is recovered.
- **Subequations (b) and (d):** Perturbations introduced to the system due to perturbing the continuity equation. They only affect acoustic waves ( $f$  and  $g$ ).
- **Subequations (c):** Perturbations introduced to the system due to perturbing the momentum equation. They only affect acoustic waves ( $f$  and  $g$ ).
- **Subequations (d):** Perturbations introduced to the system due to perturbing the energy equation. They affect both acoustic and entropy waves ( $f$ ,  $g$  and  $\alpha$ ).

After using the same set of boundary conditions as in the unperturbed problem (Eqs. 2.22, 2.24, 2.25) and then Laplace transform using  $g = Ge^{st}$  one gets the wave forms in

the frequency domain, for example for  $f_{ii}$  it would be:

$$\begin{aligned}
\mathcal{L}(f_{ii}) = & R_u G_1 e^{-s\tau_u} + \frac{1}{2(M_1 + 1)} \left( \mathcal{M}_{p_1} \bar{c}_1 \left( R_u G_1 e^{-s\tau_u} + G_1 e^{-s\tau_a} \right) \dots \right. \\
& + \frac{\mathcal{M}_{u_1}}{\bar{\rho}_1} \left( R_u G_1 e^{-s\tau_u} - G_1 e^{-s\tau_a} \right) \dots \\
& \left. + \frac{\mathcal{M}_{r_1}}{\bar{c}_1} \left( R_u G_1 e^{-s\tau_u} + G_1 e^{-s\tau_a} + A_0 e^{-s\tau_a} \right) \right) \dots \\
& + \frac{1}{2(M_1 + 1)} \left( \mathcal{F}_{p_1} \left( R_u G_1 e^{-s\tau_u} + G_1 e^{-s\tau_a} \right) \dots \right. \\
& + \frac{\mathcal{F}_{u_1}}{\bar{\rho}_1 \bar{c}_1} \left( R_u G_1 e^{-s\tau_u} - G_1 e^{-s\tau_a} \right) \dots \\
& \left. + \frac{\mathcal{F}_{r_1}}{\bar{c}_1^2} \left( R_u G_1 e^{-s\tau_u} + G_1 e^{-s\tau_a} + A_0 e^{-s\tau_a} \right) \right) \dots \\
& + \frac{1}{2(M_1 + 1)} \left( \frac{\mathcal{Q}_{p_1}}{\bar{c}_1} \left( R_u G_1 e^{-s\tau_u} + G_1 e^{-s\tau_a} \right) \dots \right. \\
& + \frac{\mathcal{Q}_{u_1}}{\bar{\rho}_1 \bar{c}_1^2} \left( R_u G_1 e^{-s\tau_u} - G_1 e^{-s\tau_a} \right) \dots \\
& \left. + \frac{\mathcal{Q}_{r_1}}{\bar{c}_1^3} \left( R_u G_1 e^{-s\tau_u} + G_1 e^{-s\tau_a} + A_0 e^{-s\tau_a} \right) \right) \quad (\text{F.9})
\end{aligned}$$

From this expression it is clear that every wave form can be expressed as a linear superposition of two variables, for the waves upstream of the flame they are  $G_1$  and  $A_0$ , for the downstream waves they are  $F_2$  and  $\mathcal{A}_2$ . Then, the last equation can be then rearranged as:

$$\begin{aligned}
\mathcal{L}(f_{ii}) = & R_u G_1 e^{-s\tau_u} \dots \\
& + G_1 \left( \frac{1}{2(M_1 + 1)} \left( \mathcal{M}_{p_1} \bar{c}_1 \left( R_u e^{-s\tau_u} + e^{-s\tau_a} \right) + \frac{\mathcal{M}_{u_1}}{\bar{\rho}_1} \left( R_u e^{-s\tau_u} - e^{-s\tau_a} \right) \dots \right. \right. \\
& \left. \left. + \frac{\mathcal{M}_{r_1}}{\bar{c}_1} \left( R_u e^{-s\tau_u} + e^{-s\tau_a} \right) \right) \dots \right. \\
& + \frac{1}{2(M_1 + 1)} \left( \mathcal{F}_{p_1} \left( R_u e^{-s\tau_u} + e^{-s\tau_a} \right) + \frac{\mathcal{F}_{u_1}}{\bar{\rho}_1 \bar{c}_1} \left( R_u e^{-s\tau_u} - e^{-s\tau_a} \right) \dots \right. \\
& \left. \left. + \frac{\mathcal{F}_{r_1}}{\bar{c}_1^2} \left( R_u e^{-s\tau_u} + e^{-s\tau_a} \right) \right) \dots \right. \\
& + \frac{1}{2(M_1 + 1)} \left( \frac{\mathcal{Q}_{p_1}}{\bar{c}_1} \left( R_u e^{-s\tau_u} + e^{-s\tau_a} \right) + \frac{\mathcal{Q}_{u_1}}{\bar{\rho}_1 \bar{c}_1^2} \left( R_u e^{-s\tau_u} - e^{-s\tau_a} \right) \dots \right. \\
& \left. \left. + \frac{\mathcal{Q}_{r_1}}{\bar{c}_1^3} \left( R_u e^{-s\tau_u} + e^{-s\tau_a} \right) \right) \right) \dots
\end{aligned}$$

$$+ A_0 \left( \frac{1}{2(M_1 + 1)} \left( \frac{\mathcal{M}_{r_1}}{\bar{c}_1} e^{-s\tau_a} \right) + \frac{1}{2(M_1 + 1)} \left( \frac{\mathcal{F}_{r_1}}{\bar{c}_1^2} e^{-s\tau_a} \right) + \frac{1}{2(M_1 + 1)} \left( \frac{\mathcal{Q}_{r_1}}{\bar{c}_1^3} e^{-s\tau_a} \right) \right) \quad (\text{F.10})$$

In simplified form that is:

$$\mathcal{L}(f_{ii}) = F_{ii} = G_1 \left( R_u e^{-s\tau_u} + E_{F_1} \right) + A_0 (A_{F_1}) \quad (\text{F.11})$$

Where

$$\begin{aligned} E_{F_1} = & \frac{1}{2(M_1 + 1)} \left( \mathcal{M}_{p_1} \bar{c}_1 (R_u e^{-s\tau_u} + e^{-s\tau_a}) + \frac{\mathcal{M}_{u_1}}{\bar{\rho}_1} (R_u e^{-s\tau_u} - e^{-s\tau_a}) \dots \right. \\ & \left. + \frac{\mathcal{M}_{r_1}}{\bar{c}_1} (R_u e^{-s\tau_u} + e^{-s\tau_a}) \right) \dots \\ & + \frac{1}{2(M_1 + 1)} \left( \mathcal{F}_{p_1} (R_u e^{-s\tau_u} + e^{-s\tau_a}) + \frac{\mathcal{F}_{u_1}}{\bar{\rho}_1 \bar{c}_1} (R_u e^{-s\tau_u} - e^{-s\tau_a}) \dots \right. \\ & \left. + \frac{\mathcal{F}_{r_1}}{\bar{c}_1^2} (R_u e^{-s\tau_u} + e^{-s\tau_a}) \right) \dots \\ & + \frac{1}{2(M_1 + 1)} \left( \frac{\mathcal{Q}_{p_1}}{\bar{c}_1} (R_u e^{-s\tau_u} + e^{-s\tau_a}) + \frac{\mathcal{Q}_{u_1}}{\bar{\rho}_1 \bar{c}_1^2} (R_u e^{-s\tau_u} - e^{-s\tau_a}) \dots \right. \\ & \left. + \frac{\mathcal{Q}_{r_1}}{\bar{c}_1^3} (R_u e^{-s\tau_u} + e^{-s\tau_a}) \right) \end{aligned} \quad (\text{F.12})$$

$$A_{F_1} = \frac{1}{2(M_1 + 1)} \left( \frac{\mathcal{M}_{r_1}}{\bar{c}_1} e^{-s\tau_a} \right) + \frac{1}{2(M_1 + 1)} \left( \frac{\mathcal{F}_{r_1}}{\bar{c}_1^2} e^{-s\tau_a} \right) + \frac{1}{2(M_1 + 1)} \left( \frac{\mathcal{Q}_{r_1}}{\bar{c}_1^3} e^{-s\tau_a} \right) \quad (\text{F.13})$$

Similarly:

$$\mathcal{L}(g_{ii}) = G_{ii} = G_1(1 + E_{G_1}) + A_0(A_{G_1}) \quad (\text{F.14})$$

$$\mathcal{L}(\alpha_{ii}) = \mathcal{A}_{ii} = G_1(E_{A_1}) + A_0(1 + A_{A_1}) \quad (\text{F.15})$$

$$\mathcal{L}(f_{iii}) = F_{iii} = F_2(1 + E_{F_2}) + \mathcal{A}_2(A_{F_2}) \quad (\text{F.16})$$

$$\mathcal{L}(g_{iii}) = G_{iii} = F_2(R_d e^{-s\tau_d} + E_{G_2}) + \mathcal{A}_2(A_{G_2}) \quad (\text{F.17})$$

$$\mathcal{L}(\alpha_{iii}) = \mathcal{A}_{iii} = F_2(E_{A_2}) + \mathcal{A}_2(1 + A_{A_2}) \quad (\text{F.18})$$

Where

$$\begin{aligned} E_{G_1} = & \frac{1}{2(M_1 - 1)} \left( \mathcal{M}_{p_1} \bar{c}_1 (R_u e^{-s(\tau_u - \tau_a)} + 1) + \frac{\mathcal{M}_{u_1}}{\bar{\rho}_1} (R_u e^{-s(\tau_u - \tau_a)} - 1) \dots \right. \\ & \left. + \frac{\mathcal{M}_{r_1}}{\bar{c}_1} (R_u e^{-s(\tau_u - \tau_a)} + 1) \right) \dots \\ & - \frac{1}{2(M_1 - 1)} \left( \mathcal{F}_{p_1} (R_u e^{-s(\tau_u - \tau_a)} + 1) + \frac{\mathcal{F}_{u_1}}{\bar{\rho}_1 \bar{c}_1} (R_u e^{-s(\tau_u - \tau_a)} - 1) \dots \right) \end{aligned}$$

$$\begin{aligned}
& + \frac{\mathcal{F}_{r_1}}{\bar{c}_1^2} \left( R_u e^{-s(\tau_u - \tau_a)} + 1 \right) \dots \\
& + \frac{1}{2(M_1 - 1)} \left( \frac{\mathcal{Q}_{p_1}}{\bar{c}_1} \left( R_u e^{-s(\tau_u - \tau_a)} + 1 \right) + \frac{\mathcal{Q}_{u_1}}{\bar{\rho}_1 \bar{c}_1^2} \left( R_u e^{-s(\tau_u - \tau_a)} - 1 \right) \dots \right. \\
& \quad \left. + \frac{\mathcal{Q}_{r_1}}{\bar{c}_1^3} \left( R_u e^{-s(\tau_u - \tau_a)} + 1 \right) \right) \quad (F.19)
\end{aligned}$$

$$\begin{aligned}
A_{G_1} &= \frac{1}{2(M_1 - 1)} \left( \frac{\mathcal{M}_{r_1}}{\bar{c}_1} e^{s(\tau_\alpha + \tau_a)} \right) - \frac{1}{2(M_1 - 1)} \left( \frac{\mathcal{F}_{r_1}}{\bar{c}_1^2} e^{s(\tau_\alpha + \tau_a)} \right) \dots \\
& + \frac{1}{2(M_1 - 1)} \left( \frac{\mathcal{E}_{r_1}}{\bar{c}_1^3} e^{s(\tau_\alpha + \tau_a)} \right) \quad (F.20)
\end{aligned}$$

$$\begin{aligned}
E_{A_1} &= -\frac{1}{M_1} \left( \frac{\mathcal{Q}_{p_1}}{\bar{c}_1} \left( R_u e^{-s(\tau_u + \tau_\alpha)} + e^{-s(\tau_a + \tau_\alpha)} \right) \dots \right. \\
& \quad + \frac{\mathcal{Q}_{u_1}}{\bar{\rho}_1 \bar{c}_1^2} \left( R_u e^{-s(\tau_u + \tau_\alpha)} - e^{-s(\tau_a + \tau_\alpha)} \right) \dots \\
& \quad \left. + \frac{\mathcal{Q}_{r_1}}{\bar{c}_1^3} \left( R_u e^{-s(\tau_u + \tau_\alpha)} + e^{-s(\tau_a + \tau_\alpha)} \right) \right) \quad (F.21)
\end{aligned}$$

$$A_{A_1} = -\frac{1}{M_1} \left( \frac{\mathcal{Q}_{r_1}}{\bar{c}_1^3} \right) \quad (F.22)$$

$$\begin{aligned}
E_{F_2} &= -\frac{1}{2(M_2 + 1)} \left( \mathcal{M}_{p_2} \bar{c}_2 \left( 1 + R_d e^{-s(\tau_d - \tau_c)} \right) + \frac{\mathcal{M}_{u_2}}{\bar{\rho}_2} \left( 1 - R_d e^{-s(\tau_d - \tau_c)} \right) \dots \right. \\
& \quad \left. + \frac{\mathcal{M}_{r_2}}{\bar{c}_2} \left( 1 + R_d e^{-s(\tau_d - \tau_c)} \right) \right) \dots \\
& - \frac{1}{2(M_2 + 1)} \left( \mathcal{F}_{p_2} \left( 1 + R_d e^{-s(\tau_d - \tau_c)} \right) + \frac{\mathcal{F}_{u_2}}{\bar{\rho}_2 \bar{c}_2} \left( 1 - R_d e^{-s(\tau_d - \tau_c)} \right) \dots \right. \\
& \quad \left. + \frac{\mathcal{F}_{r_2}}{\bar{c}_2^2} \left( 1 + R_d e^{-s(\tau_d - \tau_c)} \right) \right) \dots \\
& - \frac{1}{2(M_2 + 1)} \left( \frac{\mathcal{Q}_{p_2}}{\bar{c}_2} \left( 1 + R_d e^{-s(\tau_d - \tau_c)} \right) + \frac{\mathcal{Q}_{u_2}}{\bar{\rho}_2 \bar{c}_2^2} \left( 1 - R_d e^{-s(\tau_d - \tau_c)} \right) \dots \right. \\
& \quad \left. + \frac{\mathcal{Q}_{r_2}}{\bar{c}_2^3} \left( 1 + R_d e^{-s(\tau_d - \tau_c)} \right) \right) \quad (F.23)
\end{aligned}$$

$$A_{F_2} = -\frac{1}{2(M_2 + 1)} \left( \frac{\mathcal{M}_{r_2}}{\bar{c}_2} e^{-s\tau_\gamma} \right) - \frac{1}{2(M_2 + 1)} \left( \frac{\mathcal{F}_{r_2}}{\bar{c}_2^2} e^{-s\tau_\gamma} \right) - \frac{1}{2(M_2 + 1)} \left( \frac{\mathcal{Q}_{r_2}}{\bar{c}_2^3} e^{-s\tau_\gamma} \right) \quad (F.24)$$

$$E_{G_2} = -\frac{1}{2(M_2 - 1)} \left( \mathcal{M}_{p_2} \bar{c}_2 \left( e^{-s\tau_c} + R_d e^{-s\tau_d} \right) + \frac{\mathcal{M}_{u_2}}{\bar{\rho}_2} \left( e^{-s\tau_c} - R_d e^{-s\tau_d} \right) \dots \right)$$

$$\begin{aligned}
& + \frac{\mathcal{M}_{r_2}}{\bar{c}_2} \left( e^{-s\tau_c} + R_d e^{-s\tau_d} \right) \dots \\
& + \frac{1}{2(M_2 - 1)} \left( \mathcal{F}_{p_2} \left( e^{-s\tau_c} + R_d e^{-s\tau_d} \right) + \frac{\mathcal{F}_{u_2}}{\bar{\rho}_2 \bar{c}_2} \left( e^{-s\tau_c} - R_d e^{-s\tau_d} \right) \dots \right. \\
& \quad \left. + \frac{\mathcal{F}_{r_2}}{\bar{c}_2^2} \left( e^{-s\tau_c} + R_d e^{-s\tau_d} \right) \right) \dots \\
& - \frac{1}{2(M_2 - 1)} \left( \frac{\mathcal{Q}_{p_2}}{\bar{c}_2} \left( e^{-s\tau_c} + R_d e^{-s\tau_d} \right) + \frac{\mathcal{Q}_{u_2}}{\bar{\rho}_2 \bar{c}_2^2} \left( e^{-s\tau_c} - R_d e^{-s\tau_d} \right) \dots \right. \\
& \quad \left. + \frac{\mathcal{Q}_{r_2}}{\bar{c}_2^3} \left( e^{-s\tau_c} + R_d e^{-s\tau_d} \right) \right) \tag{F.25}
\end{aligned}$$

$$\begin{aligned}
A_{G_2} &= - \frac{1}{2(M_2 - 1)} \left( \mathcal{M}_{r_2} \bar{c}_2 e^{-s(\tau_c + \tau_d)} \right) + \frac{1}{2(M_2 - 1)} \left( \frac{\mathcal{F}_{r_2}}{\bar{c}_2^2} e^{-s(\tau_c + \tau_d)} \right) \dots \\
& - \frac{1}{2(M_2 - 1)} \left( \frac{\mathcal{Q}_{r_2}}{\bar{c}_2^3} e^{-s(\tau_c + \tau_d)} \right) \tag{F.26}
\end{aligned}$$

$$\begin{aligned}
E_{A_2} &= - \frac{1}{M_2} \left( \frac{\mathcal{Q}_{p_2}}{\bar{c}_2} \left( e^{s\tau_\gamma} + R_d e^{-s(\tau_d - \tau_c - \tau_\gamma)} \right) + \frac{\mathcal{Q}_{u_2}}{\bar{\rho}_2 \bar{c}_2^2} \left( e^{s\tau_\gamma} - R_d e^{-s(\tau_d - \tau_c - \tau_\gamma)} \right) \dots \right. \\
& \quad \left. + \frac{\mathcal{Q}_{r_2}}{\bar{c}_2^3} \left( e^{s\tau_\gamma} + R_d e^{-s(\tau_d - \tau_c - \tau_\gamma)} \right) \right) \tag{F.27}
\end{aligned}$$

$$A_{A_2} = - \frac{1}{M_2} \left( \frac{\mathcal{Q}_{r_2}}{\bar{c}_2^3} \right) \tag{F.28}$$

Note that the term labeled with  $E$  corresponds to the acoustic fluctuations and the term labeled with  $A$  corresponds to entropy fluctuations. Finally, substitute these expressions into the jump conditions (Eq. 2.4) in the frequency domain to get:

$$(\mathbf{L} + \delta\mathbf{L}) \hat{\mathbf{q}} = \mathbf{X} + \delta\mathbf{X} \tag{F.29}$$

Where  $\mathbf{L}$ ,  $\hat{\mathbf{q}}$  and  $\mathbf{X}$  are given by Eq. (2.26), and  $\delta\mathbf{L}$  and  $\delta\mathbf{X}$  are:

$$\delta\mathbf{L} = \mathbf{M} + \mathbf{Q} + \delta\mathbf{M} + \delta\mathbf{Q} \tag{F.30}$$

The matrices  $\delta\mathbf{M}$  and  $\delta\mathbf{Q}$  are:

$$\delta\mathbf{M} = \begin{bmatrix} \delta\mathbf{M}_{11} & \delta\mathbf{M}_{12} & \delta\mathbf{M}_{13} \\ \delta\mathbf{M}_{21} & \delta\mathbf{M}_{22} & \delta\mathbf{M}_{23} \\ \delta\mathbf{M}_{31} & \delta\mathbf{M}_{32} & \delta\mathbf{M}_{33} \end{bmatrix} \quad \delta\mathbf{Q} = \begin{bmatrix} 0 & 0 & 0 \\ 0 & 0 & 0 \\ 0 & \delta\mathbf{Q}_{32} & 0 \end{bmatrix}$$

With components:

$$\delta M_{11} = \frac{\bar{c}_1}{\bar{c}_2} ((M_2 + 1)A_{F_2} + (M_2 - 1)A_{G_2} + M_2 A_{A_2}) \quad (\text{F.31a})$$

$$\delta M_{12} = -(M_1 + 1)E_{F_1} - (M_1 - 1)E_{G_1} - M_1 E_{A_1} \quad (\text{F.31b})$$

$$\delta M_{13} = \frac{\bar{c}_1}{\bar{c}_2} ((M_2 + 1)E_{F_2} + (M_2 - 1)E_{G_2} + M_2 E_{A_2}) \quad (\text{F.31c})$$

$$\delta M_{21} = (M_2 + 1)^2 A_{F_2} + (M_2 - 1)^2 A_{G_2} + M_2^2 A_{A_2} \quad (\text{F.31d})$$

$$\delta M_{22} = -(M_1 + 1)^2 E_{F_1} - (M_1 - 1)^2 E_{G_1} - M_1^2 E_{A_1} \quad (\text{F.31e})$$

$$\delta M_{23} = (M_2 + 1)^2 E_{F_2} + (M_2 - 1)^2 E_{G_2} + M_2^2 E_{A_2} \quad (\text{F.31f})$$

$$\begin{aligned} \delta M_{31} = & \frac{\bar{c}_2}{\bar{c}_1} \left( \left( \frac{1 + \gamma M_2}{\gamma - 1} + \frac{M_2^2}{2} (3 + M_2) \right) A_{F_2} \cdots \right. \\ & \left. + \left( \frac{-1 + \gamma M_2}{\gamma - 1} - \frac{M_2^2}{2} (3 - M_2) \right) A_{G_2} + \frac{M_2^3}{2} A_{A_2} \right) \end{aligned} \quad (\text{F.31g})$$

$$\begin{aligned} \delta M_{32} = & \left( \frac{-1 - \gamma M_1}{\gamma - 1} - \frac{M_1^2}{2} (3 + M_1) \right) E_{F_1} \cdots \\ & + \left( \frac{1 - \gamma M_1}{\gamma - 1} + \frac{M_1^2}{2} (3 - M_1) \right) E_{G_1} - \frac{M_1^3}{2} E_{A_1} \end{aligned} \quad (\text{F.31h})$$

$$\begin{aligned} \delta M_{33} = & \frac{\bar{c}_2}{\bar{c}_1} \left( \left( \frac{1 + \gamma M_2}{\gamma - 1} + \frac{M_2^2}{2} (3 + M_2) \right) E_{F_2} \cdots \right. \\ & \left. + \left( \frac{-1 + \gamma M_2}{\gamma - 1} - \frac{M_2^2}{2} (3 - M_2) \right) E_{G_2} + \frac{M_2^3}{2} E_{A_2} \right) \end{aligned} \quad (\text{F.31i})$$



The only entry of  $\delta Q$  matrix is:

$$\delta Q_{32} = \frac{\beta}{\rho_1 \bar{c}_1^2} e^{-s\tau} (E_{G_1} - E_{F_1}) \quad (\text{F.32})$$

and the vector of perturbed forcing terms is:

$$\delta \mathbf{X} = A_0 \begin{bmatrix} (M_1 + 1)A_{F_1} + (M_1 - 1)A_{G_1} + M_1 A_{A_1} \\ (M_1 + 1)^2 A_{F_1} + (M_1 - 1)^2 A_{G_1} + M_1^2 A_{A_1} \\ \left( \frac{1 + \gamma M_1}{\gamma - 1} + \frac{M_1^2}{2} (3 + M_1) \right) A_{F_1} + \left( \frac{-1 + \gamma M_1}{\gamma - 1} - \frac{M_1^2}{2} (3 - M_1) \right) A_{G_1} + \frac{M_1^3}{2} A_{A_1} \end{bmatrix} \quad (\text{F.33})$$



# Appendix G

## Structural Sensitivity Taylor Tests

Taylor tests as described in section 3.3 are shown here for all computed structural sensitivity devices variables.

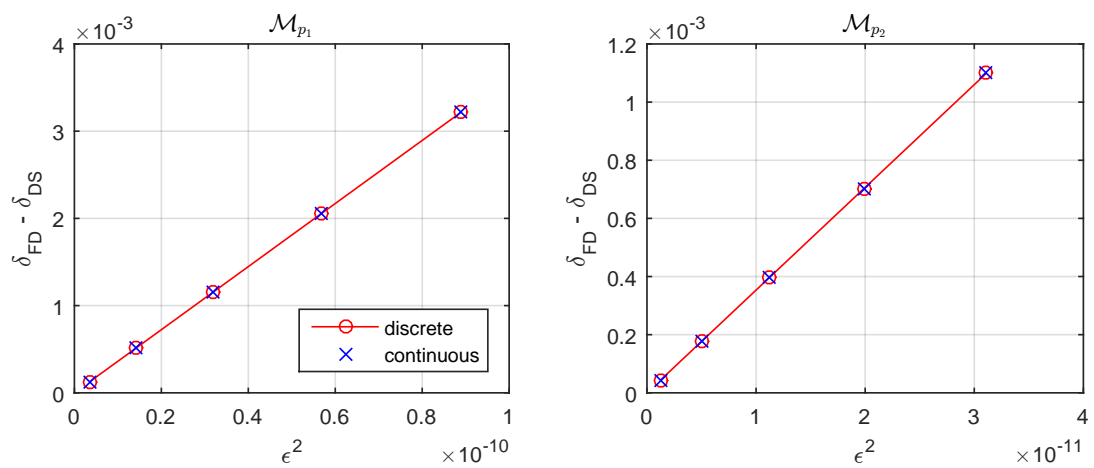


Fig. G.1 Testing structural sensitivity of continuity equation - pressure device.

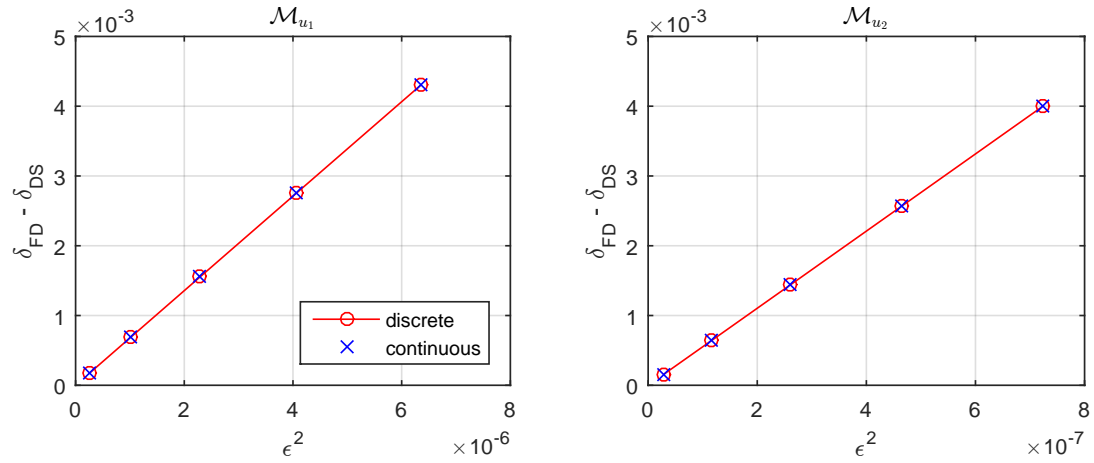


Fig. G.2 Testing structural sensitivity of continuity equation - velocity device.

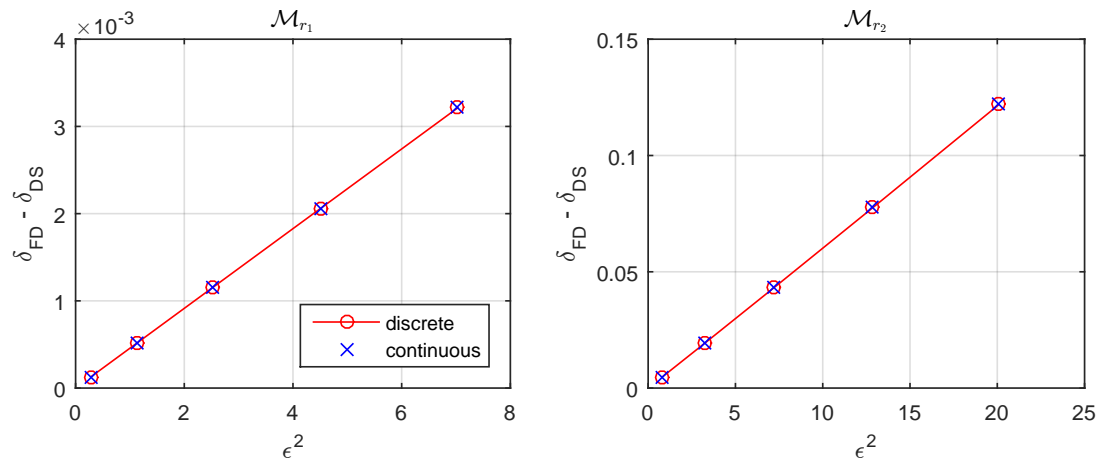


Fig. G.3 Testing structural sensitivity of continuity equation - density device.

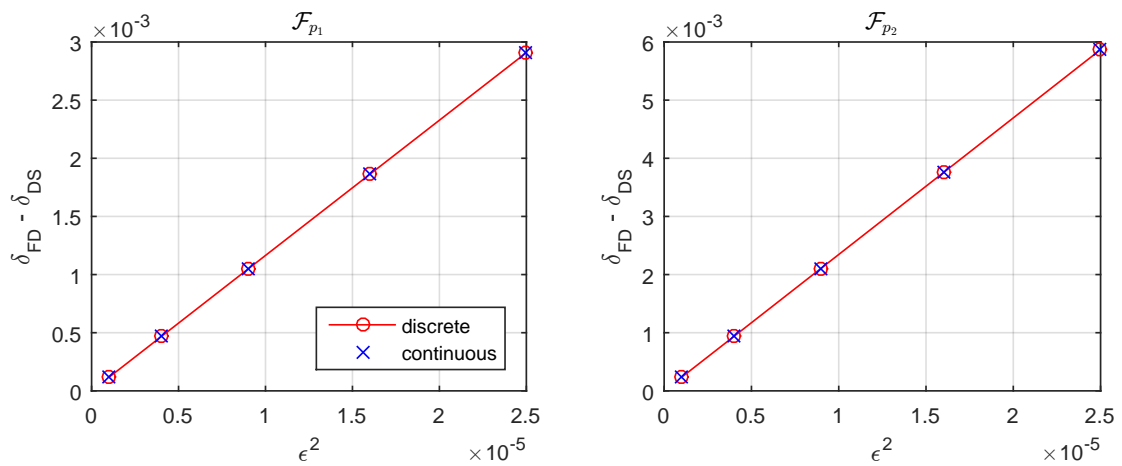


Fig. G.4 Testing structural sensitivity of momentum equation - pressure device.

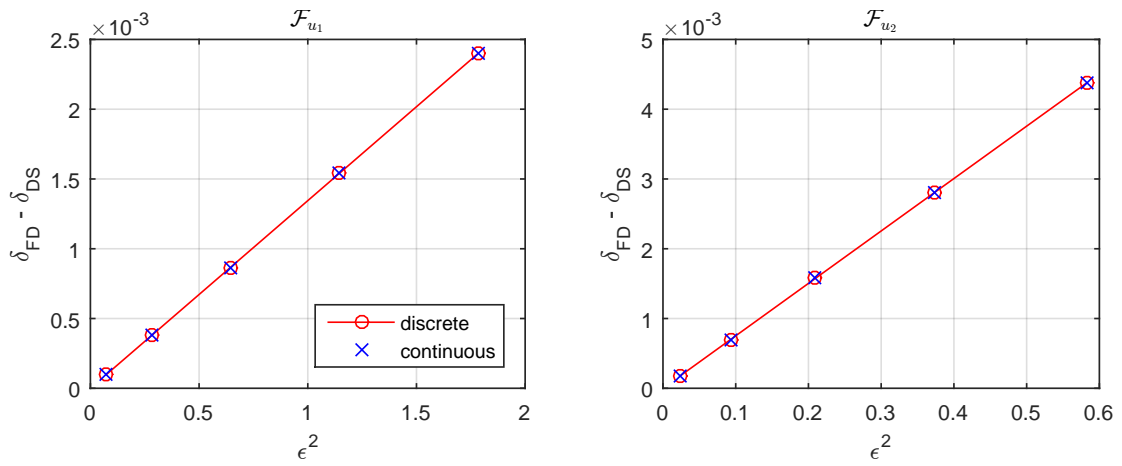


Fig. G.5 Testing structural sensitivity of momentum equation - velocity device.

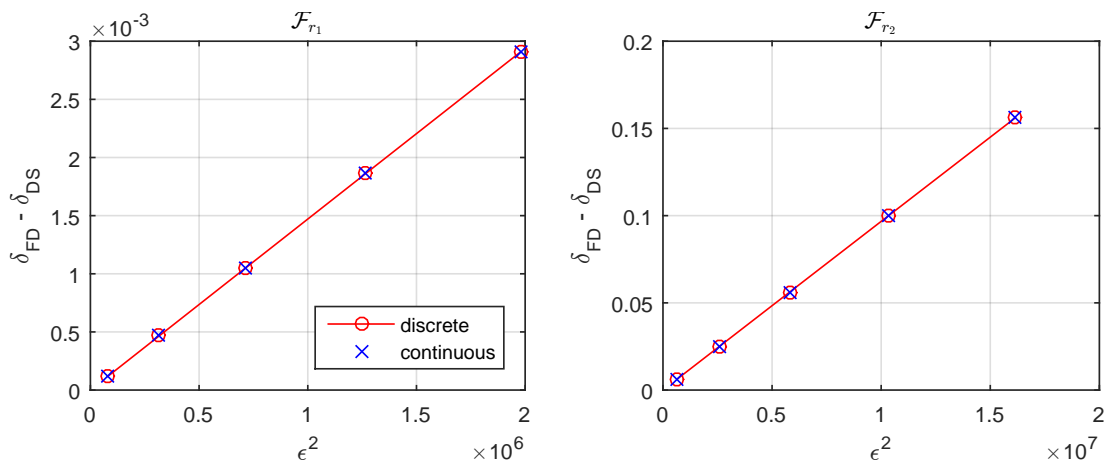


Fig. G.6 Testing structural sensitivity of momentum equation - density device.

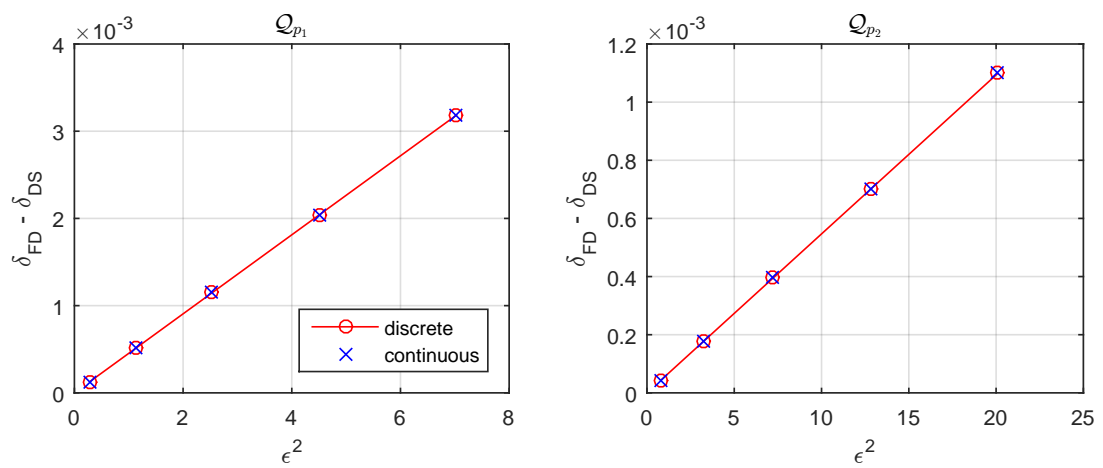


Fig. G.7 Testing structural sensitivity of Energy equation - pressure device.

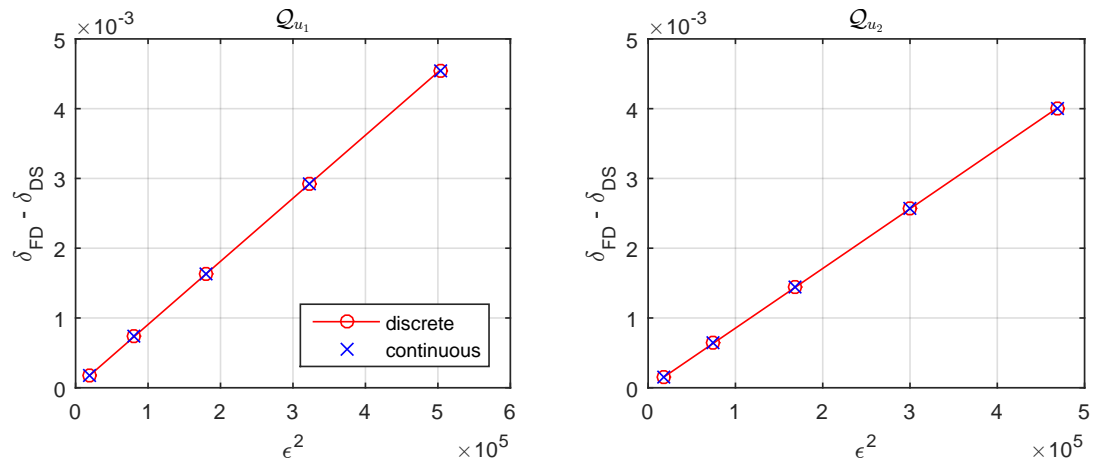


Fig. G.8 Testing structural sensitivity of Energy equation - velocity device.

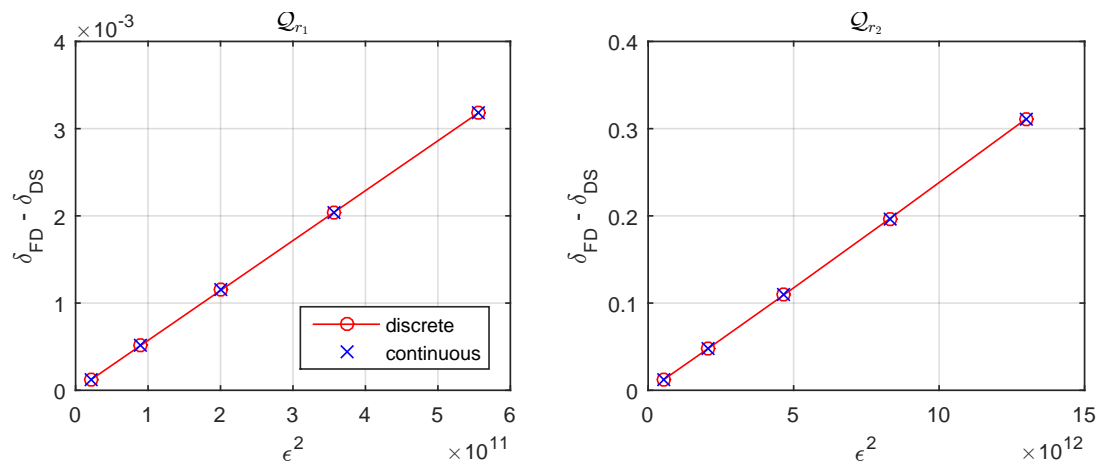


Fig. G.9 Testing structural sensitivity of Energy equation - density device.

# Appendix H

## Derivation of adjoint equations (adding a perturbation)

The following derivation of adjoint equations will follow after slightly changing a parameter in the system so that the eigenvalue drift can also be computed. Begin with the governing equations in the frequency domain using  $\rho'(t) = \hat{\rho}e^{st}$ .

$$s\hat{\rho} + \bar{u}\frac{\partial\hat{\rho}}{\partial x} + \bar{\rho}\frac{\partial\hat{u}}{\partial x} = 0 \quad (\text{H.1a})$$

$$\bar{\rho}s\hat{u} + \bar{\rho}\bar{u}\frac{\partial\hat{u}}{\partial x} + \frac{\partial\hat{p}}{\partial x} = 0 \quad (\text{H.1b})$$

$$s\hat{p} + \bar{u}\frac{\partial\hat{p}}{\partial x} + \gamma\bar{p}\frac{\partial\hat{u}}{\partial x} = 0 \quad (\text{H.1c})$$

Which are defined on

$$x \in [0, b^-) \cup (b^+, L] \quad (\text{H.2})$$

The jump conditions are only defined on  $x = b$ . The subscript 1 used in the flame model refers to the velocity upstream (i.e  $u'_1 = u(b^-)$ ):

$$[\hat{\rho}\bar{u} + \bar{\rho}\hat{u}]_{b^-}^{b^+} = 0 \quad (\text{H.3a})$$

$$[\hat{p} + 2\bar{\rho}\bar{u}\hat{u} + \bar{\rho}\hat{u}^2]_{b^-}^{b^+} = 0 \quad (\text{H.3b})$$

$$\left[ \frac{\gamma}{(\gamma - 1)} (\hat{p}\bar{u} + \bar{p}\hat{u}) + \frac{1}{2} (3\bar{\rho}\bar{u}^2\hat{u} + \bar{u}^3\hat{\rho}) \right]_{b^-}^{b^+} - \beta\hat{u}_1 e^{-s\tau} = 0 \quad (\text{H.3c})$$

By introducing a small perturbation into one of the governing equations or into one of the base state variables, the eigenvalue drift alongside the adjoint equations can be

derived. In this case a small change to the time delay ( $\tau$ ) is introduced to the system:

$$\tau \rightarrow \tau + \delta\tau \quad (\text{H.4})$$

This change will cause the variables to change for example from  $\hat{u} \rightarrow \hat{u} + \delta\hat{u}$  and also the eigenvalue  $s \rightarrow s + \delta s$ . Mean flow variables are not affected. Gathering only first order terms, the set of equations become:

$$F_1 \equiv s\delta\hat{\rho} + \delta s\hat{\rho} + \bar{u}\frac{d\delta\hat{\rho}}{dx} + \bar{\rho}\frac{d\delta\hat{u}}{dx} = 0 \quad (\text{H.5a})$$

$$F_2 \equiv \bar{\rho}s\delta\hat{u} + \bar{\rho}\delta s\hat{u} + \bar{\rho}\bar{u}\frac{d\delta\hat{u}}{dx} + \frac{d\delta\hat{\rho}}{dx} = 0 \quad (\text{H.5b})$$

$$F_3 \equiv s\delta\hat{p} + \delta s\hat{p} + \bar{u}\frac{d\delta\hat{p}}{dx} + \gamma\bar{p}\frac{d\delta\hat{u}}{dx} = 0 \quad (\text{H.5c})$$

For the jump conditions note that the term with the time delay is linearized using a Taylor expansion in two variables.

$$J_1 \equiv [\delta\hat{\rho}\bar{u} + \bar{\rho}\delta\hat{u}]_{b^-}^{b^+} = 0 \quad (\text{H.6a})$$

$$J_2 \equiv [\delta\hat{p} + 2\bar{\rho}\bar{u}\delta\hat{u} + \delta\hat{\rho}\bar{u}^2]_{b^-}^{b^+} = 0 \quad (\text{H.6b})$$

$$J_3 \equiv \left[ \frac{\gamma}{(\gamma-1)} (\delta\hat{p}\bar{u} + \bar{p}\delta\hat{u}) + \frac{1}{2} (3\bar{\rho}\bar{u}^2\delta\hat{u} + \bar{u}^3\delta\hat{\rho}) \right]_{b^-}^{b^+} \dots \\ - \beta e^{-s\tau} (\delta\hat{u}_1 - \hat{u}_1\tau\delta s - \hat{u}_1s\delta\tau) = 0 \quad (\text{H.6c})$$

Define the following inner products:

$$\langle \mathbf{a}, \mathbf{b} \rangle = \int_0^{b^-} \mathbf{a}^* \cdot \mathbf{b} \, dx \quad (\text{H.7})$$

$$\{ \mathbf{a}, \mathbf{b} \} = \int_{b^+}^L \mathbf{a}^* \cdot \mathbf{b} \, dx \quad (\text{H.8})$$

$$(a, b) = a^* \cdot b \quad (\text{H.9})$$

Define two sets of adjoint variables  $\hat{\rho}^+(x)$ ,  $\hat{u}^+(x, t)$ ,  $\hat{p}^+(x, t)$  defined on the whole domain (except at the flame  $x = b$ ) and  $f(t)$ ,  $g(t)$ ,  $h(t)$  defined only at the flame position. Create a functional:

$$\mathcal{L} \equiv \langle \hat{\rho}^+, F_1 \rangle + \langle \hat{u}^+, F_2 \rangle + \langle \hat{p}^+, F_3 \rangle + (f, J_1) + (g, J_2) + (h, J_3) + \dots \\ + \{ \hat{\rho}^+, F_1 \} + \{ \hat{u}^+, F_2 \} + \{ \hat{p}^+, F_3 \} \quad (\text{H.10})$$

Considering each term:

$$\begin{aligned} \langle \hat{\rho}^+, F_1 \rangle &= \left[ \hat{\rho}^{+*} \bar{u}_1 \delta \hat{\rho} + \hat{\rho}^{+*} \bar{\rho}_1 \delta \hat{u} \right]_0^{b^-} + \langle \hat{\rho}^+ s^*, \delta \hat{\rho} \rangle + \langle \hat{\rho}^+ \delta s^*, \hat{\rho} \rangle - \left\langle \bar{u}_1 \frac{d\hat{\rho}^+}{dx}, \delta \hat{\rho} \right\rangle \dots \\ &\quad - \left\langle \bar{\rho}_1 \frac{d\hat{\rho}^+}{dx}, \delta \hat{u} \right\rangle \end{aligned} \quad (\text{H.11a})$$

$$\begin{aligned} \langle \hat{u}^+, F_2 \rangle &= \left[ \hat{u}^{+*} \bar{\rho}_1 \bar{u}_1 \delta \hat{u} + \hat{u}^{+*} \delta \hat{\rho} \right]_0^{b^-} + \langle \hat{u}^+ \bar{\rho}_1 s^*, \delta \hat{u} \rangle + \langle \hat{u}^+ \bar{\rho}_1 \delta s^*, \hat{u} \rangle \dots \\ &\quad - \left\langle \bar{\rho}_1 \bar{u}_1 \frac{d\hat{u}^+}{dx}, \delta \hat{u} \right\rangle - \left\langle \frac{d\hat{u}^+}{dx}, \delta \hat{\rho} \right\rangle \end{aligned} \quad (\text{H.11b})$$

$$\begin{aligned} \langle \hat{p}^+, F_3 \rangle &= \left[ \hat{p}^{+*} \bar{u}_1 \delta \hat{p} + \hat{p}^{+*} \gamma \bar{p}_1 \delta \hat{u} \right]_0^{b^-} + \langle \hat{p}^+ s^*, \delta \hat{p} \rangle + \langle \hat{p}^+ \delta s^*, \hat{p} \rangle - \left\langle \bar{u}_1 \frac{d\hat{p}^+}{dx}, \delta \hat{p} \right\rangle \dots \\ &\quad - \left\langle \gamma \bar{p}_1 \frac{d\hat{p}^+}{dx}, \delta \hat{u} \right\rangle \end{aligned} \quad (\text{H.11c})$$

$$(f, J_1) = [f^* \delta \hat{\rho} \bar{u} + f^* \bar{\rho} \delta \hat{u}]_{b^-}^{b^+} \quad (\text{H.11d})$$

$$(g, J_2) = [g^* \delta \hat{p} + g^* 2 \bar{\rho} \bar{u} \delta \hat{u} + g^* \delta \hat{\rho} \bar{u}^2]_{b^-}^{b^+} \quad (\text{H.11e})$$

$$\begin{aligned} (h, J_3) &= \left[ \frac{\gamma}{(\gamma - 1)} (h^* \delta \hat{p} \bar{u} + h^* \bar{p} \delta \hat{u}) + \frac{1}{2} (h^* 3 \bar{\rho} \bar{u}^2 \delta \hat{u} + h^* \bar{u}^3 \delta \hat{\rho}) \right]_{b^-}^{b^+} \dots \\ &\quad - h^* \beta e^{-s\tau} (\delta \hat{u}_1 - \hat{u}_1 \tau \delta s - \hat{u}_1 s \delta \tau) \end{aligned} \quad (\text{H.11f})$$

$$\begin{aligned} \{ \hat{\rho}^+, F_1 \} &= \left[ \hat{\rho}^{+*} \bar{u}_2 \delta \hat{\rho} + \hat{\rho}^{+*} \bar{\rho}_2 \delta \hat{u} \right]_{b^+}^L + \{ \hat{\rho}^+ s^*, \delta \hat{\rho} \} + \{ \hat{\rho}^+ \delta s^*, \hat{\rho} \} - \left\{ \bar{u}_2 \frac{d\hat{\rho}^+}{dx}, \delta \hat{\rho} \right\} \dots \\ &\quad - \left\{ \bar{\rho}_2 \frac{d\hat{\rho}^+}{dx}, \delta \hat{u} \right\} \end{aligned} \quad (\text{H.11g})$$

$$\begin{aligned} \{ \hat{u}^+, F_2 \} &= \left[ \hat{u}^{+*} \bar{\rho}_2 \bar{u}_2 \delta \hat{u} + \hat{u}^{+*} \delta \hat{\rho} \right]_{b^+}^L + \{ \hat{u}^+ \bar{\rho}_2 s^*, \delta \hat{u} \} + \{ \hat{u}^+ \bar{\rho}_2 \delta s^*, \hat{u} \} \dots \\ &\quad - \left\{ \bar{\rho}_2 \bar{u}_2 \frac{d\hat{u}^+}{dx}, \delta \hat{u} \right\} - \left\{ \frac{d\hat{u}^+}{dx}, \delta \hat{\rho} \right\} \end{aligned} \quad (\text{H.11h})$$

$$\begin{aligned} \{ \hat{p}^+, F_3 \} &= \left[ \hat{p}^{+*} \bar{u}_2 \delta \hat{p} + \hat{p}^{+*} \gamma \bar{p}_2 \delta \hat{u} \right]_{b^+}^L + \{ \hat{p}^+ s^*, \delta \hat{p} \} + \{ \hat{p}^+ \delta s^*, \hat{p} \} - \left\{ \bar{u}_2 \frac{d\hat{p}^+}{dx}, \delta \hat{p} \right\} \dots \\ &\quad - \left\{ \gamma \bar{p}_2 \frac{d\hat{p}^+}{dx}, \delta \hat{u} \right\} \end{aligned} \quad (\text{H.11i})$$

Arranging the functional in terms of native variables (i.e  $\delta \hat{u}$ ):

$$\begin{aligned} \mathcal{L} &= \left\langle \hat{\rho}^+ s^* - \bar{u}_1 \frac{d\hat{\rho}^+}{dx}, \delta \hat{\rho} \right\rangle + \left\langle \hat{u}^+ \bar{\rho}_1 s^* - \bar{\rho}_1 \bar{u}_1 \frac{d\hat{u}^+}{dx} - \bar{\rho}_1 \frac{d\hat{\rho}^+}{dx} - \gamma \bar{p}_1 \frac{d\hat{p}^+}{dx}, \delta \hat{u} \right\rangle \dots \\ &\quad + \left\langle \hat{p}^+ s^* - \bar{u}_1 \frac{d\hat{p}^+}{dx} - \frac{d\hat{u}^+}{dx}, \delta \hat{p} \right\rangle \dots \end{aligned} \quad (\text{H.12a})$$

$$\begin{aligned}
& + \left\{ \hat{\rho}^+ s^* - \bar{u}_2 \frac{d\hat{\rho}^+}{dx}, \delta\hat{\rho} \right\} + \left\{ \hat{u}^+ \bar{\rho}_2 s^* - \bar{\rho}_2 \bar{u}_2 \frac{d\hat{u}^+}{dx} - \bar{\rho}_2 \frac{d\hat{\rho}^+}{dx} - \gamma \bar{p}_2 \frac{d\hat{p}^+}{dx}, \delta\hat{u} \right\} \dots \\
& + \left\{ \hat{p}^+ s^* - \bar{u}_2 \frac{d\hat{p}^+}{dx} - \frac{d\hat{u}^+}{dx}, \delta\hat{p} \right\} \dots \tag{H.12b}
\end{aligned}$$

$$\begin{aligned}
& + \langle \hat{\rho}^+ \delta s^*, \hat{\rho} \rangle + \langle \hat{u}^+ \bar{\rho}_1 \delta s^*, \hat{u} \rangle + \langle \hat{p}^+ \delta s^*, \hat{p} \rangle + \{ \hat{\rho}^+ \delta s^*, \hat{\rho} \} + \{ \hat{u}^+ \bar{\rho}_2 \delta s^*, \hat{u} \} \dots \\
& + \{ \hat{p}^+ \delta s^*, \hat{p} \} + h^* \beta \hat{u}_1 e^{-s\tau} (\tau \delta s + s \delta \tau) \dots \tag{H.12c}
\end{aligned}$$

$$\begin{aligned}
& + \left[ \delta\hat{\rho}(\hat{\rho}^{+*} \bar{u}_1) + \delta\hat{u}(\hat{\rho}^{+*} \bar{\rho}_1 + \hat{u}^{+*} \bar{\rho}_1 \bar{u}_1 + \hat{p}^{+*} \gamma \bar{p}_1) + \delta\hat{p}(\hat{u}^{+*} + \hat{p}^{+*} \bar{u}_1) \right]_{b^-} \dots \\
& + \left[ \delta\hat{\rho} \left( f^* \bar{u} + g^* \bar{u}^2 + \frac{1}{2} h^* \bar{u}^3 \right) + \delta\hat{u} \left( f^* \bar{\rho} + g^* 2\bar{\rho} \bar{u} + \frac{\gamma}{(\gamma-1)} h^* \bar{p} + \frac{3}{2} h^* \bar{\rho} \bar{u}^2 \right) \right] \dots \\
& + \delta\hat{p} \left( g^* + \frac{\gamma}{(\gamma-1)} h^* \bar{u} \right) \Big]_{b^-}^{b^+} - h^* \beta \delta\hat{u}_1 e^{-s\tau} \dots \\
& + \left[ \delta\hat{\rho}(\hat{\rho}^{+*} \bar{u}_2) + \delta\hat{u}(\hat{\rho}^{+*} \bar{\rho}_2 + \hat{u}^{+*} \bar{\rho}_2 \bar{u}_2 + \hat{p}^{+*} \gamma \bar{p}_2) + \delta\hat{p}(\hat{u}^{+*} + \hat{p}^{+*} \bar{u}_2) \right]_{b^+}^L \tag{H.12d}
\end{aligned}$$

The derivative of  $\mathcal{L}$  with respect to  $\delta\hat{\rho}$ ,  $\delta\hat{u}$ ,  $\delta\hat{p}$  must be zero for any value; hence, each of the rows in equation H.12 can be interpreted as:

- Equations (H.12a) and (H.12b) give the **adjoint equations**:

$$-\hat{\rho}^+ s^* + \bar{u} \frac{d\hat{\rho}^+}{dx} = 0 \tag{H.13a}$$

$$-\hat{u}^+ \bar{\rho} s^* + \bar{\rho} \bar{u} \frac{d\hat{u}^+}{dx} + \bar{\rho} \frac{d\hat{\rho}^+}{dx} + \gamma \bar{p} \frac{d\hat{p}^+}{dx} = 0 \tag{H.13b}$$

$$-\hat{p}^+ s^* + \bar{u} \frac{d\hat{p}^+}{dx} + \frac{d\hat{u}^+}{dx} = 0 \tag{H.13c}$$

From these equations by looking at the sign of the eigenvalue ( $s$ ) it is easy to see that the adjoint equations evolve backwards in time. Also note that the adjoint eigenvalue is the negative complex conjugate of the direct one. That is, if one wishes to recover the adjoint equations in the time domain, then one must use  $p'(x, t) = \hat{p}(x) e^{-s^* t}$ .

- Equation (H.12c) gives the **eigenvalue drift** for the slight change introduced in the system, note that  $\delta s$  is a number hence it comes out of the inner product:

$$\begin{aligned}
& \delta s \left( \langle \hat{\rho}^+, \hat{\rho} \rangle + \langle \hat{u}^+ \bar{\rho}_1, \hat{u} \rangle + \langle \hat{p}^+, \hat{p} \rangle + \{ \hat{\rho}^+, \hat{\rho} \} + \{ \hat{u}^+ \bar{\rho}_2, \hat{u} \} + \{ \hat{p}^+, \hat{p} \} \dots \right. \\
& \left. + h^* \tau \beta \hat{u}_1 e^{-s\tau} \right) + h^* s \delta \tau \beta \hat{u}_1 e^{-s\tau} = 0 \tag{H.14}
\end{aligned}$$

Then the eigenvalue drift with respect to the slight change done in the system ( $\delta\tau$ ) is:

$$\frac{\delta s}{\delta\tau} = \frac{-h^* s \beta \hat{u}_1 e^{-s\tau}}{\langle \hat{\rho}^+, \hat{\rho} \rangle + \langle \hat{u}^+ \bar{\rho}_1, \hat{u} \rangle + \langle \hat{p}^+, \hat{p} \rangle + \{\hat{\rho}^+, \hat{\rho}\} + \{\hat{u}^+ \bar{\rho}_2, \hat{u}\} + \{\hat{p}^+, \hat{p}\} + h^* \tau \beta \hat{u}_1 e^{-s\tau}} \quad (\text{H.15})$$

This equation is only valid to compute the eigenvalue drift with respect to a change in the time delay; however, if the interest is to know the eigenvalue drift with respect to any other perturbation added to the system, the only thing that changes in the equation is the numerator.

- Equation (H.12d) gives the boundary terms and jump conditions.

